NOTICE

The quality of this microform is heavily dependent upon the quality of the original thesis submitted for microfilming. Every effort has been made to ensure the highest quality of reproduction possible.

If pages are missing, contact the university which granted the degree.

Some pages may have indistinct print especially if the original pages were typed with a poor typewriter ribbon or if the university sent us an inferior photocopy.

Previously copyrighted materials (journal articles, published tests, etc.) are not filmed.

Reproduction in full or in part of this microform is governed by the Canadian Copyright Act, R.S.C. 1970, c. C-30.

AVIS

La qualité de cette microforme dépend grandement de la qualité de la thèse soumise au microfilmage. Nous avons tout fait pour assurer une qualité supérieure de reproduction.

S'il manque des pages, veuillez communiquer avec l'université qui a conféré le grade.

La qualité d'impression de certaines pages peut laisser à désirer, surtout si les pages originales ont été dactylographiées à l'aide d'un ruban usé ou si l'université nous a fait parvenir une photocopie de qualité inférieure.

Les documents qui font déjà l'objet d'un droit d'auteur (articles de revue, tests publiés, etc.) ne sont pas microfilmés.

La reproduction, même partielle, de cette microforme est soumise à la Loi canadienne sur le droit d'auteur, SRC 1970, c. C-30.

Canada

METAMORPHISM AND MIGMATIZATION IN THE WHITEWATER-MOJIKIT LAKES AREA, ENGLISH RIVER SUBPROVINCE, N.W. ONTARIO

by

Mark Richard Digel

A thesis submitted to the School of Graduate Studies in partial fulfillment of the requirements for the degree of M.Sc. in Geology

UNIVERSITY OF OTTAWA

OTTAWA, CANADA, 1988

ISBN 0-315-46753-3

UNIVERSITÉ D'OTTAWA
UNIVERSITY OF OTTAWA

Abstract

The Whitewater-Mojikit Lakes study-area forms part of a large area of orthopyroxene-zone, high-grade metamorphic rocks, located within the English River Subprovince of the Superior Province, northern Ontario. The area is underlain by Archean metasedimentary rock, primarily metagreywacke containing thin metapelite layers as well as mafic hornblende gneiss layers of unknown origin. Pre-metamorphic grey, hornblende-biotite metatonalite plutons are intrusive into the metasedimentary rock.

Late Archean Metamorphism is within the orthopyroxene-zone of high-grade metamorphism throughout most of the study-area, as defined by the presence of orthopyroxene in mafic hornblende gneiss layers. Cordierite-garnet-K feldspar-zone high-grade assemblages in metapelite persist into the orthopyroxene-zone. Metagreywacke is comprised of the simple assemblage, biotite-garnet-plagioclase-quartz-ilmenite, regardless of metamorphic grade. Metamorphic grade decreases in the extreme southeastern portion of the study-area, with sillimanite-K feldspar-zone high-grade and muscovite-quartz-zone medium-grade assemblages recognized in metapelite.

Metamorphism has resulted in two phases of migmatization in metapelite and metagreywacke: 1) an early phase of internal (in situ) migmatization, and 2) a later phase of external migmatites which is responsible for most of the migmatitic leucosome in the study-area. The early phase is believed to have been derived by partial melting at or near the granite solidus, although a subsolidus origin can not be ruled out. The leucosome of the later phase of migmatization has been derived by partial melting of primarily metagreywacke at depth, and was subsequently emplaced at the level presently exposed. Late, white, biotite pegmatite dikes intrude the metasedimentary rocks, and may represent the latest crystallized melts of external migmatization.

Key words: Canadian Shield, cordierite-garnet-K feldspar-zone, English River Subprovince, high-grade metamorphism, metagreywacke, metapelite, migmatization, muscovite-quartz-zone, orthopyroxene-zone, Superior Province

TABLE OF CONTENTS

LIST OF TABLES

LIST OF FIGURES

LIST OF PLATES

1. INTRODUCTION

1.1 Location and Exposure

The study-area is in northwestern Ontario, approximately 210 km north of Thunder Bay. It is located within sheet 51I of the Canadian NTS system. The area is bounded by the lakes Whitewater (NW), Smoothrock (SW), and Mojikit (SE), and by the Ogoki Reservoir (NE).

Mapping was restricted to shoreline outcroppings given the considerable size of the study-area and the general lack of exposure inland. Access is limited to canoe and float plane as there are no roads of any type within the study-area. The relief is generally low and drainage is poor.

1.2 Previous Work

The most extensive geological investigations in the English River Subprovince were undertaken by the Ontario Geological Survey as a regional mapping project in the mid 1970's (summarized in Breaks et al. 1978). The OGS study however, includes only the extreme western-most portion of the present study-area.

Previous geological work in the study-area includes reconnaissance-scale mapping by the OGS (Pye and Harris 1965, Davies et al. 1966, Sage et al. 1974) and a compilation map (Stott 1984). The most recent work was regional-scale shoreline mapping in a portion of the area by the Geological Survey of Canada in 1982 (Percival 1983a).

1.3 Regional Geological Setting

The English River Subprovince (ERSp), within which the study-area lies, is located within the Superior Province of the Canadian Shield. Until recently the ERSp was defined to include a northern metasedimentary domain and a southern plutonic domain (Beakhouse 1977, Breaks et al. 1978). Card and Ciesielski (1986) have redefined the ERSp to represent only the previously defined northern metasedimentary domain. The southern plutonic domain has been subdivided into two separate subprovinces, namely the Bird River and Winnipeg River Subprovinces (figure 1.1). This represents a logical separation as there are no strong lithologic, structural, or chronological similarities to link together the northern and southern domains (cf. Krogh et al. 1976, Breaks et al. 1978). The Superior Province subdivisions of Card and Ciesielski (1986) will be adopted in this study.

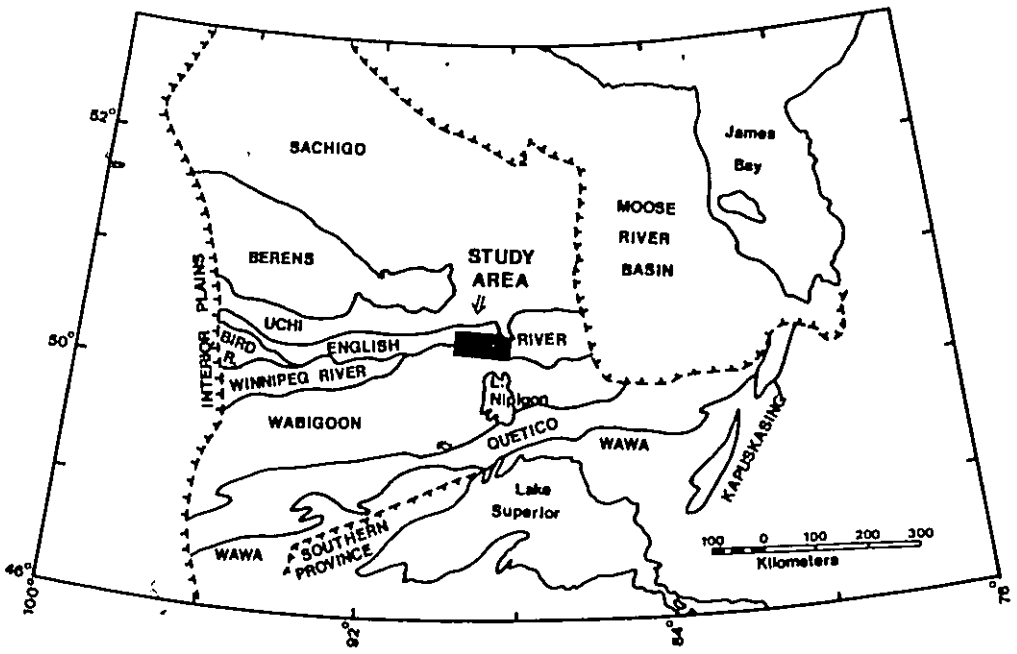

Figure 1.1. Subdivision of the Superior Province of the Canadian Precambrian Shield, proposed by Card and Ciesielski (1986). Includes the location of the present study-area.

The English River Subprovince is dominated by high-grade biotite and garnet-bearing metasedimentary rocks of predominantly greywacke composition with smaller amounts of rock of pelitic composition, and exhibits varying degrees of migmatization. The only other mappable rock types are pre-metamorphic granitoid plutons of dominantly tonalite composition, and younger, Proterozoic gabbro dikes and sills (Breaks et al. 1978). Radiometric dating indicates that all rocks, with the exception of the late gabbro dikes and sills, were emplaced and/or metamorphosed during the late Archean (Krogh et al. 1976).

Directly north of the ERSp lies the Uchi Subprovince which is a volcano-plutonic terrain. To the south the ERSp is in contact with three subprovinces which, from west to east are: the Bird River, the Winnipeg River, and the Wabigoon. The Bird River and Wabigoon Subprovinces are volcano-plutonic terrains while the Winnipeg River Subprovince is a plutonic terrain. The ERSp is distinguished from the adjoining belts by its paucity of metavolcanic and post-metamorphic felsic plutons.

Metamorphic grade throughout most of the ERSp is high-grade, with several large areas of orthopyroxene-zone high-grade metamorphism (grade classification after Winkler 1979). A thin discontinuous area of medium-grade metamorphism is locally observed at the margins of the Subprovince (Breaks et al. 1978). However, there is generally an abrupt increase from medium and low grades in adjoining subprovinces to high-grade conditions within the ERSp. The abrupt transition in metamorphic grade is caused by post metamorphic faults which appear to be guided by the interface between the English River and the adjoining subprovinces. Exceptions to this trend include the contact of the ERSp with: 1) the Winnipeg River Subprovince, which is fault bounded but which has also been metamorphosed to generally high-grade conditions, and 2) small portions of the contact with the Uchi

Subprovince, in which the progressive metamorphic zonation from low grade conditions in the Uchi Subprovince to high-grade conditions in the ERSp is still intact (Breaks et al. 1978).

1.4 Scope of the Present Study

The Whitewater-Mojikit Lakes study-area is a high-grade migmatite terrain underlain dominantly by metagreywacke, containing layers of metapelite. It therefore provides an excellent opportunity to study and contrast the metamorphism and migmatization of pelite and greywacke. Previous studies in the English River subprovince have attributed migmatite generation to melting of metasedimentary rock without giving much thought to the nature of the protolith nor the different behaviour of pelite and greywacke compositions to migmatization (Harris 1976, Harris and Goodwin 1976, Breaks et al. 1978). In addition at least two generations of migmatite can be recognized in the study-area. Much of the leucosome for the later generation of migmatite appears to have been generated at depth and emplaced at the level of exposure which is now exposed at the surface. The origin and generation of these granitoid rocks will be investigated. Subsolidus and melting phase equilibria in model systems of compositions appropriate to the metasedimentary rocks will be discussed.

In chapter 2 some terminology and theory concerning migmatites will be discussed. Chapter 3 describes the general geology and petrology of the main rock types in the study-area. The chemical composition of the migmatitic metasedimentary rocks and their constituent minerals is discussed in chapter 4. Chapter 5 describes the metamorphism and early migmatite generation, with emphasis on phase equilibria in the metasedimentary rocks. The pressure temperature conditions deduced by geothermometry and geobarometry are discussed in chapter 6. The structural

geology is described in chapter 7. The later generation of migmatite is discussed in detail in chapter 8, and a model for the development of migmatite is presented. Chapter 9 summarizes the major findings of this study and points to areas where more research is needed.

1.5 Symbols

The following is a list of symbols used within the thesis.

Mineral abbreviations

And - Andalusite	Mgt - Magnetite
Ap - Apatite	Ms - Muscovite
Bt - Biotite	Opx - Orthopyroxene
Cdt - Cordierite	Pl - Plagioclase feldspar
Co - Corundum	Qtz - Quartz
Grt - Garnet	Sil - Sillimanite
Gph - Graphite	Sp - Spinel
Ilm - Ilmenite	Trm - Tourmaline
Kfs - K feldspar	

Model Geochemical Systems

KFmASH (Fm) - K_2O-(FeO+MgO)-Al_2O_3-SiO_2-H_2O

KMASH (M) - K_2O-MgO-Al_2O_3-SiO_2-H_2O

KFASH (F) - K_2O-FeO-Al_2O_3-SiO_2-H_2O

KMFASH (MF) - K_2O-MgO-FeO-Al_2O_3-SiO_2-H_2O

KNMFASH (NMF) - K_2O-Na_2O-MgO-FeO-Al_2O_3-SiO_2-H_2O

Reactions in model systems are coded to the model system and numbered. The model system codes are listed above in parentheses. The reactions and reaction numbers are listed in tables 5.1 through 5.3.

Example: MF-1 is a reaction in the system KMFASH. NMF-1 is a reaction in the system KNMFASH.

Other Abbreviations

P - Total lithostatic pressure (= P_{total})

T - Temperature

a_{H2O} - Activity of water

P_{H2O} - Hydrostatic pressure

X_C^P - Mole fraction of component C in mineral phase P

Or - Orthoclase component

Ab - Albite component

An - Anorthite component

1.6 Acknowledgements

I would like to thank Dr. Ralph Kretz, for many interesting discussions, for his supervision of the thesis, and for reading this and all earlier versions of the manuscript. Dr. John Percival is thanked for suggesting the project, providing logistical support, and for a thorough critical review of an earlier version of the manuscript. I would also like to thank Dr. G. Skippen, Dr. Andre Lalonde for their critical appraisals.

Field work, in 1984, was funded by the Geological Survey of Canada, and in 1985, by a National Sciences and Engineering Council research grant to R. Kretz. Microprobe facilities were provided at the Geological Survey of Canada, in Ottawa.

A special note of appreciation is extended to my wife, Catherine, and my daughter, Haley, for their tremendous encouragement and patience. I also thank my wife for producing most of the drafting.

2. TERMINOLOGY OF MIGMATITES

2.1 Definition of a Migmatite

There is no universally accepted definition of a migmatite or classification of migmatite structures. For this reason a classification of migmatite structures is discussed which is broadly enough defined to be applicable to any migmatite complex.

Before any migmatite classification can be considered it is important that the term migmatite be clearly and unambiguously defined. The following definition of a migmatite is proposed which in this author's opinion is consistent with the common usage of the term in recent literature. In order to term a rock a migmatite it must satisfy the following criteria:

1) it must be a composite metamorphic rock comprising at least two parts; a mafic rich (compared to other part) part and a leucocratic part which is composed predominantly of quartz and feldspar. The leucocratic portion of a migmatite is referred to as the leucosome (Mehnert 1968). The more mafic part of a migmatite is referred as either; the mesosome[1] if it does not appear to have been depleted in felsic minerals during migmatization, or the melanosome if it does appear to have been depleted during migmatization (Johannes 1983).

2) The different portions of the rock must be intermixed such that the rock mass cannot be properly described by considering

---

[1] Paleosome refers the the unmigmatized equivalent of a migmatized rock. It differs from mesosome in that mesosome is an unmigmatized portion of a migmatized rock. The paleosome refers to the rock before migmatization.

the leucosome and mesosome and/or melanosome portions as separate rock units, and such that the leucosome does not form discrete intrusive bodies (e.g. dikes, sills, and plutons). For example, a biotite schist crosscut by pegmatite dikes would not constitute a migmatite.

3) The composite nature of the rock must not simply reflect an original inhomogeneous protolith, rather it must be the result of some metamorphic, metasomatic, or igneous process which has changed the rock either by the introduction of new material or by the re-arrangement of the existing chemical constituents. For example, a rock comprising metamorphosed finely interlayered basalt and rhyolite is not a migmatite, although it may satisfy the first two criteria.

There are two parts to the description of a migmatite; the first part involves a description based on pre-migmatitic rock composition or rock type (e.g. garnet-biotite migmatite), much in the way that non-migmatitic metamorphic rocks are described; the second part involves a description of the megascopic structure of the migmatite (i.e. contact relations between leucosome and mesosome and/or melanosome fractions: e.g. stromatic migmatite). Many terms presently used to describe migmatite also imply the process by which the migmatite formed (e.g. anatexite, diatexite). Interpretation of the origin of a migmatite requires detailed petrological study and even then one indisputable process may not be proven. Genetic terms should therefore be avoided in migmatite description. If further detailed study allows interpretation of the origin of the migmatite then a genetic qualifier may be added to the name. This approach will be taken in this study.

Mehnert (1968, chapter 2) has proposed a useful descriptive classification of migmatite structures, of which a slightly modified version will be used in this study. Mehnert's classification was simplified in an attempt to make it more universally applicable. Some of Mehnert's terms were thought (by this author) to be too narrowly defined. The terms agmatitic, stromatic, phlebitic, augen, schollen, schlieren, and nebulose are retained, as defined by Mehnert. Diktyonitic and ptygmatic structures are considered to be variations of a phlebitic (vein) structure and are not included. Stictolithic (fleck) structure describes the distribution of mafics within the leucosome and not the structure of the migmatite and therefore is not included. A folded structure is a modification of a pre-existing migmatite structure and since any migmatite structure may be modified by deformation the term does not define a unique migmatite structure. Dilation (Surreitic structure) is a genetic term and therefore is not included. Podiform, a new migmatite structural term, is introduced to describe migmatite in which the leucosome occurs as isolated pods and patches within the migmatite. This classification of migmatite structures is summarized in table 2.1, and will be used in this study.

2.2 Mechanisms of Migmatization

After having described a migmatite the next logical step is to investigate the origin of the migmatite or the mechanism(s) of migmatization. Migmatization is defined as any process which results in the formation of a migmatite. The different mechanisms of migmatization have been discussed previously, however the classification scheme, based on the conservation of matter during migmatization (i.e. open versus closed system migmatization) (e.g. White 1966, Misch 1968, Mehnert 1968, Yardley

Table 2.1. Classification of mesoscopic migmatite structures (slightly modified after Mehnert, 1968)

Structure	Description
a) Structures in which mesosome (paleosome) is commonly preserved	
Augen	The leucosome forms eye shaped lenses, which constitute a single grain, commonly a feldspar. Mehnert suggests that "augen" shaped aggregates of more than one mineral are not true augen, which is followed here.
Agmatitic	Rock has a brecciated appearance with leucosome filling the space between angular mesosome/melanosome fragments. The rock will have the appearance that if the leucosome was removed the fragments of mesosome/melanosome would fit back together.
Phlebitic	A structure in which the leucosome forms veins within the leucosome. The definition of this term has been expanded to include ptygmatic and diktyonic (net-like) structures from Mehnert's original classification.
Podiform	The leucosome forms isolated pods or patches within the mesosome/melanosome. The "pods" may be regular or irregular, and may form in the heterokinetic spaces in boudinage rocks thus encompassing the surreitic or dilation structure of Mehnert's classification.
Stromatic	A layered structure defined by alternating layers of mesosome/melanosome and leucosome. Layering is generally parallel to the foliation produced by the stress field at the time of migmatization.
Schollic	Mesosome/melanosome form somewhat rounded rafts within the leucosome. This structure requires a relatively high proportion of leucosome. Deformation structures within the rafts (Schollen) may be common but interaction of mesosome with the leucosome is by definition minor.
b) Structures in which mesosome (paleosome) is generally not preserved.	
Schlieric	Schlieric structures differ from schollic structures in that by definition there has been considerable interaction between the leucosome and schollen with are therefore termed schlieren. Schlieren migmatites are very heterogeneous and "turbulent" in appearance.
Nebulitic	Melanosome and leucosome portions are longer readily identified. Instead they form diffuse portions of the rock distinguished by slight variations in mineral content. Nebulose migmatites are rather homogeneous although small scale clustering of mafic minerals may be common. Nebulose migmatites resemble igneous rocks and only a regional view of the migmatization may allow their recognition.

1978) has limited application for most migmatite structures which are not amenable to mass balance calculations. A more universally applicable classification of migmatite mechanisms is proposed.

There are two broad categories of migmatization processes, which include; igneous (magmatic) processes, and metamorphic (subsolidus) processes (summarized in Yardley 1978). Each process may take place either by:

1) The introduction of matter (usually components of the leucosome) into the rock mass, which will be called "External migmatization".

2) The rearrangement of the existing chemical constituents into separate leucosome and melanosome fractions, which will be called "Internal migmatization".

This results in four distinct migmatization mechanisms, external and internal igneous migmatization, and external and internal subsolidus migmatization, as summarized in table 2.2.

Table 2.2. Matrix showing the different mechanisms of migmatization

	Migmatization process	
Origin of leucosome forming material	IGNEOUS	METAMORPHIC
INTERNAL	Partial melting (anatectic)	Metamorphic Differentiation
EXTERNAL	Igneous injection	External metasomatism

Internal anatectic migmatization or partial melting involves the preferential melting, segregation, and subsequent crystallization of a portion of a rock mass to form an igneous leucosome. The solid portion of the rock depleted in the leucosome-forming components forms the melanosome. Internal metamorphic migmatization or metamorphic differentiation also involves the segregation of a mesosome into separate leucosome and melanosome fractions, however, segregation results from metamorphic rather than melting processes.

External igneous migmatization, more commonly referred to as igneous injection, involves the introduction of a leucosome into a rock mass as a magma. External solid state migmatization or external metasomatism involves the infiltration of materials into the rock mass to form a leucosome by metamorphic processes (Yardley, 1978). In contrast to internal migmatization, with external migmatization the chemical and mineralogical composition of the mesosome may remain unchanged.

The concepts of external and internal migmatization are used instead of the commonly used concepts of open and closed system[2] migmatization (e.g. Olsen 1983 and 1985) because the latter are more restrictive in their scope. For example, the internal migmatization of a volume of rock in which some of the segregated leucosome migrates out of the rock is open system migmatization, but is very different from open system igneous injection. Also in many migmatite terrains it may be much easier to establish an internal or external source for the leucosome, than it is to

---

[2] The "system" refers the largest volume of rock undergoing migmatization which is undergoing the same migmatization process and resulting in the formation of the same migmatite leucosome. In a finely layered rock the size of the system for internal migmatization will be quite small (restricted to individual layers), whereas for external migmatization of the same rock the size of the system may be quite large.

perform mass balance calculations (which are applicable only to certain migmatite structures) to establish whether migmatization took place in an open or closed system. The concepts of open and closed system migmatization may still be applied to internal and external migmatization, when the question can be answered.

By definition external migmatization is an open system process. The external leucosome components may however react with or assimilate some of the mesosome, resulting in an internal component to the leucosome and the development of separate mesosome, melanosome, and leucosome fractions. Internal migmatization may take place in a closed system if there has been no loss of matter during segregation, or in an open system if matter (usually leucosome constituents), migrates out of the system during migmatization.

2.3 Distinction Between Different Migmatization Mechanisms

2.3.1 Distinction Between Internal and External Migmatites

An important task when studying migmatite is to determine whether migmatization has resulted from internal and external or external processes. Petrologists typically rely on mass balance calculations to answer this question. A detailed description of mass balance procedures is given in Olsen (1983 and 1985). Unfortunately mass balance calculations are suitable only to a limited number of migmatites which contain mesosome, melanosome, and leucosome fractions, and which have a simple migmatite structure. There is also the problem that the rock may be layered and that the protolith of the leucosome + melanosome fraction may not be the observed mesosome composition. Mass balance calculations performed on a migmatite derived from a layered protolith in which only layers of suitable

composition were migmatized will yield anomalous results. Strictly speaking any migmatite containing mesosome, leucosome, and melanosome fractions must contain some heterogeneity which leads to the preferential migmatization of certain layers or zones while others remain unaffected. Mass balance calculations are useful only for migmatites in which the mineral phases were distributed homogeneously throughout the paleosome. For such a rock to undergo migmatization and preserve leucosome, melanosome and mesosome requires that the paleosome contained textural or structural heterogeneities, or that the distribution and/or composition of volatile components in the paleosome was heterogeneous (ie. something to cause preferential migmatization of some layers while others remain unaffected).

Unfortunately we can only reasonably assume to know the nature of the protolith heterogeneity for migmatite which mass balance calculations indicate were derived in a closed system. When mass balance calculations indicate that there are excess components, then migmatization may in fact have operated in an open system, or migmatization may have occurred preferentially in certain layers or zones of an originally heterogeneous protolith.

Other factors such as the presence of characteristic migmatite structures, leucosome chemical compositions, or leucosome mineral assemblages may provide evidence of an internal component to migmatization. Alternatively constancy of mesosome composition, in areas with different proportions and/or compositions of leucosome may indicate a largely external source for the leucosome. Comparing the composition of leucosome plus mesosome and/or melanosome with equivalent unmigmatized rocks from lower grades may also provide information, although quantitative mass balance estimations would be incorrect.

2.3.2 Distinction Between Anatectic and Subsolidus Migmatite

Are there unique textural or chemical features of anatectic migmatite and internal subsolidus migmatite which allow them to be distinguished? Some features which may be useful include; plagioclase composition, leucosome composition, syn-migmatitic fold structures, and leucosome textures. A good recent discussion of the problem is found in Ashworth (1985).

It has been very well established that during anatexis the albite component of plagioclase feldspar is strongly fractionated into the melt phase (see Bowen 1913, Johannes 1978). Only with extensive internal partial melting will the composition of the plagioclase crystallized from the melt phase approach that in the remaining solid rock. The melting phenomenon of plagioclase has been used as a criteria to reject an anatectic origin for internal migmatite in which plagioclase composition does not differ between coexisting leucosome and melanosome fractions (Kretz 1966, Misch 1968).

Therefore with internal anatectic migmatite the leucosome should be significantly more sodic than paleosome or melanosome plagioclase unless one of the following conditions is true (cf. Yardley 1978):

1) Plagioclase underwent nearly complete melting, which is probably not possible at temperatures and pressures present within the crust (Wyllie 1977).

2) Segregation of the melt phase and residual plagioclase was negligible, allowing re-equilibration during crystallization (Ashworth 1985).

3) Plagioclase compositions underwent subsolidus re-equilibration throughout the migmatite. The common occurrence

> of widely variable plagioclase compositions in coexisting layers in many metamorphic rocks suggests that re-equilibration does not take place (Yardley 1978).

Obviously there is not necessarily any relationship in plagioclase composition between leucosome and mesosome in external migmatite.

The similarity of many leucosome compositions to experimental eutectic granite or tonalite melt compositions has been used as a criteria for an antatectic origin to migmatite (see Winkler 1979). However in the absence of evidence that subsolidus migmatization can not form leucosome of similar compositions, leucosome composition cannot be used as a definitive criteria. Migmatite leucosome whose compositions depart strongly from experimental melt compositions may argue against an anatectic origin. However the influence of additional components not included in experimental studies, and the possibility that the leucosome was only partially molten should be considered. Experimental studies in the granite and tonalite systems, may not provide an accurate estimation of melt compositions produced by complex melting reactions in natural rocks.

McLellan (1984) compared the development of syn-migmatitic folds in anatectic and subsolidus migmatite. She found that subsolidus migmatite formed harmonic fold structures, while anatectic migmatite formed disharmonic structures. McLellan concluded that in the presence of greater than about 30% melt phase a rock will deform as a "melt dominated" system, and that the deformation of a melt dominated migmatite will produce disharmonic fold structures in response to the strong competency contrast between the solid and molten portions of the rock. The presence of disharmonic fold structures in migmatite may therefore indicate that the leucosome was partially molten at the time of deformation.

A discussion of the textural properties of migmatite, which may help distinguish between anatectic and subsolidus migmatite may be found in Ashworth and McLellan (1985).

The mechanisms of subsolidus migmatization are not well understood, and perhaps partly for this reason most high grade migmatite terrains are discussed in terms of anatectic migmatization (Lindh and Wahlgren 1985). There is however internal migmatite formed in areas where metamorphic temperatures were never high enough to form granitic melts and therefore must have formed by subsolidus processes (e.g. Sawyer and Robin 1986).

Even in most high grade migmatite terrains, it can seldom be shown conclusively that conditions were suitable for anatexis, since the requirements for fusion vary not only as a function of pressure and temperature but also as a function of a_{H2O}, and the composition of the paleosome. Any thorough discussion of the migmatization of a metamorphic terrain should therefore include some consideration of both anatectic and subsolidus migmatization.

3. GENERAL GEOLOGY

3.1 Introduction

The lithology of the Whitewater-Mojikit Lakes study-area (figure 3.1) is dominated by migmatite, gneiss, and schist in which biotite and garnet are the major mafic minerals. Concordant layers of mafic gneiss, are minor but widespread. Intrusive into the migmatite and gneiss are early, foliated-to-gneissic, grey biotite-hornblende metatonalite plutons. Syn-metamorphic, biotite-garnet granitoid rock forms a network of layers and masses in migmatite and gneiss. Late, post-metamorphic, massive, white, biotite granite pegmatite dykes crosscut migmatite and gneiss and biotite-garnet granitoid rock. Massive pink, biotite leucogranite dykes intrude metatonalite plutons. Un-metamorphosed gabbro dykes and sills intrude all rock units. The relative timing of emplacement/deposition and the estimated overall proportions of the main lithologic components are summarized in table 3.1. Sample locations referred to in the text are shown in figure 3.2.

Four metamorphic zones were mapped (metamorphic classification is adapted from Winkler 1979), they are:

High-Grade

1) Orthopyroxene-zone (granulite): Most of the study-area experienced orthopyroxene-zone, high-grade metamorphic conditions, based on the widespread occurrence of metamorphic orthopyroxene in mafic gneiss and locally in metatonalite.

2) Cordierite-garnet-K feldspar-zone: A small area in the most northern part of the study-area contains cordierite-garnet-K feldspar in association with biotite and quartz. Orthopyroxene

is absent in associated mafic gneiss. Cordierite-garnet-K feldspar-zone assemblages, in compositionally suitable rock layers, persist into the orthopyroxene-zone.

3) Sillimanite-K feldspar-zone: Sillimanite-K feldspar-zone assemblages occur in a small area in the southern part of the study-area.

Medium-Grade

4) Muscovite-quartz-zone: Muscovite-quartz-zone assemblages are restricted to a small area, within 2 km of the southern subprovince boundary in the southeastern part of the study-area.

Table 3.1 Relative timing of deposition/emplacement of main lithologic components (oldest to youngest) in the Whitewater-Mojikit Lakes study-area

Age	Lithologic Unit	Estimated Overall Proportion
Archean	MG_1 Migmatite and Gneiss	55%
	Grey metatonalite	5%
	MG_2 Leucosome	30%
	White Bt Pegmatite and Pink Bt Granite	<1%
Proterozoic	Gabbro Dykes and Sills	10%

The distribution of metamorphic zones in the study-area is shown in figure 3.1. The boundary between metamorphic zones is approximate due to the patchy distribution of rock layers containing the appropriate index

Figure 3.1. Geological compilation map of the Whitewater-Mojikit Lakes area. Geology after Pye and Harris (1965), Davies et al. (1966), Sage et al. (1977), Percival (1983), Digel in Percival et al. (1984), Stott (1984), Digel (present study).

Legend

Proterozoic:

7 Gabbro (Logan Sills)

Archean:

6 Ms-Bt Granite and Pegmatite

5 a) Foliated Hbl-Bt metatonalite
b) Layered metatonalite gneiss

4 Leucocratic Bt-Grt-Kfs gneiss

3 Migmatized Bt-Grt metagreywacke with minor metapelite and mafic gneiss
a) mainly stromatic structures
b) mainly schlieren structures
c) mainly nebulose structures

2 Hbl-Cpx metagabbro (Wabigoon subprovince)

1 Mafic to intermediate metavolcanics (Wabigoon subprovince unsubdivided)

Isograds:

Sil-Kfs (Ms+Qtz=Kfs+Sil+H_2O)

Cdt-Grt-Kfs (Bt+Sil+Qtz+Pl=Kfs+Cdt+Grt+Melt) or
(Bt+Sil+Qtz+Pl=Kfs+Cdt+Grt+H_2O)

Opx-in Reaction unknown

Metamorphic zones:

I	Ms-Qtz
II	Sil-Kfs
III	Cdt-Grt-Kfs
IV	Opx

Structural Data:

Foliation

Lineation

Mylonite zone

Other Data:

N/O No outcroppings

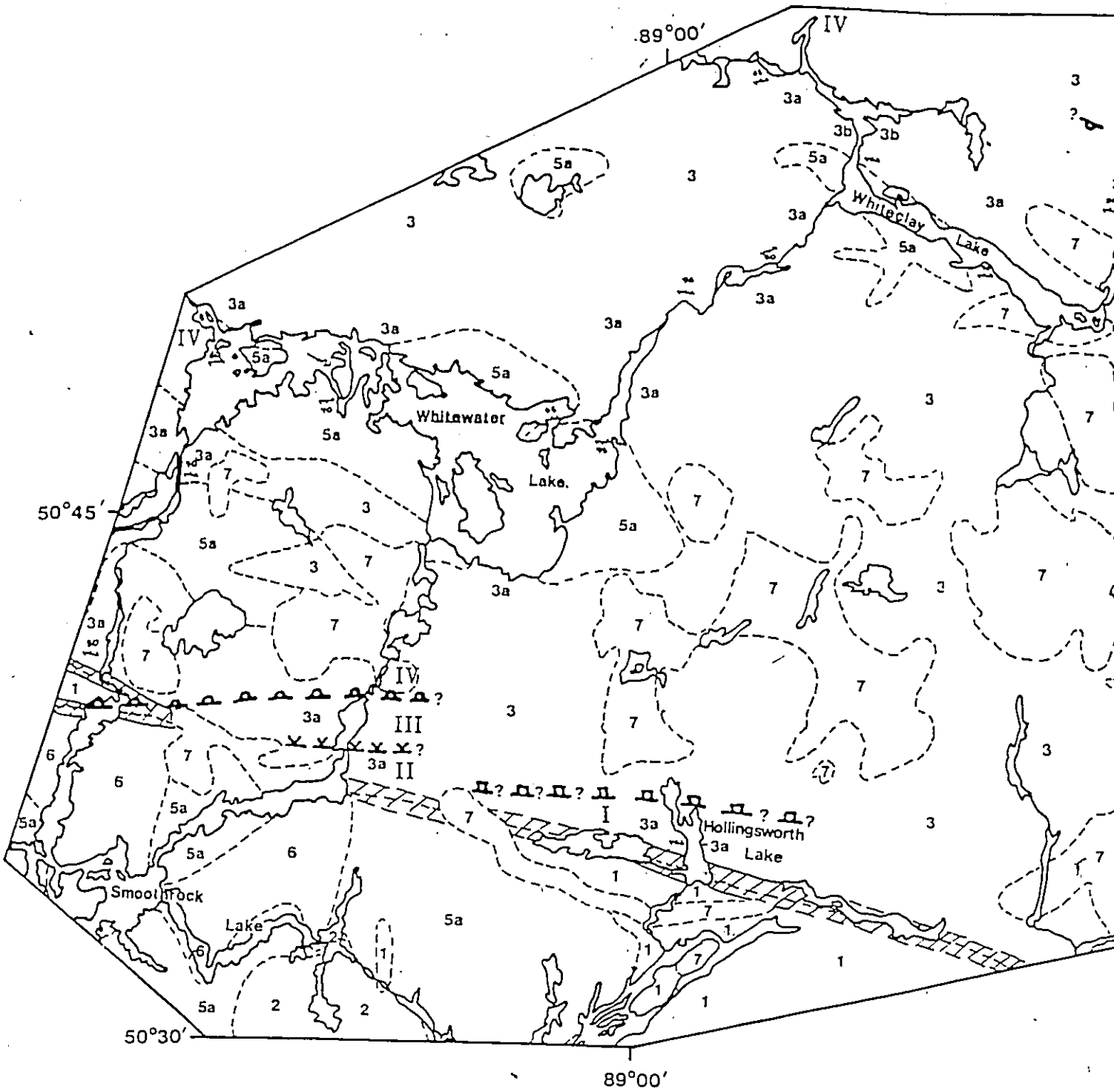
89°00'
50°45'
50°30'
Whitewater
Lake.
Whiteclay
Lake
Hollingsworth
Lake
Smoothrock
Lake
IV
III
II
I

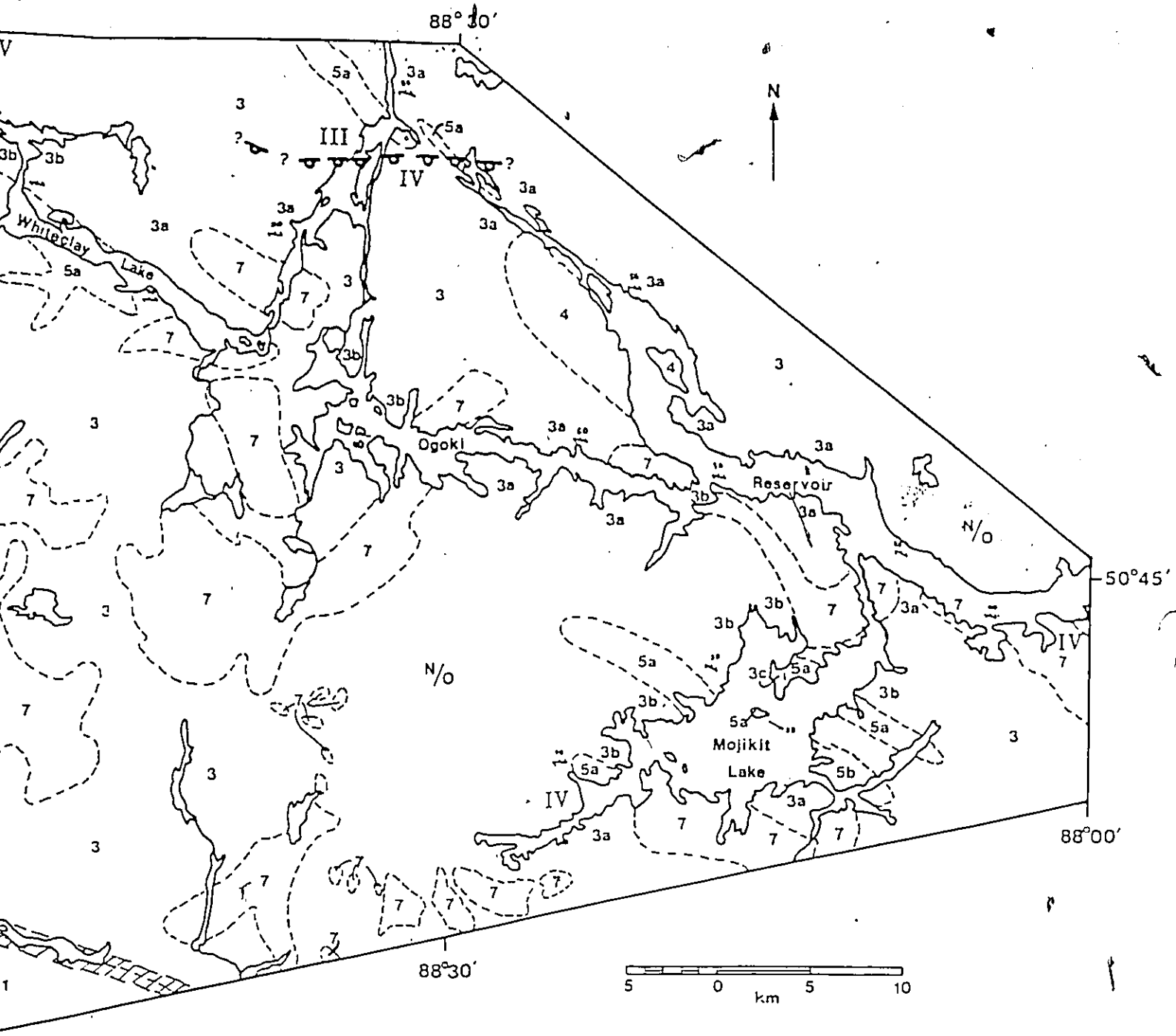
88° 30'
N
III
IV
Whiteclay Lake
Ogoki Reservoir
Mojikit Lake
N/O
50°45'
88°00'
88°30'
5 0 5 10
km

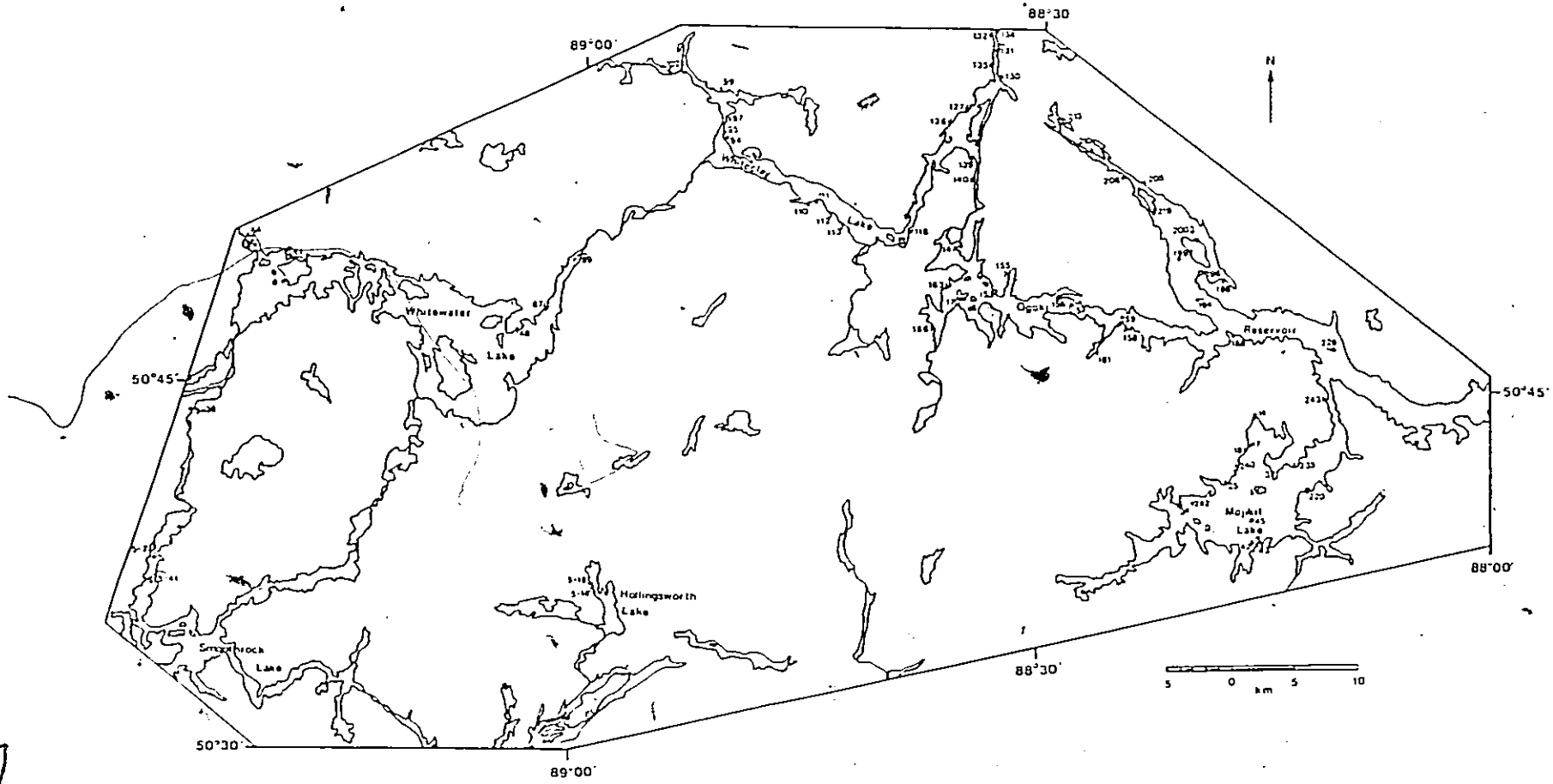

Figure 3.2. Sample location map

minerals. Since the major part of the study-area underwent orthopyroxene-zone metamorphism, this chapter will focus on the orthopyroxene-zone rocks. The metamorphism is discussed further in chapter 5. In the remainder of this chapter the field description, petrography, distribution, and contact relationships of each lithologic unit will be discussed. Assemblages for all rock types present are listed in table 3.2.

3.2 Migmatite and Gneiss (Map unit 3, figure 3.1)

Biotite- and garnet-bearing migmatite and gneiss constitute the dominant mappable unit in the study-area. They are interpreted to be derived from a sedimentary protolith, based on the recognition of relict sedimentary structures in lower grade portions of the ERSp (Breaks et al. 1978) and by their chemical similarity to sedimentary rock types. The metasedimentary rocks comprise two main compositions: 1) greywacke composition, with biotite and garnet as the main mafic minerals, and 2) pelite composition containing biotite, garnet, and one or more of muscovite, cordierite, and sillimanite. The terms metagreywacke (1) and metapelite (2) will be used to describe these rock types. Minor rock units include; leucocratic biotite-garnet-K feldspar gneiss, mafic hornblende gneiss, and garnet-clinopyroxene-magnetite layered gneiss.

No clearly recognizable primary sedimentary structures are preserved in the study-area, although possible relict graded bedding was observed at location 157 in figure 3.2. At this location 0.2 to 1.0 m wide layers of metapelite in metagreywacke exhibit a gradational and consistent increase in aluminous minerals (garnet and cordierite) across the layers (plate 3.1). Layering, parallel to the alignment of biotite grains, defined by subtle but abrupt variations in grain size, as observed in some

Table 3.2. Observed mineral assemblages

Rock Type	No.	Zone[1]	Assemblage
MG_2 migmatite leucosome	A-1	m to o	Pl Qtz Kfs Bt Grt Ilm (Cdt) (Trm)
MG_1 Metapelite melanosome	A-2a	c,o	Bt Cdt Grt Sil Pl (Kfs)[3] Ilm (Sp) (Qtz absent)
MG_1 Metapelite melanosome	A-2b	c,o	Bt Cdt Grt Pl Qtz (Kfs)[3] Ilm (Gph) (Qtz bearing)
MG_1 Metapelite melanosome	A-2c	c	Bt Cdt Grt Pl Qtz Sil Kfs Ilm
MG_1 metapelite leucosome	A-2d	c,o	Kfs Qtz
Metapelite	A-3	s	Bt Pl Sil Qtz Kfs Opq
Metapelite	A-4	m	Bt Pl Qtz Sil Ms Opq
Metagreywacke mesosome	A-5a	m to o	Pl Qtz Bt Grt Ilm
MG_1 metagreywacke leucosome	A-5b	o[2]	Pl Qtz Kfs Bt
Mafic Hbl Gneiss	A-6	s	Pl Hbl Qtz Opq (Cpx) (Bt-rare)
Mafic Hbl Gneiss	A-7	o	Pl Hbl Opx Cpx Opq (Qtz)
Mafic Hbl Gneiss	A-8	o	Pl Hbl Opx Grt Opq (Qtz) (Bt-rare)
Mafic Hbl Gneiss	A-9	o	Pl Hbl Grt Opx Cpx Opq (Qtz)
Mafic Hbl Gneiss	A-10	o	Pl Hbl Opx (Qtz)
Bt-Grt-Kfs leucocratic gneiss	A-11	o[2]	Pl Qtz Bt Grt Kfs Ilm
Grey metatonalite	A-12	o[2]	Pl (Hbl) Bt Qtz Ilm (Opx Cpx) (Opx Grt)
White Bt pegmatite & Pink Bt granite	A-13	o[2]	Kfs Pl Qtz Bt Ilm
Smoothrock lake pluton	A-14	m,s	Pl Qtz Kfs Bt Ms (Grt)

() Mineral or mineral pairs not present in all samples examined.
1 Metamorphic zones: m = Ms-Qtz , s = Sil-Kfs, c = Cdt-Grt-Kfs , o = Opx
2 Rock type not observed at other metamorphic grades.
3 minor Kfs was present in approximetely 1/3 of the samples examined.

a)

b)

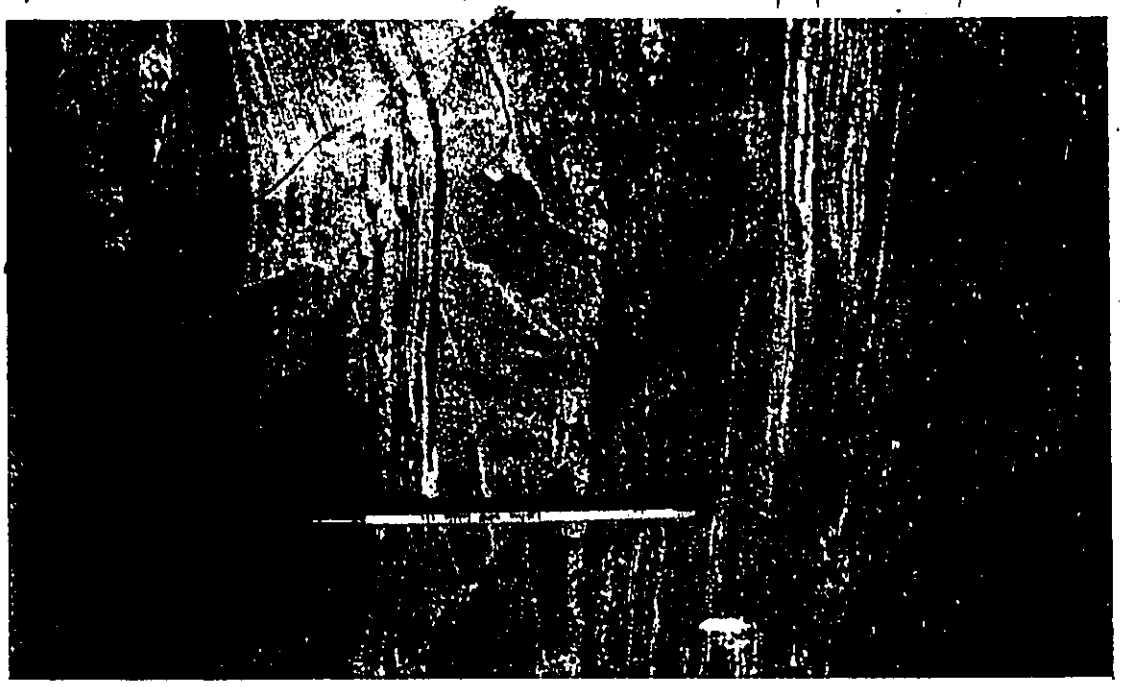

Plate 3.1. Relict sedimentary structures in metasedimentary rock. (a)Interlayered metagreywacke and metapelite, showing evidence of possible relict graded bedding in metapelite. The increase in grainsize across metapelite layers corresponds to an increase in aluminous minerals. This may be a relic of the upwarding fining sequence of a graded bed. (b) Intersection of lithologic layering (S_0) with metamorphic foliation (S_1).

metagreywacke thin sections. The alignment of biotite grains (S_1) was locally observed to intersect the lithologic layering at a low angle, which may represent an original bedding (S_0) surface. In general however, all contacts between supracrustal rocks are sharp and conformable.

Metagreywacke constitutes about 85% of the migmatite and gneiss and commonly comprises entire large outcroppings and outcropping areas. Metapelite makes up about 10% of the migmatite and gneiss. Metapelite forms layers within metagreywacke, which are usually less than 2 m in width, and although widespread they are patchy in their distribution. A variety of minor rock types, constituting less than 5% of the migmatite and gneiss unit, are associated with metagreywacke and metapelite. Mafic hornblende gneiss occurs as 1 to 10 m wide discontinuous layers and blocks within metagreywacke. Layered garnet-clinopyroxene-magnetite gneiss occurs as elongate blocks which are typically highly folded. Leucocratic biotite-garnet-K feldspar gneiss occurs as concordant layers within metasedimentary rock or as larger pluton-like bodies. The origin of the mafic gneiss and leucocratic biotite-garnet-K feldspar gneiss is problematic and will be discussed later.

Within the cordierite-garnet-K feldspar- and orthopyroxene-zones most outcrops of metapelite and some outcrops of metagreywacke are migmatite in that mesosome/melanosome fractions are interlayered with a granitoid[1] leucosome, in a manner satisfying the criteria outlined in chapter 2. Two distinct generations of migmatite were recognised in the metasedimentary rock. An earlier generation of internal (in situ) leucosome, referred as

---

[1] "Granitoid" refers to rocks which fall within the IUGS quartz-alkali feldspar-plagioclase (QAP) ternary diagram of Streckeisen (1976). "Granitic" refers to rocks which fall within the granite field of the QAP diagram. Similarly, "tonalitic" refers to rocks which fall within the tonalite field.

the MG_1 event, is recognised in metapelite and locally in metagreywacke. A later generation of externally derived leucosome, referred to as the MG_2 event, has invaded the study-area. The mineral assemblage, mineral proportions and migmatitic structure of MG_1 leucosome, in metapelite and metagreywacke, are distinct from one another. Furthermore MG_1 leucosome is distinct in migmatitic structure, mineral assemblage, and mineral proportions, compared to MG_2 leucosome. In contrast to MG_1 leucosome, which is restricted to individual lithologic layers, MG_2 leucosome forms larger bodies, which commonly cross lithologic boundaries. Wherever crosscutting relationships are observed, MG_2 leucosome crosscuts MG_1 migmatite leucosome, indicating that MG_1 leucosome predates, at least in part, MG_2 leucosome.

MG_1 leucosome will be described with in the sections on metagreywacke and metapelite. Because MG_2 leucosome is not restricted to any one rock type, it will be discussed separately. Modal estimates of migmatite and gneiss components are presented in tables 4.1-4.4.

3.2.1 Contact Relationships Between White, Biotite-Garnet Granite (MG_2 Leucosome), and MG_1 Migmatite

Cross-cutting relationships between MG_2 leucosome, and MG_1 migmatite are usually only developed where the proportion of granite exceeds about 30%. Where the proportion is lower MG_2 leucosome generally forms conformable layers and lenses within the MG_1 migmatite and gneiss, ranging from several mm to several m in width (plate 3.2a&b). Even where the proportion of MG_2 is high, evidence of an intrusive relationships may not be present. Instead, contacts between MG_2 leucosome and MG_1 metagreywacke and metapelite migmatites are often diffuse or schlieric (plate 3.2e).

Plate 3.2. Variations in MG_2 migmatite structures in metasedimentary rock. (a) Stromatic structures in metagreywacke with a very low proportion of leucosome. (b) Stromatic structures in metagreywacke with a higher proportion of leucosome. Note the subordinate development of schlieren structures. (c) Vein structure in metagreywacke. (d) Schollen structures in metagreywacke. (e) Schlieren structures in metagreywacke with minor metapelite. (f) Biotite-and garnet-rich clot in schlieren migmatite.

a)

b)

c)

d)

e)

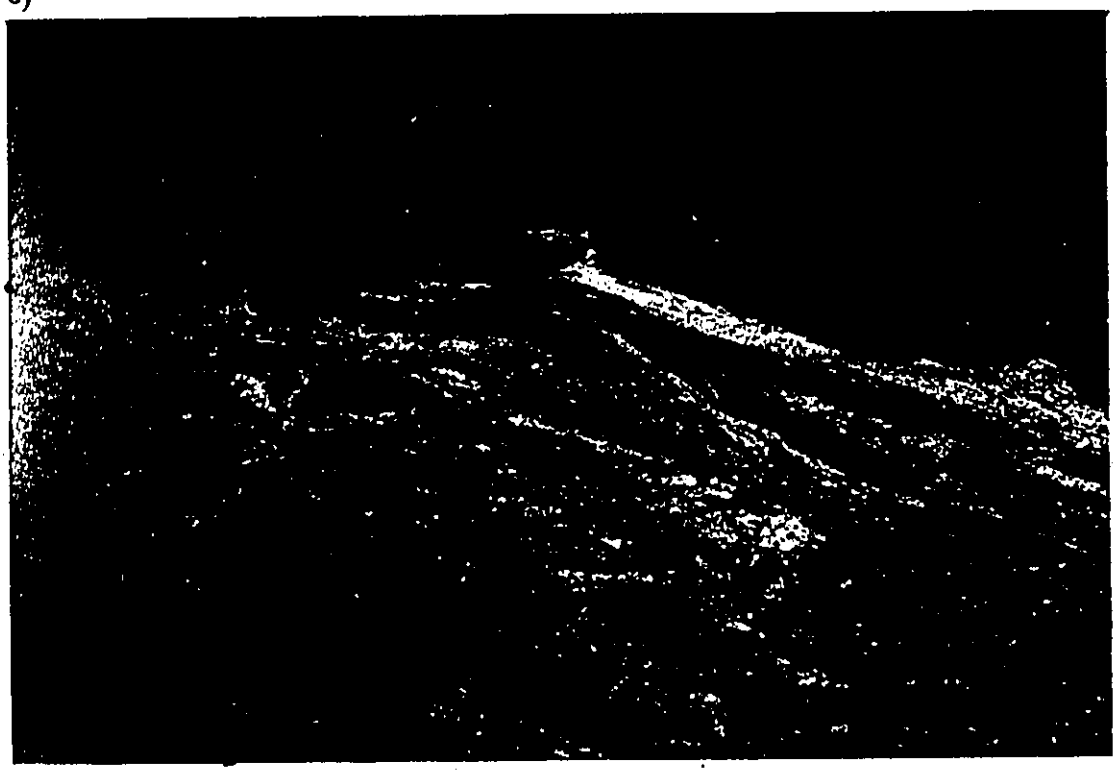

f)

Relationships between MG_2 leucosome, and metagreywacke and metapelite can be more appropriately described using migmatite terminology, than with intrusive terminology. MG_2 leucosome is therefore considered as a separate generation of migmatite leucosome rather than distinct intrusive bodies, and will be described as such.

The presence of MG_2 leucosome is persistent throughout the study-area. MG_2 leucosome makes up an average of 30% of the MG_2 migmatite and gneiss, although at individual outcrops the proportion varies from 0 to 95%. The migmatite structure developed is directly related to the proportion of MG_2 leucosome present. Stromatic structures are predominant where the proportion of MG_2 leucosome is low (plates 3.2a,b), with vein structures developed locally (plate 3.2c). With an increasing proportion of MG_2 leucosome stromatic structures give way to schollen and schlieren structures (plates 3.2d,e). Schollen are angular to rounded mesosome inclusions within the leucosome, and retain their pre-migmatitic appearance and composition, and exhibit sharp contacts with leucosome. Where schlieren structures are developed, metasedimentary inclusions (schlieren) are either: 1) irregular sub-m scale inclusions of more or less recognizable metasedimentary rock, exhibiting diffuse and gradational contacts with the leucosome, or 2) clots and lenses rich in biotite and garnet (with or without cordierite and/or sillimanite), with only minor plagioclase and/or quartz (plate 3.2f).

The mesosome of the MG_2 leucosome is either MG_1 migmatite or non-migmatitic metasedimentary rock. Stromatic and schollen migmatites contain mesosome whose mineral assemblage, appearance, and chemical composition (discussed in chapter 4) do not differ from mesosome where MG_2 migmatites

are not present. Where stromatic and schollen structures are developed, the volume of MG_2 leucosome is clearly too large to have been derived from the included mesosome, except where the proportion of MG_2 leucosome is very low. MG_2 stromatic and schollen migmatite structures differ only in the mesosome to leucosome ratio and in the mesosome-leucosome contact relationships.

Schlieren migmatite differs from stromatic and schollen migmatite in that, by definition, there has been interaction between the leucosome and mesosome, which has altered the composition and appearance of the mesosome. Although MG_2 schlieren migmatite is inhomogeneous on too large a scale to allow quantitative mass balance estimation or to determine schlieren or leucosome compositions, the schlieren plus leucosome composition is clearly too felsic to represent a metagreywacke. There must, therefore, be a considerable external component to the leucosome of schlieren migmatite.

Stromatic, schollen, and schlieren structures are rarely completely isolated at any outcropping. Rather these terms represent ideal endmember structures which occur in variable proportions in natural migmatites. For example, plate 3.2b shows MG_2 migmatite with a predominant stromatic structure, but with some schlieren structure developed. In the central portion of the ERSp the proportion of MG_2 leucosome seems to increase towards the east in the study-area, with stromatic migmatite predominant in the west, and a higher proportion of schollen and schlieren migmatite in the east.

Breaks et al. (1978) described similar migmatite to the west. MG_1 migmatite and stromatic MG_2 migmatite correspond to the metatexite in the classification scheme used by Breaks et al., while schollen and schlieren migmatite correspond to diatexite. They did not distinguish between different generations of migmatite leucosome.

MG_2 leucosome is present in metasedimentary rocks of all metamorphic zones observed. However, with decreasing grade, MG_2 leucosome forms larger and more recognizable intrusive layers which commonly form small stocks and layers up to several tens of meters wide. In areas of muscovite-quartz-zone and sillimanite-K feldspar-zone metamorphism the description of the rocks as migmatite becomes tenuous, and intrusive terminology becomes more appropriate. Schlieren structures were only observed in cordierite-garnet-K feldspar-zone and orthopyroxene-zone MG_2 migmatite.

3.2.2 MG_2 Leucosome

MG_2 leucosomes vary from granite to tonalite in composition although most are granite. MG_2 leucosome is characterized by assemblage A-1 (table 3.2), and all white in colour. Cordierite is present as a minor phase in MG_2 leucosome in many samples. Orthopyroxene was observed in MG_2 leucosome at two locations in the field (stations 17 and 188 in in figure 3.2), but was not observed in thin section. Percival (1983a) also reported the rare occurrence of orthopyroxene in white granitoid rock.

The texture of MG_2 leucosome is generally allotriomorphic seriate. The one notable exception to this general rule is tonalitic MG_2 leucosome, in which minerals more commonly exhibit granoblastic textures. The proportion of mafic minerals in MG_2 leucosome varies considerably, although most contain less than 5% (see table 4.1).

Plagioclase, which rarely occurs as coarse euhedral megacrysts, is oligoclase in composition and exhibits weak normal zoning. Aligned biotite grains are commonly clustered with garnet. Isolated biotite grains and biotite clusters however, generally show no preferred orientation, except where the leucosome has been deformed. Garnets are medium- to coarse-grained rounded anhedral, and are commonly cut by chlorite- and biotite-

filled fractures. Rare inclusions of quartz, plagioclase, sillimanite, and green spinel were observed in generally inclusion free garnet.

Cordierite is a minor phase (<1%) in MG_2 leucosome, occurring as coarse euhedral to subhedral tabular grains, randomly distributed throughout the rock (plate 3.3). Concentrations of cordierite (up to 20% of the rock) are locally present, in MG_2 leucosome, near the contact with metapelite where schollen and schlieren structures are developed and rarely adjacent to stromatic structures. Cordierite is variably altered to a fine-grained mixture of chlorite and white mica, however pristine cordierite is common.

Muscovite is present locally as a secondary mineral in MG_2 leucosome, generally crosscutting the pre-existing biotite foliation. Muscovite which may be primary was observed locally in MG_2 leucosome in the muscovite-quartz-zone. Subhedral andalusite was observed in one sample (Station 64).

3.2.3 Nebulose Migmatite

Migmatite with nebulose structure was recognized in a small area of less than 2 km square at the north end of Mojikit Lake (see figure 3.1). The overall appearance of the nebulose migmatite, is that of a foliated mafic granitoid rock in which small clots of fine- to medium-grained biotite and garnet occur as, evenly distributed, oriented inclusions, within a matrix of medium- to coarse-grained plagioclase (often as euhedral megacrysts), quartz, fine- to medium-grained garnet, and oriented biotite (plate 3.4). Medium- to coarse-grained anhedral microcline is developed in nebulose migmatite only at the margins of metapelite inclusions, or where nebulose migmatite is gradational into MG_2 schlieren migmatite.

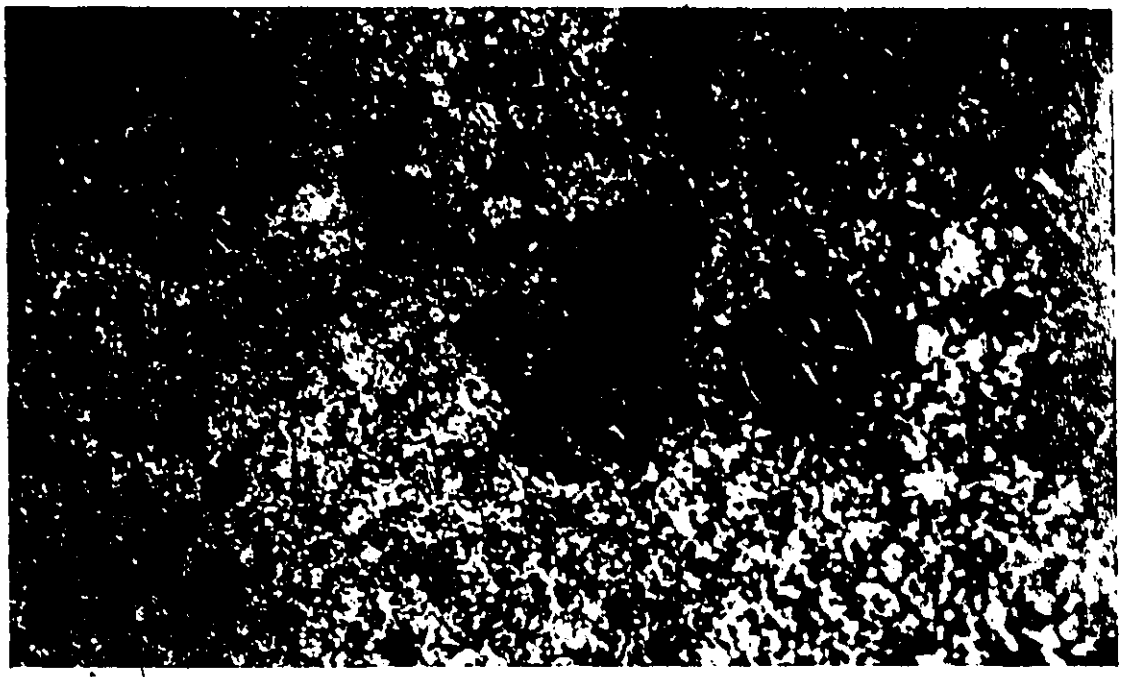

Plate 3.3. Coarse subhedral tabular cordierite in MG_2 leucosome.

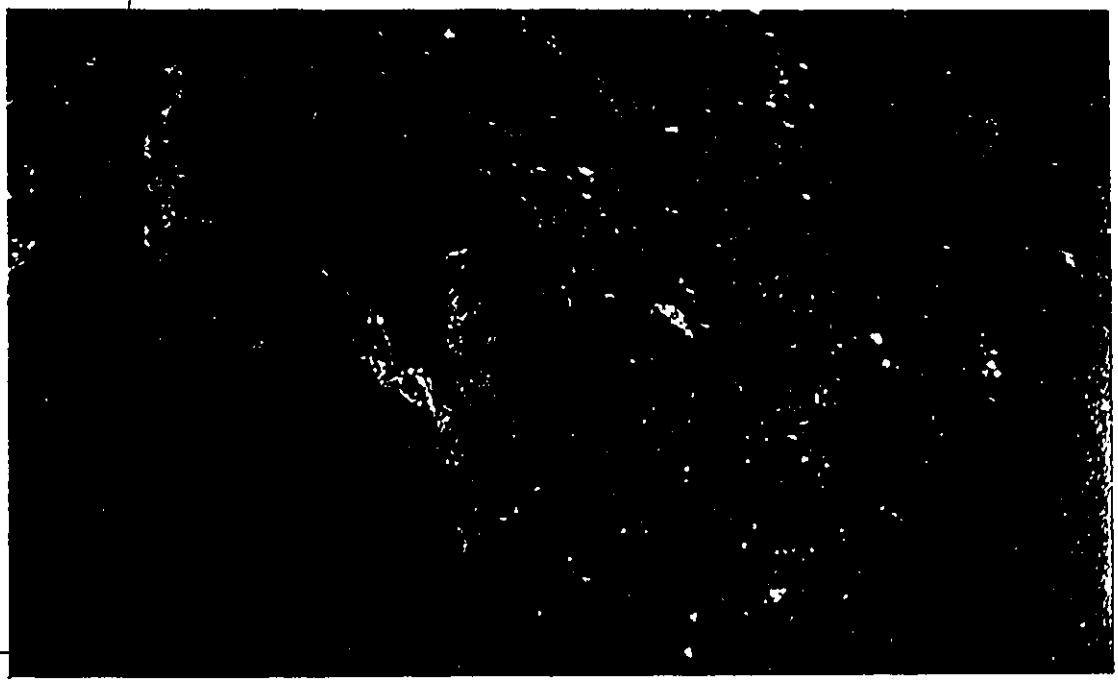

Plate 3.4. MG_2 nebulose migmatite developed in metagreywacke.

MG_2 nebulose migmatite contains rounded inclusions of metasedimentary rock and mafic gneiss. Discordant contacts between nebulose migmatite and MG_2 stromatic metagreywacke migmatite were observed at one outcropping (Station 3 in figure 3.2). However, more typically, nebulose migmatite grades into schlieren migmatite, suggesting that nebulose migmatite may be a variety of MG_2 migmatite.

3.2.4 Muscovite-Quartz- and Sillimanite-K feldspar-Zone Metapelite

Muscovite-quartz-zone metapelite, characterized by assemblage A-1, is fine- to medium-grained and schistose. Medium-grained biotite and muscovite grains are aligned forming the foliation in the rock. Fine-grained sillimanite is usually present, and is oriented parallel to the mica alignment.

Sillimanite-K feldspar-zone metapelite, characterized by assemblage A-2, is medium-grained schistose. Small lenses of plagioclase and quartz were observed, although the rock is characteristically mesoscopically homogeneous. Sillimanite-K feldspar-zone metapelite differs from muscovite-quartz-zone metapelite by the absence of muscovite and the presence of K feldspar. The isograd separating the muscovite-quartz- and sillimanite-K feldspar-zones is only approximate, due to the patchy distribution of the metapelite layers.

3.2.5 Cordierite-Garnet-K feldspar-zone Metapelite

Cordierite-garnet-K feldspar-zone and orthopyroxene-zone metapelite contains 5 to 25% of isolated lenses and pods of granitoid MG_1 leucosome. The dominant migmatite structures are podiform and stromatic (plate 3.5) (Note: this discussion is exclusive of MG_2 migmatization). Melanosome of

a)

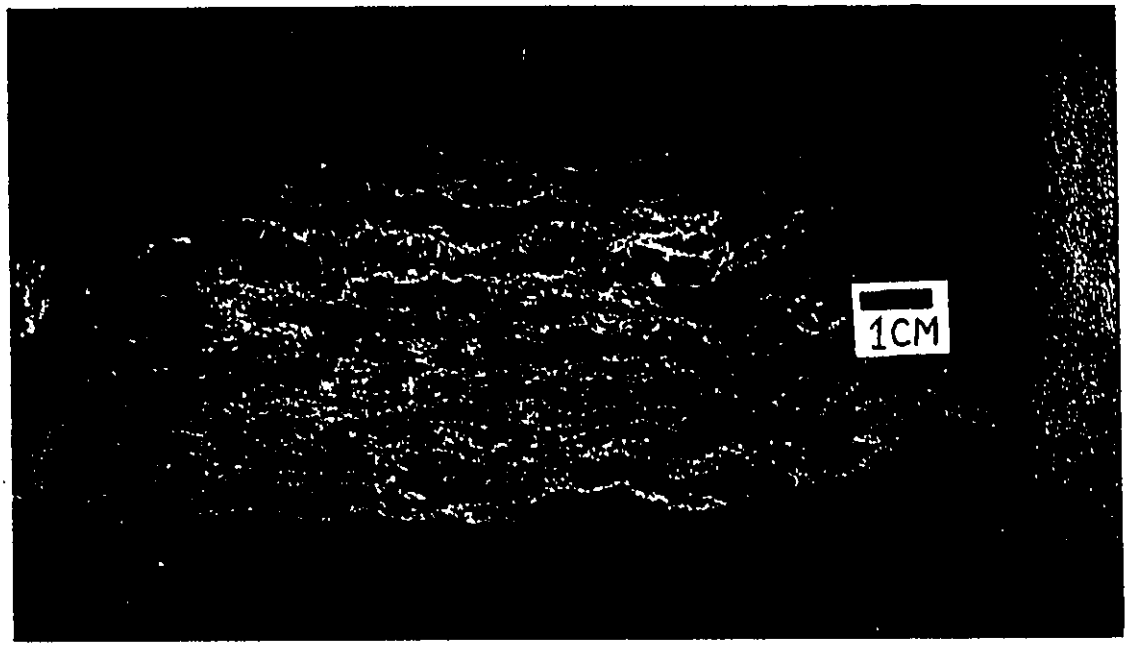

b)

Plate 3.5. MG_1 migmatite structures in metapelite, (a) Stromatic. K feldspar in leucosome stained orange. (b) Podiform. Leucosome concentrated in area between metapelite boudins.

cordierite-garnet-K feldspar-zone and orthopyroxene-zone metapelite consist of either assemblage A-2a or A-2b. Assemblage A-2c was observed at one location only (Station 134 in figure 3.2). Accessory zircon and ilmenite are common to all metapelite melanosome. MG_1 metapelite leucosome consists of the simple assemblage, microcline-quartz (A-2d). Biotite and plagioclase are minor phases which together make up less than 5% of the leucosome.

Melanosome is medium- to coarse-grained inequigranular; only biotite and rare garnet exhibit subhedral to euhedral boundaries. Clustering into cordierite-rich and biotite-rich lenses gives the metapelite melanosome a gneissic texture. The alignment of biotite is much better developed in biotite-rich zones than in cordierite-rich zones.

MG_1 metapelite leucosome is medium-grained, equigranular, and allotriomorphic granular. Minor myrmekite is common at K feldspar-quartz contacts. Minor biotite in the leucosome is generally aligned parallel to the foliation in the melanosome. Contacts between melanosome and leucosome are generally sharp but irregular.

Garnet is medium-grained (0.8-2.5mm) irregular in shape, and is generally free of inclusions, although some oriented inclusions of biotite, sillimanite, and green spinel are present. Garnet is commonly completely or partially surrounded by cordierite.

Biotite occurs as fine- to medium-grained oriented plates which define the foliation in the rock. Biotite grains are commonly concentrated in decussate clusters in which grain boundaries are rational. Decussate biotite grains are much coarser (ave 4 mm) than isolated grains in contact with other phases (ave 0.5 mm). Grain boundaries and cleavage planes of

a)

b)

Plate 3.6. Sillimanite inclusions in cordierite in metapelite melanosomes. (a) Abundant fine-grained sillimanite needles as swirled and convoluted inclusion trails in cordierite from quartz-absent melanosome. (b) Minor fine-grained sillimanite inclusions restricted to the cores of cordierite grains in quartz-bearing melanosome. Bar =.25 mm.

biotite grains are commonly coated with a thin film of opaque minerals. Very-fine-grained haloed zircon inclusions in biotite are common. Secondary muscovite locally cuts the earlier biotite foliation.

Cordierite occurs as irregular grains (0.2-3 mm), which commonly exhibit polysynthetic twinning. In quartz-free metapelite, cordierite invariably contains abundant swirled and convoluted inclusion trails of fine-grained oriented sillimanite (plate 3.6a). In quartz-bearing metapelite sillimanite is restricted to cores of cordierite grains (plate 3.6b). Fine-grained oriented sillimanite occurs interleaved with biotite and in contact with plagioclase and garnet only in quartz-free metapelite. Cordierite is variably altered to a very fine-grained mixture of chlorite and white mica. Fine-grained anhedral green spinel is a common accessory mineral associated with cordierite in quartz-free metapelite.

Plagioclase and quartz grains are fine- to medium-grained and equant. Plagioclase exhibits weak, normal zoning and polysynthetic twinning is common. Quartz invariably has undulose extinction.

The alkali-feldspar granite mineral assemblage of MG_1 metapelite leucosome is very different from that of any other granitoid rock in the study-area. Where MG_1 metapelite leucosome and MG_2 leucosome were observed together, MG_2 leucosome is always distinctly more plagioclase-rich.

3.2.6 Metagreywacke

Metagreywacke is the dominant lithologic unit in the study area, and displays the same mineral assemblage (A-5a) regardless of metamorphic grade. Accessory zircon and ilmenite are common to all samples. Minor K feldspar was observed in one sample, without garnet (sample 5-59). Metagreywacke is schistose and fine-grained, except for garnet which

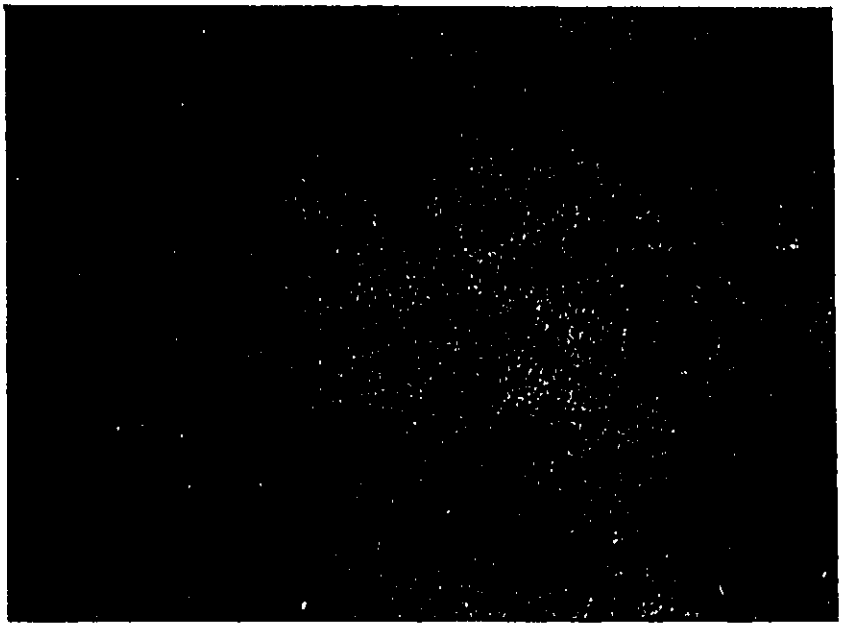

Plate 3.7. Typical example of fine-grained schistose texture in metagreywacke mesosome. Bar = 1 mm.

commonly forms rounded to irregular poikiloblasts and ranges from 0.5 to 3 mm in grain size (ave 1 mm) (see plate 3.7). Garnet greater than 1 mm in diameter is usually highly irregular in shape and poikiloblastic, whereas finer-grained garnet is commonly rounded. All other phases range from 0.3 to 0.6 mm in average grain-size. Quartz invariably shows undulose extinction. Plagioclase exhibits weak normal zoning. Plagioclase and quartz grains are anhedral and equant. The strong planar orientation of biotite plates defines the foliation in the rock.

The large proportion of MG_2 leucosome in the study-area makes the recognition of MG_1 leucosome difficult. In metapelite, MG_1 leucosome can be recognized by its isolated nature and radically different composition compared to the MG_2 leucosome. To a certain extent this criterion may be applied to help identify possible MG_1 migmatite in metagreywacke. Small isolated pods and lenses of medium-grained, white, massive granitoid leucosome were recognized locally in metagreywacke (plate 3.8). They are generally tonalite to granodiorite in composition and are free of garnet, in contrast to generally granitic MG_2 leucosome, which do contain garnet.

Melanosome, only rarely developed around MG_2 metagreywacke leucosome, consists of thin (<4mm) mantles of decussate biotite grains (see plate 3.8). Contacts between mesosome and leucosome are sharp to diffuse, and are irregular in shape. In some examples, small isolated pods of leucosome are rimmed with poikiloblastic cordierite, containing rounded inclusions of quartz.

A thin layer of biotite-orthopyroxene schist, interlayered with normal biotite-garnet metagreywacke, was observed at a single outcrop (Station 95 in figure 3.2). The mesoscopic appearance of this layer is similar to metagreywacke, although orthopyroxene is present and garnet is

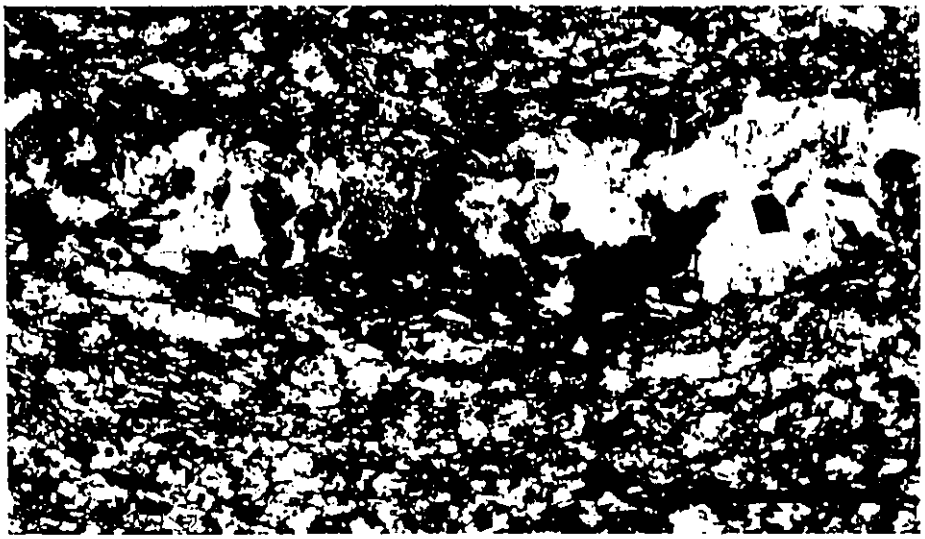

Plate 3.8. Sromatic MG_1 migmatite structures in metagreywacke. Coarser grained leucosome rimmed by biotite rich melanosome. Bar = 1 mm.

absent. The origin of biotite-orthopyroxene schist is enigmatic.

3.2.7 Mafic Hornblende Gneiss

Mafic hornblende gneiss, a minor but widespread rock unit, occurs within metasedimentary rock as either discontinuous layers, 1 to 8 m wide, where stromatic MG_2 migmatite structures predominate, or as angular blocks, 0.5 to 3 m wide, where schollen, schlieren, or nebulose MG_2 migmatite structures are predominant. The sub-orthopyroxene-zone metamorphic assemblage is A-6. The appearance of orthopyroxene in mafic hornblende gneiss defines the lower boundary of orthopyroxene-zone in the study-area. Several orthopyroxene-zone metamorphic assemblages were observed including; A-7, A-8, A-9, and A-10. Minor cummingtonite is present in many orthopyroxene-zone samples. Accessory magnetite and ilmenite are common to mafic gneiss. Mineralogical variations in orthopyroxene-zone mafic gneisses reflect compositional variations, rather than grade variations, as mafic layers containing different assemblages were found at single outcroppings.

The gneissosity results from thin (<1 cm) concordant leucocratic layers of plagioclase and quartz (plus orthopyroxene in orthopyroxene-zone gneiss). Mafic gneiss is medium-grained, granoblastic, and granular. A thin marginal zone depleted in hornblende and enriched in pyroxene and/or garnet is common in the margins of orthopyroxene-zone mafic gneiss in contact with metagreywacke (plate 3.9).

The origin of the mafic gneiss is not clear. Its mineralogy and field relationships suggests that it could have originated as mafic volcanic rock or as intrusive dykes or sills. Intercalated mafic volcanic rock and metagreywacke are reported further west in the lower grade portions of the ERSp (Breaks et al 1978).

Plate 3.9. Orthopyroxene enriched margin in Hbl-Opx mafic gneiss at the contact with metagreywacke.

Plate 3.10. Layered Grt-Cpx-Mgt gneiss.

3.2.8 Layered Garnet-Clindpyroxene-Magnetite Gneiss

Rare, thin (<1m wide) discontinuous and commonly tightly folded layers of layered garnet-clinopyroxene-magnetite gneiss (A-11) are believed to represent metamorphosed banded iron formation (Percival 1983a). The rock is comprised of alternating garnet-rich and clinopyroxene-magnetite-rich layers (plate 3.10).

3.2.9 Leucocratic Biotite-Garnet-K feldspar Gneiss (Map unit 4, minor in map unit 3)

Fine-grained leucocratic biotite-garnet-K feldspar gneiss displays assemblage A-12. Microcline is a ubiquitous but minor (<5%) phase. The gneissosity is defined by biotite-rich layers (plate 3.11). Biotite-garnet-K feldspar gneiss occurs as 1 to 10 m concordant layers within metagreywacke ranging from 1 to 3 m in thickness. It also rarely forms elongate, pluton-like bodies, up to several kilometers in width. Some concordant layers can commonly be traced for distances of several kilometres. Features of this biotite-garnet-K feldspar gneiss which distinguish it from metagreywacke include; leucocratic composition, layered structure, and the presence of K feldspar.

The origin of leucocratic biotite-garnet-K feldspar gneiss is enigmatic. The gneiss is finer-grained than any recognizable intrusive rock, with grain sizes comparable to those of the metagreywacke, and may therefore represent metamorphosed arkosic sedimentary rocks. Alternatively the gneiss may represent pre-metamorphic felsic volcanic or intrusive rock.

3.3 Intrusive Rocks

Recognizable intrusive rocks (exclusive of MG_2 leucosome) are all granitoid in composition, with the exception of Proterozoic gabbroic dykes

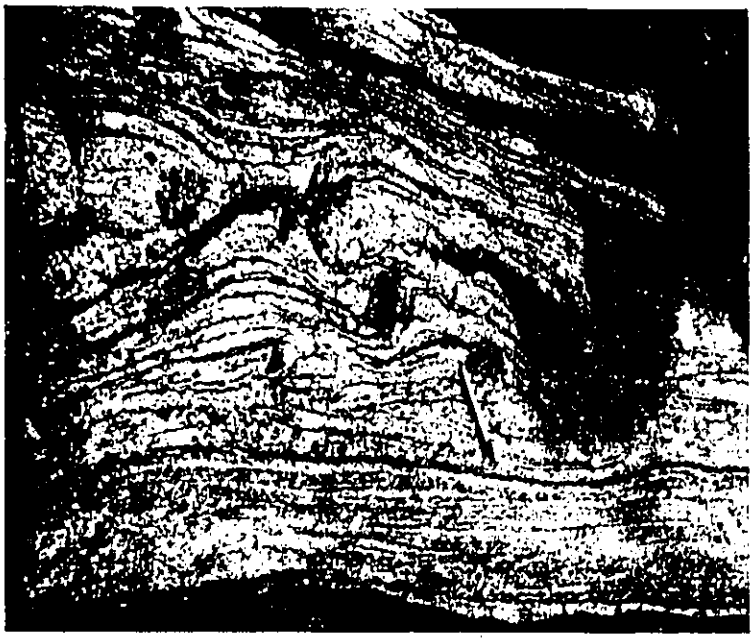

Plate 3.11. Leucocratic Bt-Grt-Kfs gneiss.

and sills. They may be broadly divided into: 1) pre-metamorphic, foliated, grey biotite-hornblende tonalite plutons, 2) post-metamorphic dykes including pink, biotite granite and white, biotite granite pegmatite, and 3) the Smoothrock Lake Pluton.

3.3.1 Grey Metatonalite (Map unit 5, figure 3.1)

Plutons of foliated to gneissic, grey biotite-hornblende tonalite are elongated parallel to the regional metamorphic fabric. Mineral foliations and lineations, defined by biotite and hornblende respectively, are parallel to those in surrounding metasedimentary rocks, and contacts are conformable. They range from several km to 10's of km in length.

Metatonalite consists of assemblage A-12. Accessory zircon and magnetite are present in all samples. Metatonalite is fine- to medium-grained and allotriomorphic granular. Most of the plutons are composed entirely of tonalite, although the largest of the plutons, the Whitewater Lake pluton, is dominantly tonalite, but also contains hornblendite, clinopyroxenite, hornblende-clinopyroxene gabbro, anorthosite, and hornblende-biotite syenite.

Orthopyroxene and clinopyroxene are generally restricted to mafic diorite xenoliths. However, metatonalite at Mojikit Lake contains orthopyroxene-garnet or orthopyroxene-clinopyroxene throughout the plutons. Discordant and isolated pods of leucocratic tonalitic pegmatite within metatonalite at Mojikit Lake, also contain coarse-grained orthopyroxene and clinopyroxene (plate 3.12).

Hornblende, although common in most metatonalite plutons, is absent from more leucocratic compositions and is minor in orthopyroxene-bearing metatonalite. Biotite is present as a stable phase in most metatonalite.

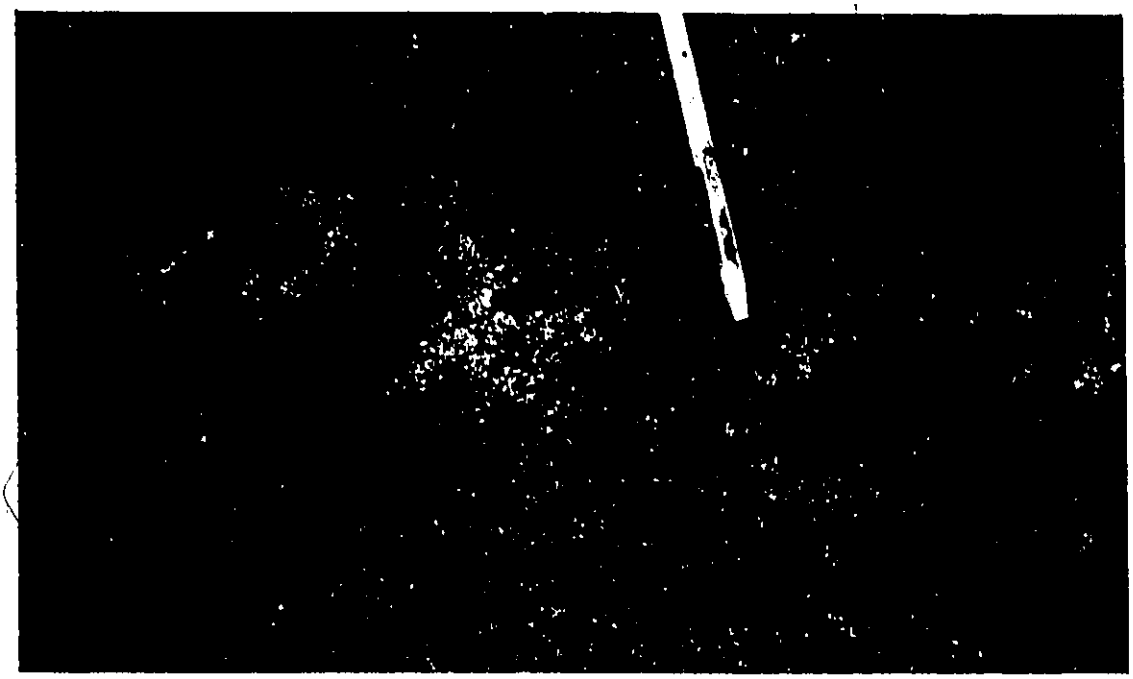

Plate 3.12. Isolated patches of Opx-Plag-Qtz pegmatite in Bt-Hbl-Opx-Cpx grey metatonalite.

Plate 3.13. Late white Bt pegmatite dike intrusive into MG_2 migmatite.

Secondary biotite grains, cross-cutting garnet and orthopyroxene, do however occur in orthopyroxene-garnet bearing metatonalite at Mojikit Lake. Orthopyroxene-bearing metatonalite contains a lower proportion of hornblende and a higher proportion of magnetite, than orthopyroxene-absent metatonalite. Garnet was observed only in one pluton (Station 1) as fine subhedral grains associated with magnetite and orthopyroxene. Minor, ragged grains of cummingtonite are common, and are usually associated with hornblende and orthopyroxene.

Metasedimentary xenoliths are locally present in metatonalite, indicating that intrusion post-dated deposition of the sedimentary rocks. The concordant orientation of the plutons and their foliated, allotriomorphic granular texture indicate that intrusion predated the main tectono-metamorphic event(s).

3.3.2 White, Biotite Granite Pegmatite Dykes

Discordant, white, biotite granite pegmatite dykes are intrusive into the metasedimentary migmatite, and clearly post-date migmatitic layering (plate 3.13). The dykes are up to several metres wide, and dyke margins are straight to irregular. White pegmatite displays assemblage A-13. Garnet and andalusite are common accessory minerals. Tourmaline was observed in one dyke. Grain size in typically extremely variable, with K feldspar grains up to 30cm long observed locally (station 170, figure 3.2).

Plagioclase is generally unzoned and untwinned. K feldspar is generally not perthitic. Garnet is medium- to coarse-grained, rounded, and is present as an accessory phase. Andalusite is coarse-grained, anhedral to tabular euhedral, and is present in about one third of the dykes examined.

a)

b)

Plate 3.14. Pink Bt granite in grey metatonalite. (a) Intrusive dikes. (b) Concordant layers.

3.3.3 Pink, Biotite Granite

Pink, biotite granite occurs as discordant dykes and concordant layers within grey metatonalite plutons (plate 3.14). It also consists of assemblage A-13, as does white, biotite pegmatite. Apatite is a common accessory phase. The granite is medium-grained, massive, and allotriomorphic irregular. The proportion of pink granite commonly increases towards the margins of grey metatonalite plutons. At one location, grey metatonalite contains concordant layers of foliated, pink, biotite granite, and is highly folded.

3.3.4 Smoothrock Lake Pluton (Map unit 6, figure 3.1)

The Smoothrock Lake Pluton is an irregularly shaped pluton of white, biotite-muscovite granite to pegmatite with assemblage A-14. It is intrusive into the Winnipeg River Subprovince immediately south of the ERSp at Smoothrock Lake. The pluton is massive suggesting post-tectonic intrusion.

4. GEOCHEMISTRY

4.1 Introduction

Whole rock and mineral chemical analyses were obtained for selected specimens from the main rock types in the study-area. Whole rock geochemistry and mineral chemistry focus mainly on rock types involved in the migmatitic evolution of the study-area, namely the metasedimentary and granitoid rocks. A discussion of analytical methods and uncertainties is given in appendix A.

4.2 Whole Rock Chemical Analysis

X-ray fluorescence analyses of major and selected minor elements were obtained for the following rock types (bracketed values indicate number of analyses); metagreywacke mesosome (11), metapelite paleosome/melanosome (6), MG_1 and MG_2 leucosomes (39), white biotite granitic pegmatite (4), pink biotite granite (2), grey metatonalite (4), and leucocratic biotite-garnet-K feldspar gneiss (2).

4.2.1 MG_2 Leucosome

In the MG_2 migmatite leucosome in this study and in granitoid rocks in general it is the proportions of feldspars and quartz which exhibit the greatest variation. The relative variations of K feldspar, plagioclase, and biotite proportions with the element concentrations can be examined from the whole rock chemical data. A modified CIPW normative calculation was performed on the major element analyses of the leucosomes, to estimate the volume proportions of minerals present. All Fe and Mg is assumed to be

present in biotite, in leucosomes (see appendix B: Metanorm calculation for procedures and justifications). Results are presented in table 4.1[1].

The normative anorthite content of plagioclase ($X_{An}/(X_{An}+X_{Ab})$) for MG_2 leucosome ranges from 16 to 26 mole %, with a mean 22 mole %. Normative K feldspar varies from 2.7-29.8 volume %. Normative mineral volume percentages were plotted on a quartz-alkali feldspar-plagioclase (QAP) diagram in figure 4.1, with subdivisions from Streckeisen (1976). MG_2 leucosomes range from monzogranite to tonalite, with most in in the monzogranite field.

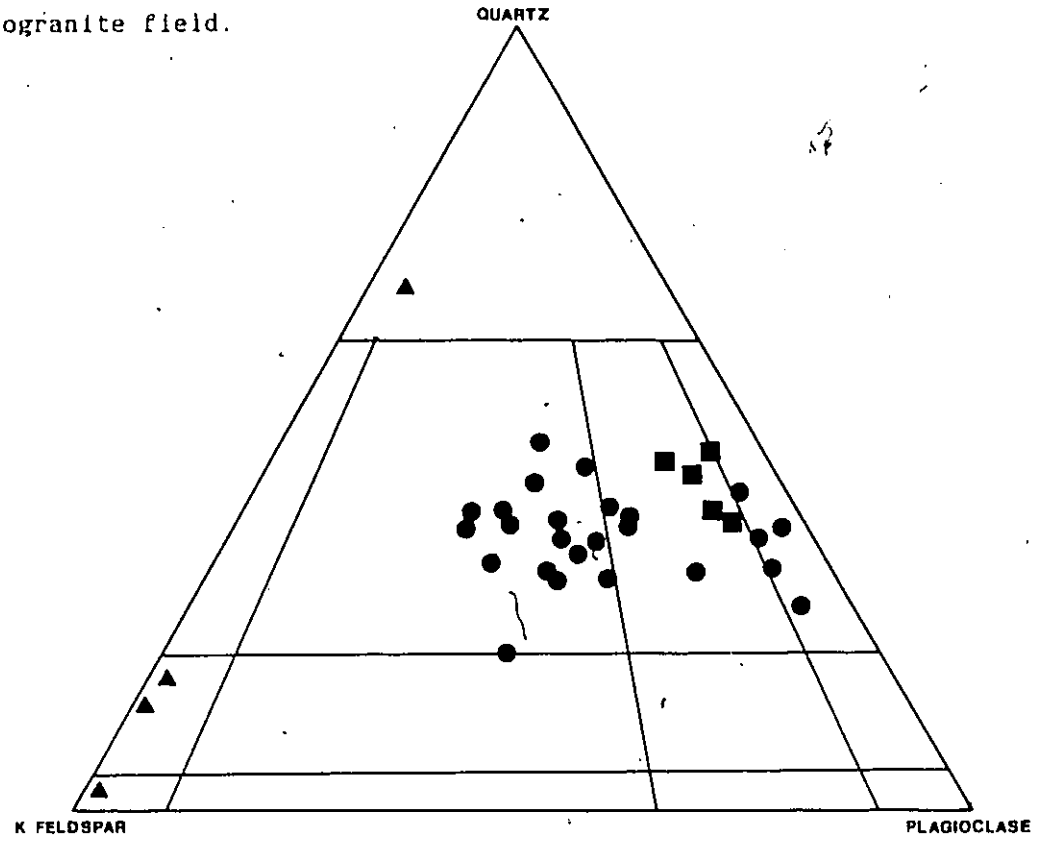

Figure 4.1. Normative QAP (Qtz-Kfs-Plag) diagram, with subdivisions from Streckeisen (1976). Circles: MG_2 leucosome, squares: MG_1 metagreywacke leucosome, triangles: MG_1 metapelite leucosome.

Plagioclase is the only leucosome phase which incorporates Ca into its structure (except for minor Ca in garnet) and therefore variations in

[1] Two samples 243cd and 159 contain cordierite as the main ferromagnesian phase and were excluded from the biotite norm calculations

Table 4.1. Chemical analyses and volume norms of MG$_2$ leucosome.

	116b	243b	42	95a	220a	102b	159	134	14a	28	220b	84c	153a	140
Wt. %														
SiO_2	68.4	70.3	74.4	75.5	72.2	71.5	72.3	74.6	74.5	67.9	74.3	73.1	70.1	71.9
TiO_2	0.28	0.23	0.10	0.08	0.23	0.31	0.12	0.05	0.01	0.42	0.07	0.05	0.13	0.27
Al_2O_3	16.8	14.9	13.3	13.2	14.3	14.4	15.5	14.7	14.6	15.0	13.9	15.5	15.3	15.5
FeO	1.51	2.35	1.21	0.50	2.10	1.94	0.87	0.51	0.87	4.11	0.56	0.86	3.65	1.51
MgO	0.82	0.87	0.41	0.34	1.05	1.16	0.50	0.26	0.23	1.84	0.47	0.37	1.50	1.03
MnO	0.01	0.06	0.02	0.01	0.03	0.01	0.01	0.02	0.00	0.05	0.01	0.02	0.06	0.02
CaO	1.52	1.13	1.02	1.07	1.37	1.45	1.41	1.01	1.04	1.36	1.78	1.82	1.57	1.70
Na_2O	4.06	3.17	2.91	2.95	2.99	2.75	3.93	4.21	4.03	2.78	3.42	3.92	3.38	3.86
K_2O	6.09	5.75	5.48	5.21	5.18	5.08	4.70	4.65	4.12	4.08	4.07	4.04	4.02	3.94
P_2O_5	0.11	0.08	0.02	0.08	0.04	0.07	0.09	0.06	0.00	0.07	0.02	0.06	0.02	0.06
Total	99.58	98.76	98.80	98.88	99.82	98.65	99.44	100.88	99.15	97.30	98.83	99.75	100.08	99.79
ppm Ba	1620	1070	840	1220	1320	1390	1120	1180	980	900	1030	950	810	1020
Cr	40	<10	30	<10	40	50	30	10	30	100	30	20	90	60
Zr	100	240	140	240	170	130	180	60	80	190	140	40	220	160
Sr	440	270	180	310	300	420	360	360	330	370	310	380	280	430
Rb	150	170	130	120	140	120	100	80	100	130	100	90	130	120
Y	<10	20	10	<10	20	<10	<10	<10	<10	10	<10	<10	10	10
Nb	<10	<10	<10	<10	<10	<10	<10	<10	<10	<10	<10	<10	<10	<10
Zn	60	50	50	50	50	50	30	20	30	80	30	30	70	50
Ni	20	<10	<10	<10	<10	20	<10	<10	<10	30	<10	<10	40	10
V	80	10	<10	<10	30	40	20	<10	<10	40	<10	<10	60	40
Volume Norm														
										*			*	
Pl	36	28	25	25	28	26	36	38	36	X	34	38	X	38
Kfs	38	34	36	35	30	29	30	31	28	X	27	26	X	22
Qtz	19	28	35	37	33	34	29	29	33	X	36	11	X	11
Bt	7	9	4	3	9	9	4	2	2	x	3	4	x	8
Grt	x	x	x	x	x	x	x	x	x	x	x	x	x	x
Cdt				x		x			t			x		
And												x		
Ilm	x	x	x	x	x	x	x	x	t	x	x	x	x	x
Co	0.3	0.6	0.3	0.5	0.5	0.9	0.9	0.0			0.3	0.9		0.9
Ap	0.2	0.2	0.0	0.2	0.1	0.1	0.2	0.1	0.0		0.0	0.1		0.1

* proportion of Grt or Cdt too large for normative calculation to a yield reasonable volume norm

x - present in minor amounts (Cdt, Ilm, and And <1%, all other phases <5%). X - > 5%

Table 4.1. continued

Wt %	97b	17a	242bg	87	127a	135ag	155	242cg	188b	113	128a	48	130a
SiO_2	63.9	73.7	74.6	73.3	72.1	73.3	69.4	66.9	70.3	69.4	74.3	73.4	71.2
TiO_2	0.52	0.01	0.21	0.01	0.01	0.08	0.21	0.08	0.23	0.08	0.14	0.04	0.12
Al_2O_3	16.9	14.6	13.0	15.6	16.1	14.9	16.6	18.4	16.7	17.6	15.1	16.3	15.7
FeO	5.68	0.54	1.60	0.39	0.87	0.59	1.52	3.13	1.91	0.78	0.68	0.34	1.18
MgO	2.33	0.42	0.90	0.10	0.44	0.42	0.80	3.16	1.06	0.35	0.50	0.21	0.70
MnO	0.07	0.02	0.03	0.02	0.02	0.01	0.02	0.04	0.03	0.02	0.01	0.01	0.03
CaO	2.12	1.57	1.14	1.30	2.27	2.07	2.77	1.10	2.74	3.03	2.80	2.85	3.40
Na_2O	3.62	2.98	2.70	4.81	3.84	4.10	4.50	2.54	4.73	5.68	4.54	5.76	4.77
K_2O	1.93	3.91	3.86	3.71	2.97	2.93	2.69	2.12	1.65	1.15	1.10	1.05	1.01
P_2O_5	0.04	0.13	0.06	0.05	0.07	0.12	0.04	0.03	0.02	0.00	0.02	0.00	0.15
Total	99.16	97.87	98.19	99.33	98.67	98.46	98.53	97.47	99.39	98.65	99.18	99.93	98.28
Ba	890	1060	1030	650	1080	1110	540	330	280	230	340	200	320
Cr	140	20	50	<10	20	30	30	20	30	10	30	20	20
Zr	240	60	150	60	60	30	100	100	90	90	180	30	50
Sr	330	320	280	360	370	400	390	170	350	480	570	410	400
Rb	150	90	80	80	50	50	90	80	50	20	20	10	20
Y	20	<10	<10	<10	<10	<10	<10	<10	<10	<10	<10	<10	<10
Nb	<10	<10	<10	<10	<10	<10	<10	<10	<10	<10	<10	<10	<10
Zn	120	90	60	110	40	20	50	70	50	60	50	30	50
Ni	70	<10	<10	<10	10	20	<10	<10	10	<10	<10	<10	10
V	90	<10	40	<10	<10	20	50	<10	30	<10	20	<10	<10
Volume Norm													
Pl	* X	29	27	44	41	42	51	* X	54	66	52	62	57
Kfs	X	26	22	25	18	19	14	x	4	6	5	6	3
Qtz	X	39	42	29	34	35	28	X	31	25	38	30	34
Bt	x	3	8	2	4	3	7	x	10	3	4	2	6
Grt	x	x	x	x	x	x	x	x	x	x	x	x	x
Cdt	x	x				x	x	X					
And													
Ilm	x	x	x	x	x	x	x	x	x	x	x	x	x
Co		1.9	1.2	0.8	1.5	0.8	0.6		1.6	0.1	0.7	0.3	0.4
Ap		0.3	0.1	0.1	0.1	0.2	0.1		0.0	0.0	0.0	0.0	0.3

* - proportion of Grt or Cdt to large for normative calculation to a yield reasonable volume norm.

x present in minor amounts (Cdt, Ilm, and And <1%, all other phases <5%). X = > 5%.

the concentration of Ca will reflect variations in plagioclase content or variations in the anorthite content of the plagioclase. Biotite and K feldspar both contain K as an essential structural constituent, however since K feldspar is volumetrically dominant over biotite, variations in K concentrations should reflect dominantly a change in K feldspar concentration in the rock. Biotite is the dominant Mg-bearing phase; minor garnet contains a much lower proportion of Mg than biotite. Variations in Mg concentration, therefore, should reflect dominantly changes in biotite concentration.

The elements fall into five groups. (1) Elements which do not show correlative variations in concentration with other elements (ie scattered). This group includes Al, Si, Mn, Y, Zr, Zn, Cr, and Nb. (2) Elements which show a positive near linear variation in concentration with Mg. This group includes Fe, Ti, Ni, and V. (3) Elements which show a negative near linear variation in concentration with K. This group includes Na and Ca. (4) Elements which show a positive near linear variation in concentration with K. This group includes Ba and Rb. (5) Elements which show a positive correlation with Ca. Sr is the only element in this group. The correlations present in groups 2,3, 4, and 5 are shown in figure 4.2 and the corresponding linear regression equation and correlation coefficients are given in table 4.2.

Elements which show a positive correlation with Mg, reflect their incorporation into biotite either as part of the biotite structure or in ilmenite inclusions which are ubiquitous in biotite.

The negative correlation of Ca and Na with K is simply a result of closure as plagioclase, K feldspar, and quartz together comprise >95 volume % of MG_2 leucosome. Quartz does not vary appreciably between different

Table 4.2. Linear regression equations and correlation coefficients (r^2) of inter-element correlations.

Oxides/Elements	Equation	r^2
FeO vs. MgO	FeO = 2.42(MgO) - 0.28	0.93
TiO_2 vs. MgO	TiO_2 = 0.25(MgO) - 0.02	0.77
Ni vs. MgO	Ni = 26.1(MgO) - 10.2	0.65
V vs. MgO	V = 38.2(MgO) - 6.7	0.61
Na_2O vs. K_2O	Na_2O = -0.37(K_2O) + 5.18	0.41
CaO vs. K_2O	CaO = -0.40(K_2O) + 3.31	0.66
Rb vs. K_2O	Rb = 25.9(K_2O) - 3.0	0.78
Ba vs. K_2O	Ba = 229.6(K_2O) + 37.83	0.79

Figure 4.2. Element correlations in MG_2 leucosome. (a) Element (weight percent element oxide or parts per million) plotted verses weight percent MgO. (b) Element versus weight percent K_2O. (c) ppm Sr versus weight percent CaO. Bars represent 95% confidence interval.

Figure 4.2a.

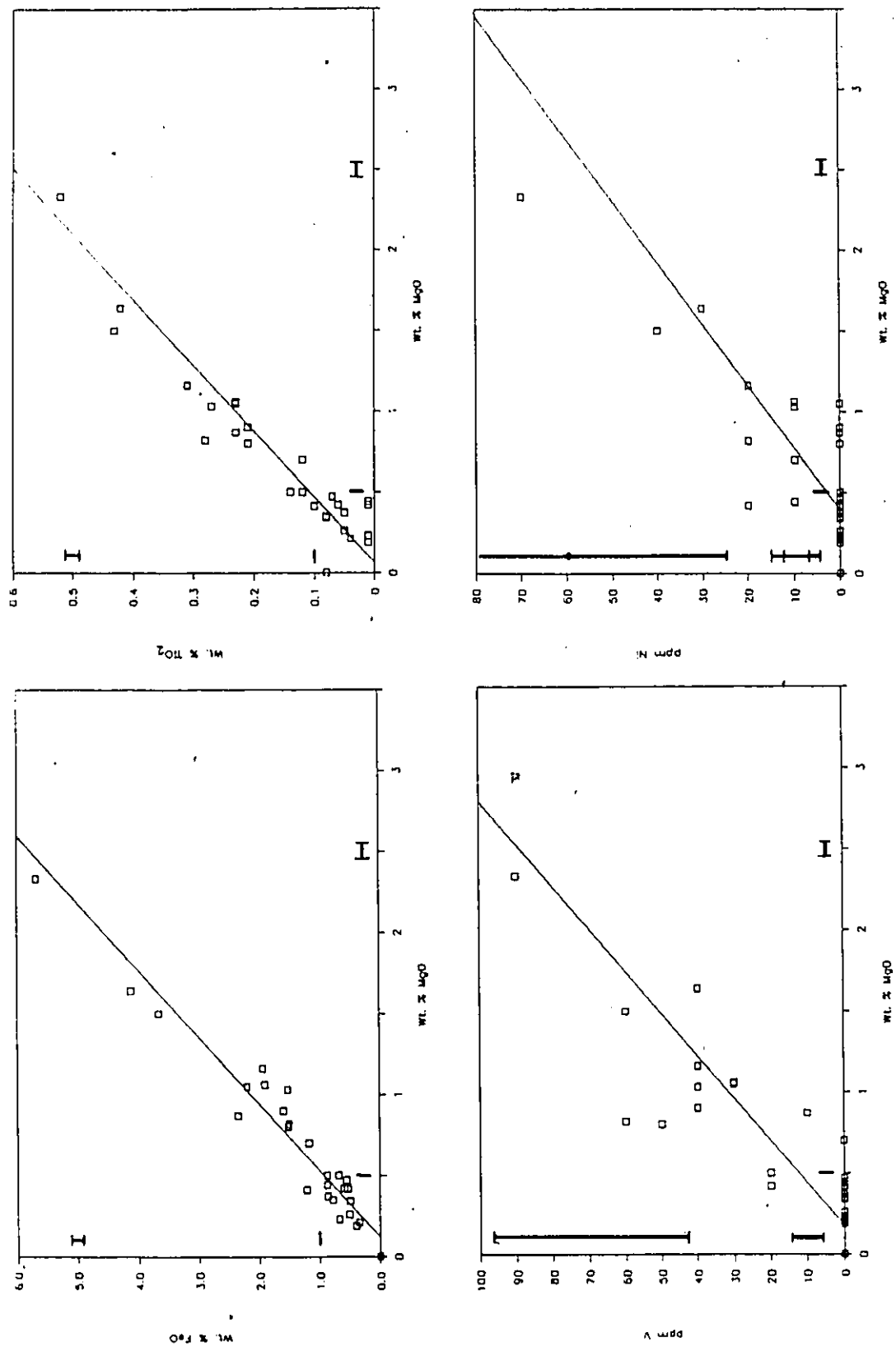

Figure 4.2b.

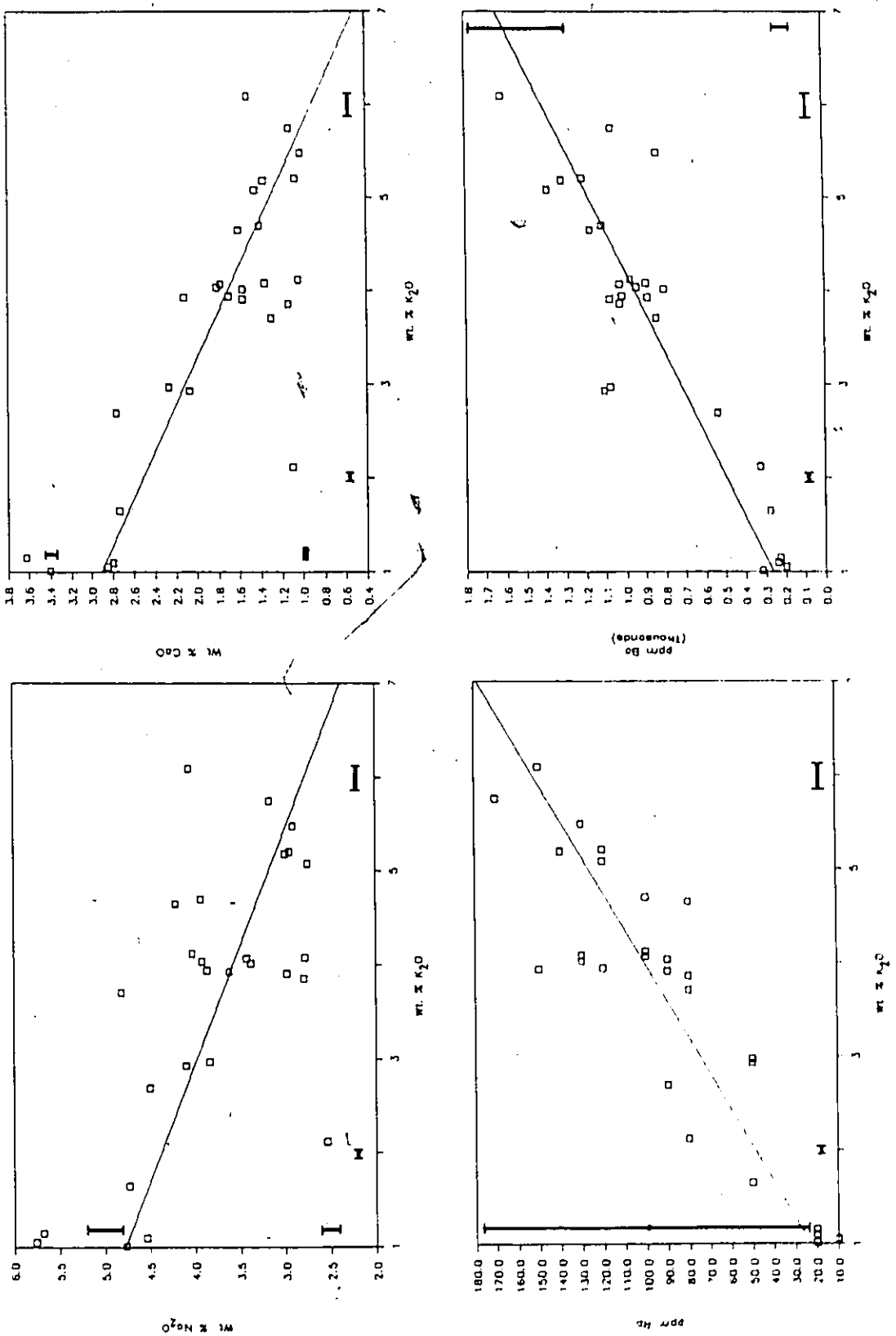

Figure 4.2c.

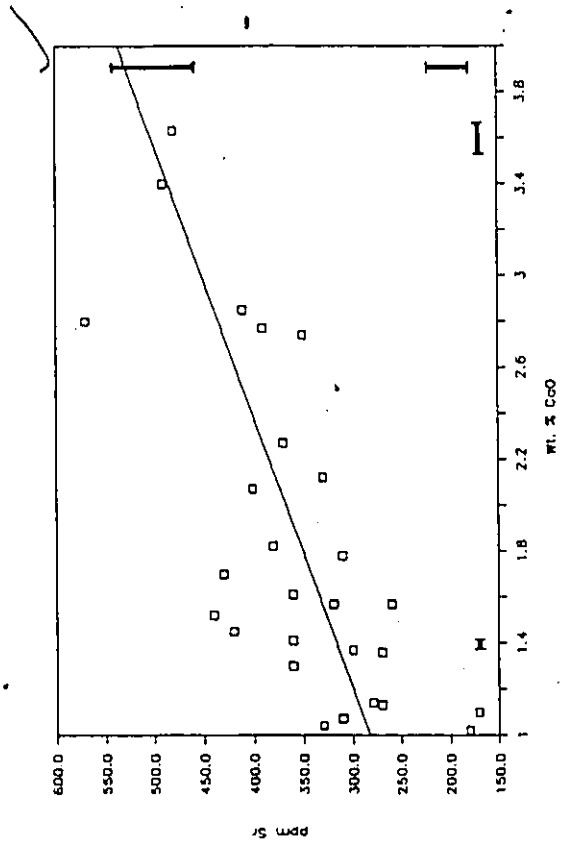
600.0
550.0
500.0
450.0
400.0
350.0
300.0
250.0
200.0
150.0
ppm Sr
1
1.4
1.8
2.2
2.6
3
3.4
3.8
Wt. % CaO

samples, therefore increases in K feldspar content (K) reflect decreases in plagioclase content (Na and Ca).

Ba, Rb, and Sr are important trace elements in that they are incorporated differently into the structures of plagioclase, K feldspar and biotite, which with quartz comprise greater than 99 volume % of most MG2 leucosome. Ba is preferentially and approximately equally incorporated into biotite and K feldspar. Rb is preferentially incorporated into biotite and to a lesser extent K feldspar. Sr is preferentially incorporated into plagioclase (Hanson 1978). This distribution of trace elements is confirmed by analysis of mineral separates (see section 4.3).

Ba and Rb show strong positive correlations with K, indicating that Ba and Rb are indeed concentrated in biotite and/or K feldspar. Ba and Rb do not, however, show any correlation with Mg indicating that inter-sample variations in Ba and Rb are not controlled by variations in biotite concentration, which is not surprising given that K feldspar is present in much higher proportions than biotite. Sr does not exhibit a correlative variation with K_2O, but does show a positive correlation with CaO (figure 4.2c).

4.2.2 Metapelite Paleosome and Melanosome

Five samples of cordierite-garnet-K feldspar-zone metapelite and one sample of muscovite-quartz-zone metapelite were analyzed (table 4.3). In the small area of muscovite-quartz- and sillimanite-K feldspar-zone metamorphic rocks, metapelite is scarce and normally restricted to thin discontinuous layers. Only one sample of metapelite suitable for whole rock analysis was found. The chemical composition of that sample is however very similar to the mean paleosome composition of metapelite from further west in the ERSp (Breaks et al. 1978) (table 4.3).

Table 4.3. Chemical Analyses and volume norms of metapelite and metagreywacke MG_1 melanosome, mesosome and paleosome.

	Metagreywacke Mesosome									Non MG_1 Migmatitic Metagreywacke		Nebulose[1] Migmatite	Metapelite Melanosome					Metapelite Paleosome	Average Paleosome (Brooks et al 76)	
Wt %	131a	135a1	243a1	61b	5-18	5 36	5-39	157a	132a	Mean	95% C I	3d	147	157e	64b	206b	240	5 14	Pelite	Wacke
SiO_2	64 8	65 3	69 4	64 7	68 3	67 8	69 0	67 1	67 5	67 9	1 3	65 6	42 1	47 1	50 4	47 9	45 6	57 7	58 4	65 6
TiO_2	0 13	0 63	0 52	0 58	0 48	0 60	0 55	0 53	0 57	0 55	0 08	0 61	1 47	1 08	0 95	1 07	1 19	0 73	0 84	0 88
Al_2O_3	14 9	15 7	14 5	16 8	15 4	15 7	13 7	15 5	15 3	15 1	1 4	16 4	31 0	26 0	24 0	23 2	28 6	19 1	19 4	15 8
FeO	6 26	5 97	4 55	5 38	4 84	5 08	5 20	5 83	5 62	5 31	0 71	5 37	13 2	12 1	10 5	11 3	9 3	7 9	8 19	5 00
MgO	3 28	2 86	2 07	2 74	1 89	2 55	2 57	2 53	2 45	2 40	0 50	2 60	6 32	6 09	5 14	5 92	4 74	4 37	3 75	2 63
MnO	0 06	0 10	0 08	0 10	0 07	0 07	0 09	0 10	0 07	0 08	0 02	0 08	0 15	0 16	0 15	0 13	0 08	0 12	0 09	0 08
CaO	2 24	2 26	2 56	3 13	2 13	2 18	2 45	2 62	2 08	2 29	0 41	2 37	0 85	1 69	2 09	1 60	1 42	1 15	1 30	2 10
Na_2O	3 27	3 67	3 65	3 58	4 12	3 26	3 01	3 41	3 64	3 49	0 74	3 85	0 77	2 27	3 16	2 64	2 60	2 27	2 06	3 20
K_2O	2 87	2 25	1 71	2 00	2 21	1 80	2 14	1 58	2 29	2 00	0 53	2 46	3 48	2 43	3 20	4 08	4 47	4 20	3 82	1 79
P_2O_5	0 13	0 07	0 10	0 11	0 11	0 07	0 12	0 15	0 08	0 11	0 06	0 02	0 01	0 05	0 09	0 04	0 02	0 13	0 12	0 12
Total	97 88	98 82	99 08	99 12	99 57	99 07	98 81	99 36	99 64	99 29		99 39	99 41	98 86	99 64	97 92	97 93	97 68	97 97	97 28
ppm Ba	310	350	470	590	290	360	510	420	320	380	150	370	600	540	670	620	540	540		210
Cr	200	180	150	160	120	170	200	170	170	170	50	160	350	320	280	320	280	220		180
Zr	170	150	160	100	130	160	190	140	150	150	40	180	230	180	150	180	230	130		100
Sr	250	280	420	300	290	290	290	270	290	290	20	180	110	160	290	190	180	170		
Rb	160	110	80	80	150	90	70	70	120	100	60	120	240	140	150	180	220	250		70
Y	20	20	20	20	20	20	20	20	20	20	0	20	20	30	30	30	30	30		
Nb	<10	<10	<10	<10	<10	<10	<10	<10	<10	<10		<10	20	10	10	10	10	<10		
Zn	120	90	100	70	80	110	100	90	180	110	70	110	230	220	160	170	220	130		80
Ni	70	40	40	50	50	80	70	80	40	60	30	40	110	150	130	140	80	50		
V	110	110	90	110	70	100	90	90	100	90	20	110	280	280	220	240	280	180		
Migmatite[2] Type	MG1	MG1	$MG_{1\,2}$	MG1	NON	NON	MG2	NON	MG2	NON & MG2		MG2	MG1	MG_{1-2}	MG_{1-2}	MG1	$MG_{1\,2}$	NON		
Volume Norm/Assemblage																				
Pl %	40	44	44	47	46	38	39	43	42	42	6	X	12	X	39	X	X	X		
Kfs	0.0	0.0	0.0	0 0	0 8	0.0	0.0	0.0	0.0	0.2	0 6	x		x	m					
Qtz	32	31	37	30	33	40	20	35	34	32	13	X		x	5	x		X		
Bt	27	21	18	19	19	17	2	15	21	15	13	X	38	X	32	X	X	X		
Grt	1	3	2	4	0	4	m	6	1	2	5	x	9	X	4	X	X			
Crd													26	X	20	X	X			
Sil													17	(x)	(m)	(x)	X	X		
Ms					m													x		
Ilm	m	m	m	m	m	m	m	m	m	m		x	m	x	m	x	x	x		
Co	0 3	0 5	0 3	0 6	0 9	1 8	0 1	0 8	0 9	0 8	1 0		0.0		0.0					
Ap	0 3	0.2	0.2	0 2	0 2	0 2	0.2	0.3	0.1	0 2	0 1		0.0		0.2					

[1] Leucosome - Melanosome composition [2] MG_1 - MG_1 migmatite MG_2 - MG_2 migmatite, $MG_{1\,2}$ - contains MG_1 and MG_2 leucosome, NON - non migmatitic

X and x represent modal percentages of > 5% and < 5% respectively for analyses not suitable for the normative calculation

m represents minor phases (<2%) present but not calculated in the volume norm

(Parentheses) enclose sillimanite which occurs only as isolated inclusions in cordierite

Cordierite-garnet-K feldspar-zone melanosome is chemically distinct from muscovite-quartz-zone metapelite and paleosome compositions for several elements (see table 4.3). Cordierite-garnet-K feldspar-zone melanosome is enriched in Mg, Fe, Al, Ti, Na, and Ca and is depleted in Si relative to paleosome compositions. These differences can be accounted for by the removal of an alkali feldspar granite fraction with the composition of MG_1 metapelite leucosome from sillimanite-K feldspar-zone metapelite (paleosome), as shown in figure 4.3. With the exception of melanosome sample no. 147 for the Na_2O + CaO vs SiO_2 diagram, paleosome element concentrations fall intermediate between leucosome and melanosome compositions, approximately on a straight line. Sample no. 147 contains very low concentration of Na_2O, and CaO which represents either original compositional differences or the removal of plagioclase. MG_1 leucosome observed in this sample contains no plagioclase.

4.2.3 MG_1 Metapelite Leucosome

Four metapelite samples showing evidence of MG_1 migmatization were selected for leucosome separation and analysis (table 4.4). All leucosome samples contain greater than 97 volume % quartz and K feldspar, with only minor plagioclase and biotite (<3 volume % total). The proportion of quartz and K feldspar exhibit considerable variation among the 4 samples, which is reflected in the whole rock analyses. Volume normative quartz and orthoclase were calculated for metapelite leucosomes (table 4.4). Three of the leucosomes have normative compositions which are similar to common granitoid compositions, while one sample (206B1) is anomalously rich in quartz, containing 64 volume % quartz, while the maximum quartz content for normal granitoid rocks is 45 volume % (Streckeisen 1976). Excluding sample 206B1, metapelite leucosome is syenogranite or quartz syenite.

Figure 4.3. Element variation diagrams showing compositional differences among leucosome and melanosome fractions of MG_1 metapelite migmatite and metapelite paleosome. a) TiO_2 vs. FeO + MgO b) Al_2O_3 vs. SiO_2 c) K_2O vs. SiO_2 d) Na_2O + CaO vs. SiO_2. X-symbols: melanosome, pluses: paleosome, diamonds: leucosome.

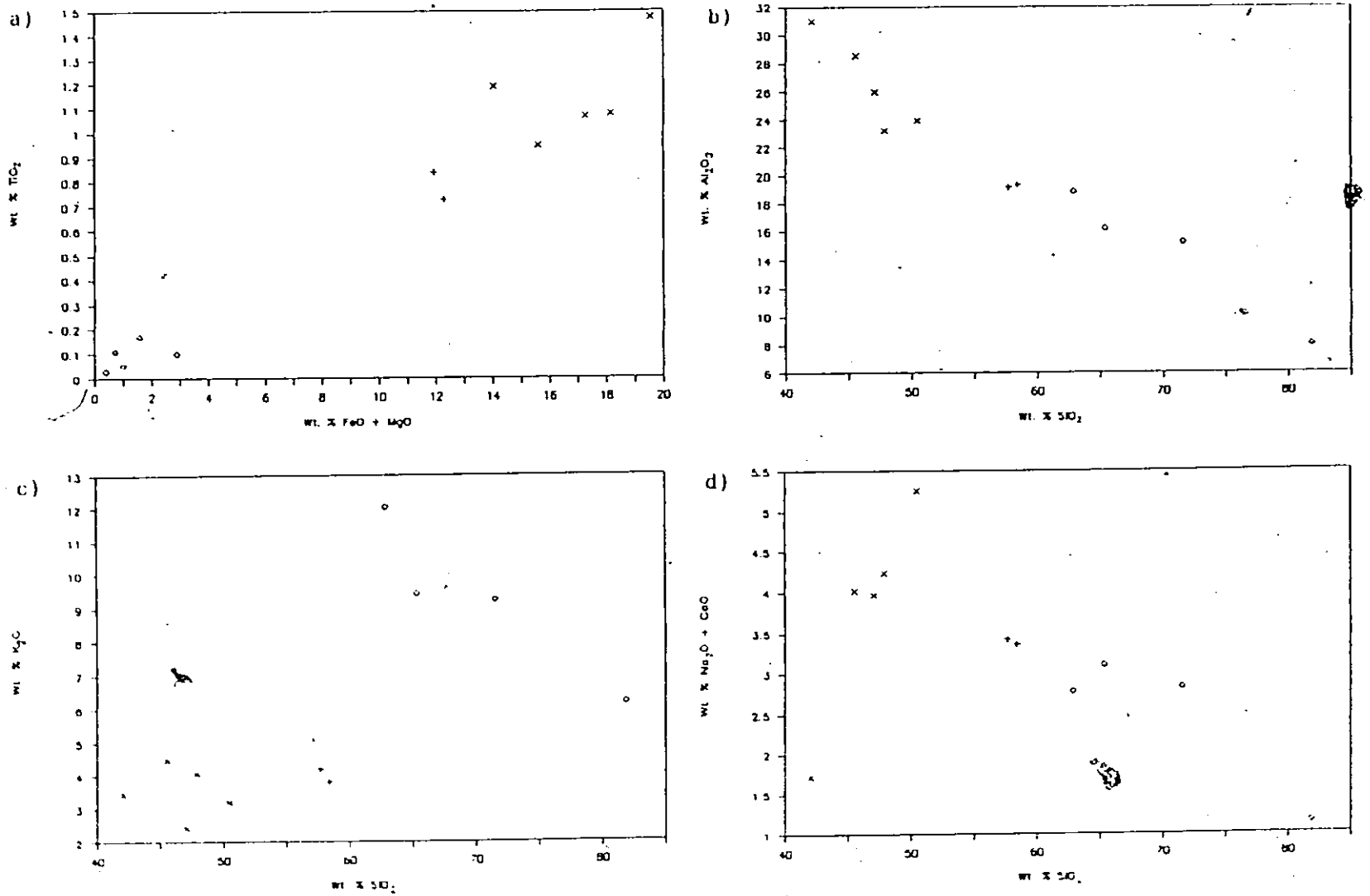
a)
Wt. % TiO_2
Wt. % FeO + MgO
b)
Wt. % Al_2O_3
Wt. % SiO_2
c)
Wt. % K_2O
Wt. % SiO_2
d)
Wt. % Na_2O + CaO
Wt. % SiO_2

Table.4.4. Chemical analyses and volume norms of MG_1 leucosome and white Bt pegmatite.

	Metapelite Leucosome				Metagreywacke Leucosome				
Wt. %	157EL	203L	206BL	240L	111CL	131AL	135AL	219EL	243BL
SiO_2	71.5	62.9	81.9	68.8	74.5	74.7	73.5	71.9	73.3
TiO_2	0.17	0.11	0.10	0.03	0.16	0.03	0.11	0.10	0.18
Al_2O_3	15.2	18.6	8.0	17.1	14.2	15.0	14.7	15.0	13.6
FeO	0.97	0.55	1.69	0.23	1.57	0.25	0.90	2.19	1.91
MgO	0.63	0.18	1.19	0.19	0.74	0.25	0.80	1.21	0.93
MnO	0.01	0.00	0.01	0.00	0.02	0.01	0.01	0.03	0.05
CaO	0.33	0.44	0.28	0.37	2.05	2.91	2.54	1.91	2.11
Na_2O	2.50	2.34	0.89	2.89	4.19	4.79	4.49	3.52	4.01
K_2O	9.24	12.04	3.20	9.94	1.91	1.28	1.73	2.44	1.64
P_2O_5	0.14	0.19	0.06	0.15	0.06	0.03	0.00	0.04	0.20
Total	100.74	97.27	97.27	99.62	99.35	99.25	98.63	98.34	98.00
ppm Ba	2580	4860	970	2840	450	400	410	520	670
Cr	40	30	40	20	40	20	20	30	60
Zr	60	70	20	90	30	40	70	70	80
Sr	400	790	170	460	320	390	370	310	410
Rb	180	160	60	180	50	30	30	50	50
Y	<10	<10	<10	10	10	<10	<10	10	10
Nb	<10	10	<10	<10	<10	<10	<10	<10	<10
Zn	30	40	50	20	60	30	40	40	40
Ni	<10	<10	40	<10	30	10	20	40	20
V	30	<10	10	20	<10	<10	20	10	30
Volume Norm									
Pl	2	1	4	1	45	54	50	39	44
Kfs	72	93	19	83	9	8	9	10	5
Qtz	21	3	67	13	39	36	36	39	41
Bt	5	2	9	1	7	2	5	10	9
Grt									
Cdt									
And									
Ilm					■	■	■	■	■
Co	0.3	1.0	1.4	0.8	0.8	0.9	0.4	1.7	0.9
Ap	0.3	0.4	0.1	0.3	0.1	0.1	0.0	0.1	0.4

■ - present in minor amounts (<1%), but not included in normative calculation.

Trace element concentrations also reflect the variable quartz/K feldspar ratio within leucosomes. This is particularly true for Ba, Rb, and Sr which would be incorporated almost totally within the K feldspar structure.

4.2.4 Metagreywacke Mesosome and MG_1 Leucosome

Variations in major and trace element content of migmatitic metagreywacke do not exceed the standard deviation of the non-migmatitic metagreywacke (see table 4.3). This indicates that the chemical composition of metagreywacke mesosome does not differ significantly from the composition of non migmatitic metagreywacke. The mean major element composition of metagreywacke in this study is very similar to metagreywacke compositions from further west in the ERSp (see table 4.3).

MG_1 metagreywacke leucosome ranges from tonalite to granodiorite (see table 4.4). Normative anorthite content in the plagioclase for the leucosomes ranges from 19 to 26 mole %. Normative orthoclase varies from 4.9 to 15.6 volume %.

4.2.5 White Pegmatite Dikes

Late white pegmatite dikes are syenogranite (table 4.5). Normative anorthite content in plagioclase ranges from 3 to 16 mole %. Normative orthoclase varies from 35.0 to 48.0 volume %.

4.2.6 Comparison of MG_1 and MG_2 Leucosome

Element oxides and trace elements which show a correlation in concentration for the MG_2 leucosomes were plotted in figure 4.4 for all leucosome types, and white pegmatite. Major element oxide and trace element concentration variations for MG_1 metagreywacke leucosome and white

Figure 4.4. Comparison of element correlations in MG_1 leucosome, white Bt pegmatite, and pink Bt leucogranite with MG_2 leucosome. (a) Element (weight percent element oxide or parts per million) element plotted verses weight percent MgO. (b) Element verses weight percent K_2O. (c) ppm Sr verses weight percent CaO. Diamonds: MG_1 metagreywacke leucosome, x-symbols: MG_1 metapelite leucosome, pluses: white Bt pegmatite, triangles: pink Bt leucogranite. Bars represent 95% confidence interval.

Figure 4.4a.

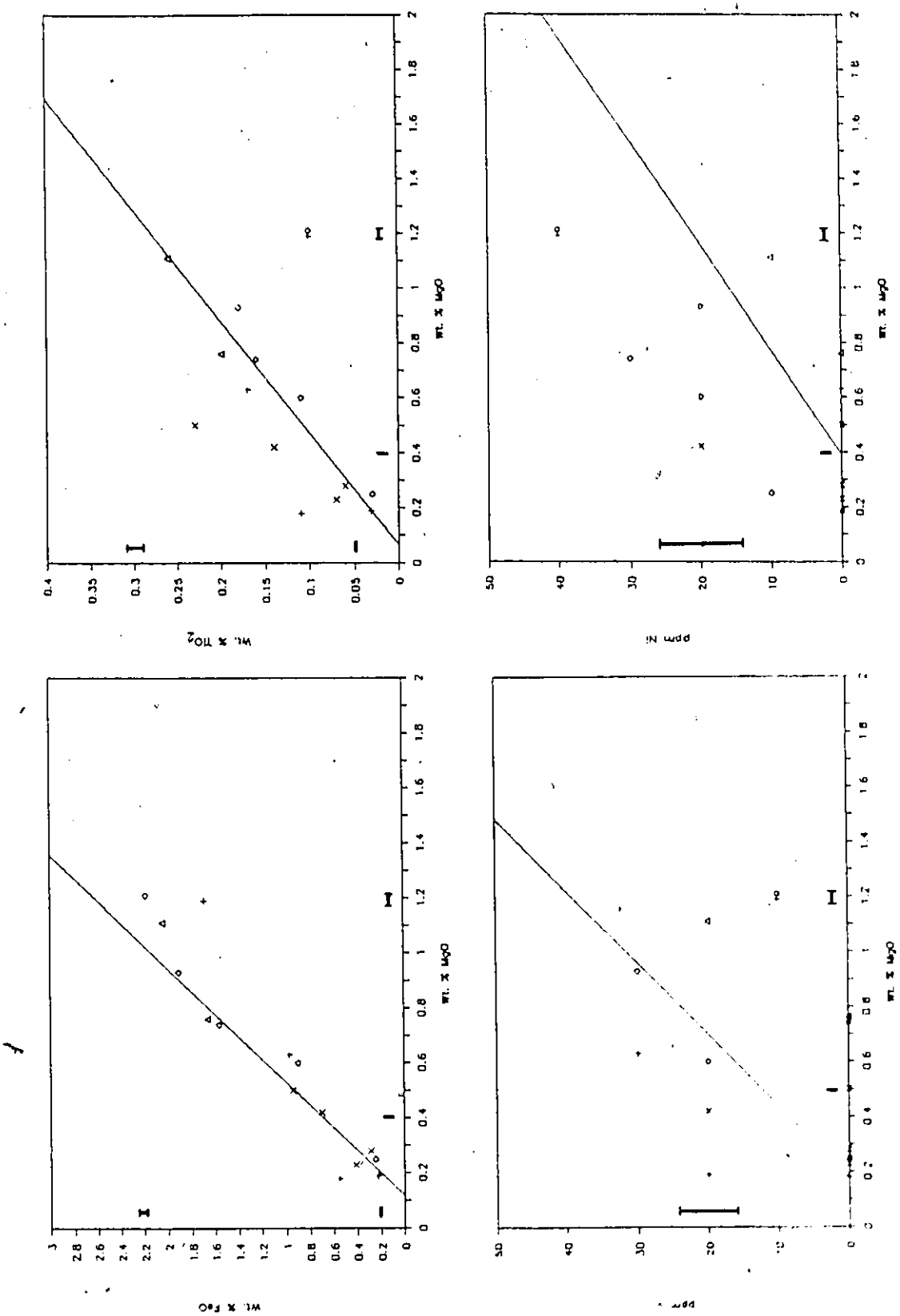

Figure 4.4b.

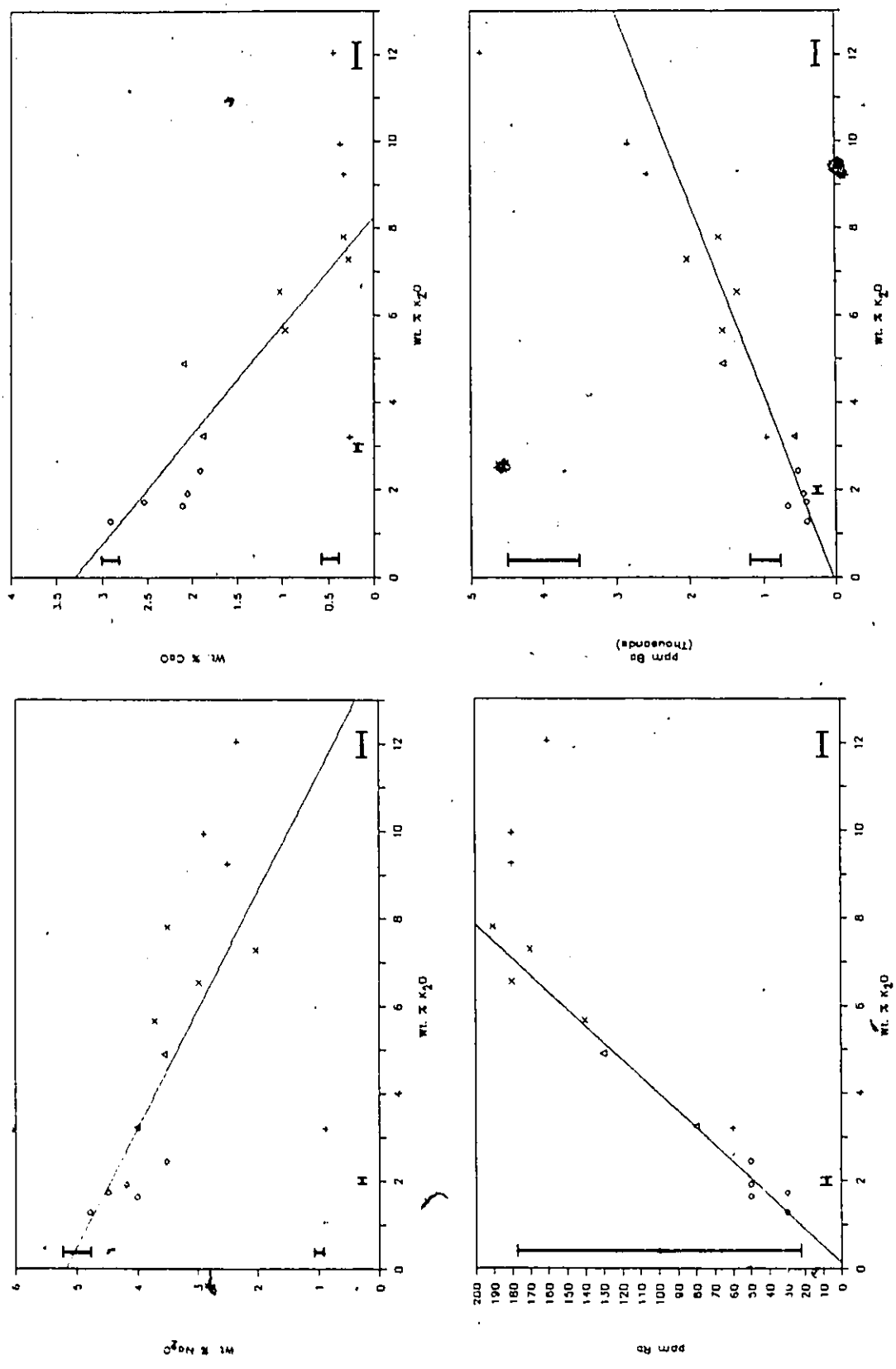
wt. % CaO
wt. % K_2O
ppm Ba (Thousands)
wt. % K_2O
wt. % Na_2O
wt. % K_2O
ppm Rb
wt. % K_2O

Figure 4.4c.

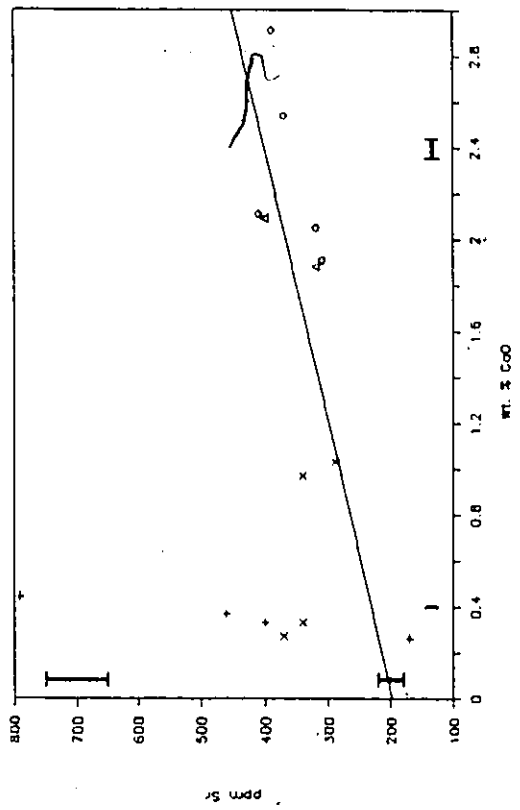

Table 4.5. Chemical analyses of other rock types.

	Grey Metatonalite				Pink Bt Granite		Leucocratic Bt-Grt-Kfs Gneiss		White Bt pegmatite			
Wt %	1A	94A	235A	45	196	94B	194H	196	170a	112b	194f	158
SiO_2	66.7	66.3	55.7	64.5	69.4	71.5	74.3	72.2	69.7	75.4	72.5	73.8
TiO_2	0.71	0.38	0.85	0.54	0.20	0.26	0.10	0.07	0.07	0.14	0.23	0.06
Al_2O_3	14.1	17.2	17.0	15.2	16.4	14.9	14.7	16.4	16.3	12.8	15.0	14.9
FeO	7.56	3.08	5.02	4.61	1.66	2.04	1.27	1.39	0.41	0.70	0.94	0.29
MgO	1.22	1.70	5.09	3.95	0.76	1.11	0.49	0.51	0.23	0.42	0.50	0.28
MnO	0.16	0.05	0.09	0.07	0.02	0.02	0.04	0.03	0.01	0.01	0.01	0.01
CaO	3.68	4.54	8.70	4.63	2.09	1.88	2.86	3.00	0.33	0.27	1.03	0.97
Na_2O	3.42	4.16	4.20	3.62	3.56	4.01	4.28	4.74	3.50	2.02	2.98	3.71
K_2O	1.00	1.27	2.31	1.66	4.90	3.23	1.63	1.31	7.80	7.28	6.54	5.66
P_2O_5	0.17	0.08	0.22	0.08	0.03	0.03	0.00	0.00	0.10	0.06	0.07	0.08
Total	98.80	98.76	98.93	98.66	99.07	98.06	99.38	99.67	98.41	99.11	99.77	99.81
ppm Ba	330	400	580	550	1560	580	700	210	1600	2040	1300	1560
Cr	10	50	220	200	<10	40	20	30	10	30	<10	10
Zr	240	110	120	140	100	230	60	40	30	30	500	120
Sr	180	530	830	410	400	320	280	320	340	370	290	340
Rb	80	40	90	70	130	80	20	30	100	170	180	140
Y	50	10	20	20	<10	<10	<10	20	<10	<10	20	<10
Nb	<10	<10	<10	<10	<10	<10	<10	<10	<10	<10	<10	<10
Zn	120	60	70	80	50	60	35	40	40	20	30	20
Ni	<10	20	100	80	<10	10	<10	<10	<10	20	<10	<10
V	30	40	140	110	<10	20	<10	<10	<10	20	<10	<10
Assemblage/Mode												
Pl	X	X	X	X	X	X	X	X	23	11	24	30
Kfs					X	X	x	x	54	49	43	39
Qtz	X	X	X	X	X	X	X	X	19	35	28	29
Bt	x	X	x	x	x	x	x	x	2	3	1	2
Grt	x						x	x		x		x
And												x
Hbl	x		X	X								
Opx	x		x									
Cpx			x									
Cum	x		x	x								
Ilm Mgt	x	x	x	x	x	x	x	x	x	x	x	x
Co									0.2	0.1	0.1	0.2
Ap	x	x	x	x					1.0	0.8	0.8	0.8

X and x represent modal percentages of > 5% and < 5% respectively.

pegmatite overlap with and follow the pattern of element concentration variations of the MG2 leucosomes, discussed in section 4.2.1. MG_1 metapelite leucosome compositions do not seem to follow the element concentration variation patterns of MG_2 for the element variations Na_2O and CaO vs. K_2O, and Rb vs. K_2O.

MG_1 metapelite leucosome and white pegmatite dikes are similar in that both are K feldspar-rich, and have low normative anorthite contents in comparison to MG_2 leucosome and MG_1 metagreywacke leucosome. They differ however, in that MG_1 metapelite leucosomes have higher proportions of K feldspar, and lower proportions of quartz.

4.3 Mineral Analyses

Energy dispersive electron microprobe analyses were obtained for minerals from selected specimens of metagreywacke mesosome and leucosome, metapelite melanosome, MG_2 leucosome, grey metatonalite, and garnet-orthopyroxene mafic hornblende gneiss. X-ray fluorescence analyses for major and selected trace elements were obtained for mineral separates from selected specimens of metagreywacke mesosome, metapelite melanosome and leucosome, and MG_2 leucosome.

4.3.1 Biotite

Analyses of biotite from metapelite, metagreywacke, MG_2 leucosome, and garnet-orthopyroxene grey metatonalite, are summarized in table 4.6. Biotite from all rocks analyzed do not differ significantly in chemical composition except for biotite in the garnet-orthopyroxene metatonalite which is significantly more Fe-rich. Biotites from metagreywacke, metapelite, and MG2 leucosome contain 44 and 55 mole % of the magnesium

Table 4.6 Average biotite analyses. a) Microprobe, b) Mineral Separates.

a)

	HQ_2 Leucosome								Bt-Ot-Opx-Hbl Metatonalite
	38		64C		163A		200		1A
wt %	Core	Edge	Core	Edge	Core	Edge	Core	Edge	
SiO_2	35.5	35.7	36.4	35.9	35.7	35.8	36.3	35.8	34.4
TiO_2	3.03	2.47	2.82	3.46	3.40	3.67	2.90	2.93	4.55
Al_2O_3	19.6	19.5	18.4	18.4	18.5	18.8	18.4	18.7	14.2
Cr_2O_3	0.07	0.06	0.00	0.00	0.07	0.06	0.09	0.06	0.00
FeO	19.2	18.8	14.7	18.1	17.9	17.8	19.3	19.0	28.1
MgO	8.8	9.6	13.8	12.8	10.8	10.8	10.9	10.7	5.8
X_2O	8.8	8.3	8.6	8.4	9.9	9.8	9.2	9.6	8.6
Total	95.52	95.70	95.42	95.98	95.93	96.77	96.15	96.93	95.67
No. of cations on the basis of 22 O									
Si	5.38	5.39	5.41	5.33	5.37	5.38	5.33	5.35	5.45
Ti	0.23	0.28	0.32	0.39	0.38	0.41	0.33	0.33	0.54
Al	3.50	3.47	3.22	3.22	3.28	3.27	3.28	3.29	2.66
Cr	0.01	0.06	2.00	0.00	0.01	0.01	0.01	0.01	0.00
Fe^{2+}	2.43	2.37	1.83	2.00	2.35	2.33	2.44	2.37	3.73
Mg	2.14	2.16	2.98	2.86	2.38	2.35	2.48	2.38	1.37
K	1.84	1.84	1.82	1.77	1.81	1.90	1.77	1.67	1.74
Total	15.64	15.55	17.68	15.58	15.58	15.63	15.60	15.61	15.61
Fe/(Fe+Mg)	0.53	0.52	0.38	0.41	0.49	0.49	0.50	0.50	0.73
2Al/(Fe+Mg)	1.53	1.53	1.34	1.33	1.43	1.43	1.33	1.38	1.04
No of Analyses	5	2	1	1	4	3	2	1	4

	Metapelite						Metagreywacke Mesosome				Nebulose Migmatite	
	64B		147		303		111C		157A		3D	
wt %	Core	Edge	Core	Edge	Core	Edge	Core	Edge	Core	Edge	Core	Edge
SiO_2	34.0	33.9	33.3	34.0	33.0	33.2	34.0	33.8	34.5	34.5	33.8	34.0
TiO_2	4.65	4.45	3.90	4.19	4.09	4.16	3.29	3.20	3.96	3.89	2.75	2.78
Al_2O_3	17.4	17.5	18.1	18.1	17.4	17.6	17.0	17.1	17.3	17.2	17.7	18.2
Cr_2O_3	0.16	0.18	0.14	0.17	0.09	0.14	0.13	0.11	0.14	0.13	0.11	0.11
FeO	18.4	18.2	19.3	18.5	20.7	18.7	18.2	18.2	18.0	18.0	17.4	17.4
MgO	11.3	11.4	10.2	10.0	9.4	9.9	11.6	11.5	13.5	13.6	12.6	12.8
X_2O	9.9	9.8	9.3	9.8	8.4	9.7	10.0	9.9	9.8	9.9	9.3	9.2
Total	96.76	95.50	96.22	96.84	96.14	96.36	96.17	95.82	96.09	96.18	95.76	96.45
No of cations on the basis of 22 O												
Si	5.38	5.38	5.32	5.38	5.31	5.33	5.42	5.42	5.40	5.41	5.38	5.35
Ti	0.52	0.50	0.44	0.47	0.47	0.47	0.37	0.36	0.44	0.43	0.31	0.31
Al	3.06	3.10	3.22	3.19	3.16	3.13	3.02	3.04	3.01	3.00	3.14	3.30
Cr	0.02	0.03	0.03	0.03	0.01	0.03	0.02	0.01	0.02	0.01	0.01	0.02
Fe^{2+}	2.06	2.04	2.44	2.31	2.66	2.50	2.30	2.31	1.46	1.50	2.18	2.16
Mg	2.61	2.64	2.29	2.23	2.14	2.22	2.60	2.58	2.98	2.99	2.62	2.63
K	1.69	1.69	1.79	1.84	1.66	1.88	1.92	1.90	1.65	1.67	1.78	1.74
Total	15.48	15.48	15.51	15.46	15.55	15.55	15.65	15.64	15.56	15.58	15.62	15.61
Fe/(Fe+Mg)	0.45	0.44	0.52	0.51	0.55	0.53	0.47	0.47	0.38	0.38	0.44	0.43
2Al/(Fe+Mg)	1.35	1.35	1.36	1.40	1.31	1.32	1.23	1.24	1.25	1.24	1.25	1.28
No of Analyses	8	7	3	3	4	3	6	6	6	6	4	4

Table 4.6b.

	Metagreywacke Mesosome		Metapelite Melanosome	MG_2 Leucosome		
wt. %	61B	157A	64B	102	188b	220A
SiO_2	36.5	40.1	37.3	36.2	36.5	35.9
TiO_2	3.25	3.34	4.04	3.09	2.64	3.07
Al_2O_3	17.9	17.9	19.1	20.4	20.0	18.6
FeO_T	17.4	14.2	16.5	17.3	18.2	18.6
MgO	12.4	11.7	11.2	10.4	10.3	11.1
CaO	0.25	0.47	0.09	0.18	0.59	0.44
Na_2O	0.18	0.45	0.14	0.05	0.18	0.11
K_2O	9.2	8.7	9.3	8.9	8.5	8.2
MnO	0.04	0.02	0.02	0.06	0.10	0.05
Total	97.10	96.88	97.63	96.49	97.01	96.11
ppm Ba	2040	1670	910	450	490	500
Cr	730	780	980	530	150	490
Zr	60	110	90	60	30	50
Sr	10	40	10	10	20	20
Rb	420	440	550	540	410	640
Y	20	20	30	20	20	30
Nb	40	40	50	50	50	90
Zn	320	400	460	410	360	430
Ni	210	150	210	190	90	140
V	580	510	880	460	360	420

end-member and have a high Al content indicating a siderophyllite composition. Zoning was not detected.

XRF analyses were obtained for selected biotite mineral separates from metagreywacke, metapelite, and MG_2 leucosome (table 4.6). Biotite from MG_2 leucosome have significantly lower concentrations of Ba, compared to biotite in metagreywacke and metapelite. The Ba concentrations in biotite separates are as follows: metagreywacke, 1670 and 2050 ppm (2 analyses); metapelite 910 ppm (1 analysis); MG_2 leucosome, 450-500 ppm (3 analyses). Otherwise the major and trace element concentrations in biotite from the different rock types do not differ systematically. The concentration of Ba, Rb, and Sr of biotite, K feldspar, and plagioclase among the various rock types is shown in figure 4.5.

4.3.2 Garnet

Microprobe analyses were obtained for garnet from metagreywacke, metapelite, MG_2 leucosome, garnet-orthopyroxene metatonalite, and garnet-orthopyroxene mafic hornblende gneiss (table 4.7). The are no distinguishable differences in major element chemistry of garnet from metapelite, metagreywacke, and MG_2 leucosome. Garnet from all 3 rock types is Fe-rich, with subordinate Mg, and minor Mn and Ca. Zoning is restricted to a thin zone at the edge of the grains (< 1/6 grain diameter), which is relatively enriched in Mg and Mn, and depleted in Fe.

Garnet from grey metatonalite and mafic hornblende gneiss is richer in Fe and Ca (and consequently depleted in Mg) than garnet in metagreywacke, metapelite, and MG_2 leucosome. Mn concentration is similar in garnet from all rock types.

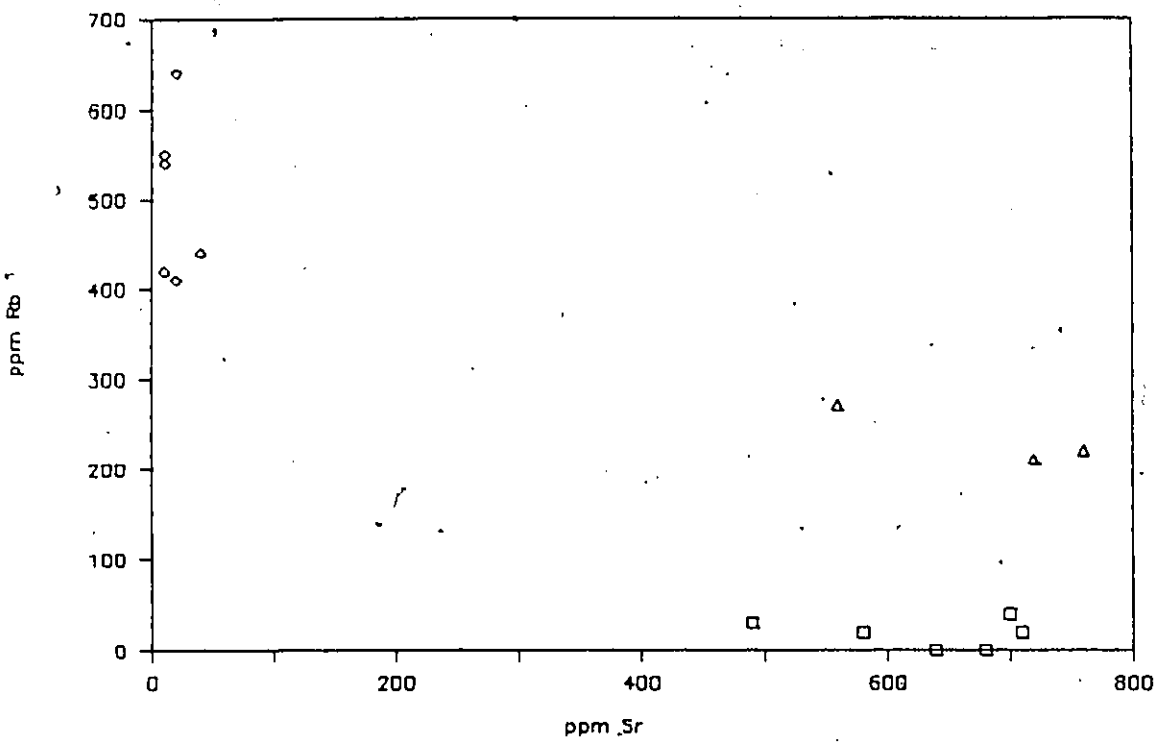

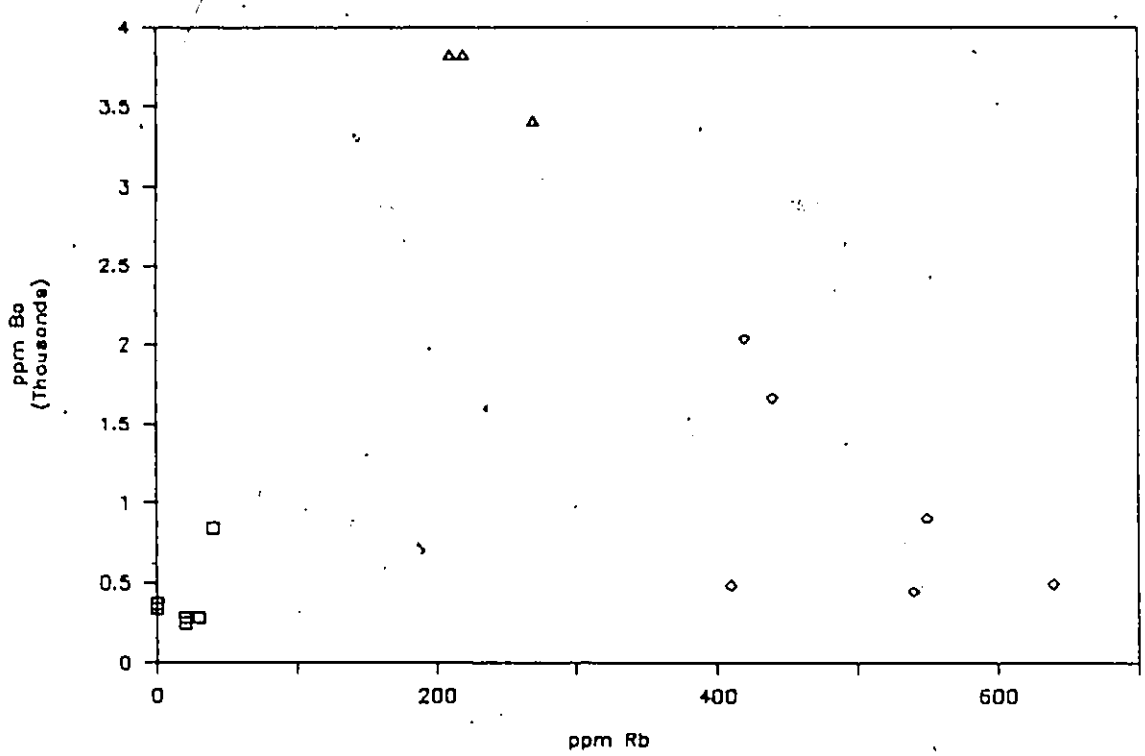

Figure 4.5. Trace element concentrations of mineral seperates. a) Rb vs. Sr b) Rb vs. Ba.

Table 4.7. Average garnet analyses (microprobe).

	Metagreywacke Mesosome						MG_2 Leucosome						MG_2 Leucosome					
	111C			157A			28*			64C			153A			200		
wt %	Core	Int	Edge	Core	Int	Edge	Core	Int.	Edge	Core	Int.	Edge	Core	Int	Edge	Core	Int.	Edge
SiO_2	37 7	37 9	37 4	37 7	38 1	37 7	37.9	37 5	37 3	37 8	37.8	37.5	37 8	37 6	37 5	37 8	37 9	37.9
Al_2O_3	21 7	21 7	21 3	21 7	21 8	21 5	21.6	21 4	21.5	22.5	22.5	22.2	21 6	21 5	21 5	21 8	21 7	21.7
Cr_2O_3	0 07	0 07	0 07	0 08	0 07	0 10	0 05	0 05	0 03	0 06	0.06	0 07	0 08	0.13	0 08	0 08	0 08	0.05
FeO	32 2	32 7	34 3	31 9	31 8	32 2	34 0	33 8	33 9	30 5	30.6	33 6	33 4	33 5	33 8	32 2	32 1	32 5
MnO	1 02	1 08	1 53	0 96	0 98	1 00	1 60	1 68	3 06	0 93	0 86	1 19	1 49	1 46	1 67	0 97	0 98	1 07
MgO	6 14	5 83	4 28	6 74	6 75	6 22	4 17	3 99	2 97	7 56	7 46	4 82	4.83	4 45	4 13	5 81	5 75	5 60
CaO	1 34	1 34	1 21	0 98	1 00	1 01	0 98	0 98	0 96	0 79	0 79	0 78	1 02	1 06	0 88	0 90	0 90	0 90
Total	100 17	100 65	100 05	100 05	100 43	99 67	100 27	99 43	99 63	100 12	99 97	100 20	99 99	99 88	99 40	99 54	99 34	99 74
No of cations on the basis of 24 O																		
Si	5 96	5 95	5 98	5 93	5 96	5 97	6 02	6 02	6 01	5 90	5 90	5 94	6.00	6 01	6 01	5 99	6 01	6 00
Al	4 04	4.02	4 01	4 03	4 02	4 00	4 04	4 05	4 08	4 13	4 14	4 15	4 05	4 04	4 07	4 06	4 05	4 05
Cr	0 01	0 01	0 01	0 01	0 01	0 01	0 01	0 01	.00	0 01	0.01	0 01	0 01	0 02	0 01	0 01	0 01	0 01
Fe^{2+}	4 24	4 30	4 58	4 19	4 16	4 26	4 52	4 54	4 57	3 98	3 99	4 45	4 44	4 47	4 49	4 28	4 26	4 30
Mn	0 14	0 14	0 21	0 13	0 13	0 13	0 22	0 23	0 42	0 12	0 11	0 16	0 20	0 20	0 23	0 13	0 13	0 14
Mg	1 44	1 39	1 02	1 58	1 58	1 47	0 99	0 95	0 71	1 76	1 74	1 14	1 16	1 06	0 98	1 37	1 36	1 32
Ca	0 23	0 23	0 21	0 17	0 17	0 17	0 17	0 17	0 17	0 13	0 13	0 13	0 17	0 18	0 15	0 15	0 15	0 15
Total	16 04	16 03	16 01	16 05	16 03	16 02	15 95	15 96	15 95	16 03	16 03	15 98	15 97	15 97	15 95	15 98	15 98	15 97
Alm	0 70	0 71	0 76	0 69	0 69	0 71	0 77	0 77	0 78	0 66	0 67	0 76	0 75	0 76	0 77	0 72	0 72	0 73
Pyr	0 24	0 23	0 17	0 26	0 26	0 24	0 17	0 16	0 12	0 29	0 29	0 19	0 19	0 18	0 17	0 23	0 23	0 22
Grss	0 04	0 04	0 03	0 03	0 03	0 03	0 03	0 03	0 03	0 02	0 02	0 02	0 03	0 03	0 03	0 03	0 03	0 03
Sps	0 02	0 02	0 03	0 02	0 02	0 02	0 04	0 04	0 07	0 02	0 02	0 03	0 03	0 03	0 04	0 02	0 02	0 02
No. of Analyses	3	3	4	5	5	6	3	3	3	2	3	3	3	1	3	3	2	3

Table 1.1 continued

	Metapelite Melanosome									Nebulose Migmatite			Hbl-Opx-Grt Mafic Gneiss					Bt Grt Opx Hbl Metatonalite	
	64b			147			203			3D			199A			139A		1A	
wt %	Core	Int	Edge	Core	Int	Edge	Core	Int	Edge	Core	Int	Edge	Core	Int	Edge	Core	Edge	Core	Edge
SiO_2	37 6	37.6	37 1	38 0	38 3	38 1	37.3	37.4	37 0	37 4	37 2	37.2	37 8	38.0	37 8	38 3	35 2	37 0	37.0
Al_2O_3	21 6	21 6	21 4	21 8	21 7	21.7	21 6	21 6	21 4	22 2	22 3	22.1	21.4	21 6	21 3	21 8	21 8	21 5	21 8
Cr_2O_3	0 09	0 09	0.09	0 04	0 09	0 07	0.08	0 07	0 03	0 08	0 06	0.11	0 05	0 03	0 05	0 06	0 06	0 07	0 09
FeO	33 4	33 4	35.0	33 0	33 5	33 5	33.0	32 8	34 6	33 2	33 3	33 9	30.3	30 5	30 7	31 6	31 7	31 8	31 5
MnO	0 88	0 88	1 05	0 99	0 98	1 03	2.51	2 41	2 69	1 62	1 62	1.75	1.82	1 78	1 84	1 21	1 22	2.74	2.72
MgO	6 04	6 04	4 75	5 18	4 89	4 89	4 90	5 15	3 78	4.73	4 75	3.92	3 16	3 06	2 73	4 26	4 05	1 98	1 46
CaO	0 86	0 86	0.87	0 99	0 93	1 05	1 00	0 99	1 07	1.03	1 08	1.06	5 22	5 14	5 38	3 38	3 34	4 66	5.08
Total	100 49	100 49	100 27	99 98	100 41	100 32	100 36	100 16	100 52	100.29	100 28	100.04	99 75	100.02	99 77	100 54	100 21	99 73	99 50
No of cations on the basis of 24 0																			
Si	5 94	5 94	5 93	6 01	6 03	6 02	5 93	5 94	5 92	5 92	5 90	5.94	6.02	6 03	6 03	6 02	6 04	5 95	6.20
Al	4 01	4 01	4 02	4 06	4 04	4.03	4 05	4 05	4 04	4.16	4 17	4.16	4 01	4 05	4 01	4 04	4 03	4 09	4.10
Cr	0 01	0 01	0 01	0 01	0 01	0 01	0 01	0 01	00	0.01	0 01	0.01	0.01	0 00	0 01	0 01	0 01	0.01	0 01
Fe^{2+}	4 41	4 41	4 68	4 36	4 42	4 43	4 39	4.33	4 63	4 40	4 41	4.52	4.03	4 05	4 10	4 16	4 18	4 29	4 24
Mn	0 12	0 12	0 14	0 13	0 13	0.14	0.34	0.32	0 37	0.22	0.22	0.24	0 25	0 24	0 25	0 16	0 16	0.37	0 37
Mg	1 42	1 42	1 13	1 22	1.15	1.15	1.20	1 22	0 90	1 12	1 12	0.93	0 75	0 72	0 65	1 00	0 95	0 47	0 45
Ca	0 15	0 15	0 15	0 17	0 16	0.18	0 17	0 17	0 18	0.17	0 18	0.18	0 89	0 86	0 92	0 57	0 57	0 80	0 87
Total	16 05	16 05	16.06	15 96	15 98	15 96	16.04	16 04	16 05	16 00	16.01	15.98	15 98	15 97	15 98	15 98	15.94	15 99	16.24
Alm	0 72	0 72	0 77	0.74	0 75	0 75	0.72	0 72	0 76	0 74	0 74	0.77	0 68	0 69	0 69	0 71	0 71	0.72	0.72
Pyr	0 23	0 23	0 19	0 21	0.20	0.20	0.19	0 20	0 15	0.19	0 19	0 16	0 13	0.12	0 11	0 17	0 16	0.08	0 08
Gros	0 02	0 02	0 02	0 03	0 03	0.03	0.03	0 03	0.03	0 03	0 03	0.03	0 15	0.15	0 16	0 10	0 10	0.14	0 15
Spes	0 02	0 02	0 02	0 02	0 02	0 02	0 06	0 05	0 06	0 04	0 04	0.04	0 04	0.04	0 04	0 03	0 03	0 06	0 06
No of Analyses	3	3	8	3	3	3	2	1	2	4	2	3	3	2	1	4	4	3	4

Table 4.8. Average cordierite analyses (microprobe).

	Metapelite Melanosome					MG_2 Leucosome	
	64B		147		203	200	
wt. %	Core	Edge	Core	Edge	Edge	Core	Edge
SiO_2	47.1	47.3	46.6	47.2	46.4	46.9	47.5
TiO_2	0.06	0.06	0.08	0.07	0.05	0.05	0.04
Al_2O_3	33.9	34.1	33.8	34.0	33.6	33.9	34.1
Cr_2O_3	0.04	0.03	0.07	0.04	0.05	0.03	0.02
FeO	7.39	7.01	7.89	7.40	7.31	7.87	7.32
MnO	0.09	0.08	0.08	0.09	0.18	0.09	0.11
MgO	9.30	9.70	8.74	8.97	9.19	9.07	9.12
CaO	0.00	0.02	0.02	0.01	0.03	0.02	0.01
Na_2O	0.03	0.14	0.13	0.10	1.05	0.12	0.19
K_2O	0.04	0.06	0.05	0.05	0.07	0.04	0.24
Total	97.95	98.48	97.51	97.92	97.90	98.03	98.65
No. of cations on the basis of 24 O							
Si	4.86	4.85	4.85	4.87	4.82	4.85	4.87
Ti	0.00	0.00	0.01	0.01	0.00	0.00	0.00
Al	4.12	4.12	4.15	4.14	4.09	4.13	4.13
Cr	0.00	0.00	0.01	0.00	0.00	0.00	0.00
Fe^{2+}	0.64	0.60	0.69	0.64	0.63	0.68	0.63
Mn	0.01	0.01	0.01	0.01	0.02	0.01	0.01
Mg	1.43	1.48	1.35	1.38	1.42	1.40	1.39
Ca	0.00	0.00	0.00	0.00	0.00	0.00	0.00
Na	0.01	0.03	0.03	0.02	0.21	0.02	0.04
K	0.01	0.01	0.01	0.01	0.01	0.00	0.03
Total	11.08	11.10	11.09	11.07	11.21	11.10	11.10
Fe/(Fe+Mg)	0.31	0.29	0.34	0.32	0.31	0.33	0.31
No. of Analyses	3	3	3	4	2	4	3

4.3.3 Cordierite

Cordierite occurs in cordierite-garnet-K feldspar-zone metapelite, in MG_2 leucosome, and rarely in thin lenses with quartz in metagreywacke. Microprobe analyses were obtained for cordierite in metapelite melanosome and MG_2 leucosome (table 4.8). Cordierite from metapelite and MG_2 leucosome is similar in composition. The average Fe/(Fe+Mg) ratio of cordierite is about 0.3. Cordierite is weakly zoned with thin rims enriched in Mg, and depleted in Fe.

4.3.4 Aluminosilicate Minerals

Sillimanite, the main aluminosilicate mineral, is restricted primarily to metapelite, but is also found rarely as inclusions in MG_2 leucosome garnet. Andalusite is present in late white pegmatite dikes, and was observed in one sample of MG_2 leucosome.

4.3.5 Feldspars

Plagioclase is present in all rock types, except MG_1 metapelite leucosome and metamorphosed banded iron formation. Microprobe analyses of plagioclase, and XRF analyses of plagioclase separates are summarized in table 4.9. Differences in anorthite content among the various rock types have been summarized previously. A plagioclase separate from metapelite melanosome contains an anomalously high Ba concentration (640 ppm), which is due to the presence of K feldspar in the separate.

K feldspar is present in MG_1 metapelite leucosome, MG_2 leucosome, and leucocratic biotite-garnet-K feldspar gneiss. Microprobe analyses of K feldspar in MG_2 leucosome, and XRF analyses of K feldspar separates from MG_2 leucosome and MG_1 metapelite leucosome are listed in table 4.10

Table 4.9. Average plagioclase analyses. a) microprobe. b) Mineral Separates.

a)

	Metapelite						Metagreywacke Mesosome						Nebulose Migmatite	
	64B		147		203		111C		157A		30	
Wt. %	Core	Edge	Core	Edge	Core	Edge	Core	Edge	Core	Edge	Core	Edge
SiO_2	62.0	61.3	59.9	59.1	59.9	59.0	60.8	60.9	61.2	60.9	61.3	60.6
Al_2O_3	24.0	24.0	25.2	26.3	25.8	26.0	24.6	23.9	24.8	24.6	24.4	24.8
FeO	0.08	0.23	0.00	0.13	0.41	0.20	0.10	0.17	0.08	0.10	0.02	0.24
CaO	5.07	5.27	6.51	7.66	8.90	7.13	5.88	5.18	6.05	5.97	5.21	5.55
Na_2O	8.39	8.23	7.76	6.86	7.42	7.45	8.10	8.31	8.07	7.94	8.72	8.52
K_2O	0.32	0.26	0.19	0.17	0.19	0.20	0.31	0.33	0.31	0.29	0.26	0.22
Total	99.89	99.34	99.52	100.21	100.61	99.98	99.75	98.77	100.48	99.83	99.85	99.93
No of cations on the basis of 32 O												
Si	11.01	10.96	10.72	10.52	10.64	10.55	10.84	10.96	10.84	10.85	10.90	10.80
Al	5.03	5.07	5.30	5.53	5.40	5.47	5.17	5.07	5.17	5.18	5.12	5.23
Ca	0.97	1.01	1.25	1.46	1.31	1.38	1.12	1.00	1.15	1.14	0.99	1.06
Na	2.89	2.85	2.69	1.87	2.55	2.58	2.80	2.80	2.77	2.74	3.01	2.95
K	0.07	0.06	0.04	0.04	0.04	0.04	0.07	0.07	0.07	0.07	0.06	0.05
Total	19.97	19.95	19.99	19.41	19.95	20.01	20.01	19.99	20.00	19.98	20.08	20.08
An	0.25	0.26	0.31	0.43	0.34	0.34	0.28	0.25	0.29	0.29	0.24	0.26
Ab	0.73	0.73	0.68	0.55	0.65	0.65	0.70	0.73	0.69	0.69	0.74	0.73
Or	0.02	0.01	0.01	0.01	0.01	0.01	0.02	0.02	0.02	0.02	0.01	0.01
No of Analyses	5	3	1	2	2	2	2	2	2	2	2	3

Table 4.9a. Continued

	MG_2 Leucosome					Bt-Gt-Opx-Hbl Metatonalite		Gt-Opx-Hbl Mafic Gneiss					
	28		64C		153A	200		1A		139B		199A	
wt %	Core	Edge	Core	Edge	Core	Core	Edge	Core	Edge	Core	Edge	Core	Edge
SiO_2	61.4	61.8	61.7	62.2	61.2	62.1	62.1	59.1	58.4	49.8	50.1	47.0	46.1
Al_2O_3	23.9	24.1	23.8	24.1	24.5	24.2	24.1	26.3	26.1	32.1	32.3	34.8	34.7
FeO	0.21	5.16	0.04	0.17	0.04	0.01	0.04	0.08	0.22	0.05	0.15	0.23	0.40
CaO	5.06	8.34	4.66	4.74	5.70	5.10	5.15	7.18	7.39	14.68	14.72	17.54	17.71
Na_2O	8.42	0.27	8.90	9.03	8.18	8.39	8.56	7.19	7.34	2.94	2.95	1.32	1.31
K_2O	0.28	0.00	0.31	0.25	0.27	0.28	0.23	0.23	0.22	0.12	0.12	0.12	0.11
Total	99.17	99.68	99.49	100.54	99.88	100.02	100.14	100.08	99.73	99.67	100.26	100.80	100.34
No. of cations on the basis of 32 O													
Si	10.99	10.98	11.01	11.00	10.88	10.99	10.99	10.51	10.49	9.11	9.11	8.58	8.48
Al	5.04	5.05	5.01	5.02	5.13	5.04	5.03	5.51	5.53	6.91	6.92	7.44	7.53
Ca	0.97	0.98	0.89	0.90	1.09	0.97	0.97	1.37	1.42	2.86	2.87	3.43	3.50
Na	2.93	2.87	3.08	3.09	2.82	2.88	2.94	2.64	2.55	1.04	1.04	0.47	0.47
K	0.07	0.08	0.07	0.06	0.06	0.06	0.05	0.05	0.05	0.03	0.03	0.03	0.03
Total	19.99	19.95	20.06	20.07	19.99	19.98	19.99	20.08	20.05	19.96	19.96	19.95	20.01
An	0.24	0.25	0.22	0.22	0.27	0.25	0.25	0.34	0.35	0.73	0.73	0.87	0.88
Ab	0.74	0.73	0.76	0.76	0.71	0.74	0.74	0.65	0.63	0.27	0.26	0.12	0.12
Or	0.02	0.02	0.02	0.01	0.02	0.02	0.01	0.01	0.01	0.01	0.01	0.01	0.01
No. of Analyses	1	1	3	3	1	2	2	3	4	4	4	2	3

Table 4.9b.

	Metagreywacke Mesosome		Metapelite Melanosome	MG_2 Leucosome		
wt. %	61B	157A	64B	102A	188b	220A
SiO_2	60.4	59.9	61.8	60.7	61.3	61.2
TiO_2	0.03	0.06	0.02	0.05	0.02	0.02
Al_2O_3	24.5	25.0	23.5	24.7	24.3	24.2
FeO_T	0.24	0.34	0.13	0.47	0.20	0.45
MgO	0.40	0.38	0.21	0.57	0.33	0.42
CaO	6.00	6.10	4.56	4.26	4.69	4.49
Na_2O	7.67	7.74	7.44	8.10	8.24	8.33
K_2O	0.78	0.47	2.29	1.17	0.87	0.83
MnO	0.00	0.00	0.02	0.00	0.02	0.00
Total	100	100	100	100	100	100
ppm Ba	370	340	840	280	250	280
Cr	30	50	<10	50	50	30
Zr	150	220	120	220	80	210
Sr	680	640	700	710	580	490
Rb	<10	<10	40	20	20	30
Y	10	<10	<10	20	<10	20
Nb	10	20	<10	20	20	40
Zn	10	40	10	70	30	40
Ni	<10	10	<10	<10	<10	<10
V	<10	10	<10	<10	<10	<10

Plagioclase composition recalculated from XRF analyses of Pl-Qtz mixture obtained by mineral separation. Qtz assumed to be pure SiO_2. (See appendix A for recalculation scheme)

Table 4.10. Average K feldspar analyses. a) Microprobe. b) Mineral Separates.

a)

	200		64C
wt. %	Core	Edge	Core
SiO_2	65.9	65.8	64.8
Al_2O_3	19.4	19.2	19.4
FeO	0.01	0.03	0.00
CaO	0.25	0.16	0.20
Na_2O	1.56	1.53	1.55
K_2O	13.0	13.1	14.3
Total	100.14	99.80	100.25
No. of cations on the basis of 32 O			
Si	11.98	11.99	11.87
Al	4.16	4.13	4.18
Ca	0.05	0.03	0.04
Na	0.55	0.54	0.55
K	3.02	3.03	3.33
Total	19.74	19.72	19.98
An	0.01	0.01	0.01
Ab	0.15	0.15	0.14
Or	0.84	0.84	0.85
No.	2	2	1

b)

wt. %	102A	188B	220A
SiO_2	63.4	62.6	64.4
TiO_2	0.02	0.12	0.01
Al_2O_3	18.7	20.4	19.0
FeO	0.11	0.22	0.08
MnO	0.01	0.00	0.00
MgO	0.17	0.76	0.17
CaO	0.56	0.28	0.29
Na_2O	1.85	1.80	1.89
K_2O	13.2	14.6	13.4
P_2O_5	0.02	0.00	0.10
Total	97.78	100.88	99.27
An	0.08	0.03	0.03
Ab	0.15	0.15	0.17
Or	0.79	0.82	0.80
ppm Ba	3830	3830	3410
Cr	10	90	20
Zr	60	320	20
Sr	780	720	560
Rb	220	210	270
Y	10	50	20
Nb	10	90	<10
Zn	10	50	<10
Ni	<10	<10	<10
V	<10	<10	<10

Table 4.11. Spinel analyses (microprobe).

	Metapelite melanosome	
	PBA82-153A[1]	
wt %	Core	Edge
SiO_2	0.67	0.26
TiO_2	0.03	0.03
Al_2O_3	54.0	54.1
Cr_2O_3	1.46	1.49
FeO	31.7	31.2
MnO	0.07	0.04
MgO	3.08	3.18
CaO	0.07	0.07
ZnO	7.97	8.65
V_2O_5	0.59	0.63
Total	99.63	99.68

1 Unpublished spinel analyses kindly provided by Dr J A. Percival

respectively. K feldspar in MG_2 leucosome (X_{Ab}^{Kfs} = 0.09-0.18) is significantly less sodic than K feldspar in MG_1 metapelite leucosome (X_{Ab}^{Kfs} = 0.23-0.32).

4.3.6 Spinel

Green spinel is restricted to cordierite-garnet-K feldspar-zone metapelite melanosome, and rarely occurs as inclusions in garnet in MG_2 leucosome. Microprobe analyses of spinel from one metapelite sample are listed in table 4.11. Green spinel is a zinc-rich hercynite, containing about 8 weight % ZnO.

5. METAMORPHISM AND MG_1 (INTERNAL) MIGMATIZATION

5.1 Introduction

A rigorous approach to the discussion of metamorphism and internal (MG_1) migmatization of metagreywacke and metapelite in the study-area will be attempted in this chapter. In order to accomplish this, phase relations will be discussed in terms of model systems, which closely approach the actual chemical constitution of the rocks studied. The system KMFASH will be used for subsolidus phase relations and the system KNMFASH for phase relations with melt considered as an additional phase. The development of the model systems will be discussed, followed by a discussion of their suitability and application to the rocks in this study.

5.2 Model Systems for the Phase Relations of the Metasedimentary Rocks

5.2.1 General Discussion

Any rock system is composed of a finite number of phases (denoted by "p") and a finite number of components (denoted by "n"). Schreinemakers (1915-1925) developed a set of rules by which the relative order of univariant reactions may be determined around an invariant point composed of n+2 mineral phases. Zen (1966) provides an excellent summary of Schreinemakers rules. In a given area subject to a range of metamorphic conditions, the total number of phases (p) for a given rock type, will commonly exceed n+2, although not within a single sample. Korzinksii (1959) designated such systems as "multisystems". For a given multisystem the total number of possible invariant points can be determined by the following equation:

$$\text{number of invariant pts.} = \frac{p!}{(n+2)!(p-n-2)!} \quad \text{(by combinatorial mathematics)}$$

Phase relations in multisystems, therefore, form a series of invariant points connected by univariant reactions, to form a petrogenetic grid.

5.2.2 Phase Relations in the System KMFASH

Vielzeuf and Boivin (1984) have developed an algorithm for multisystems based on Schreinemakers rules which arranges the univariant reactions around invariant points and then arranges the invariant points in P-T space to form a petrogenetic grid. They applied their algorithms to the systems K_2O-MgO-Al_2O_3-SiO_2-H_2O (KMASH), K_2O-FeO-Al_2O_3-SiO_2-H_2O (KFASH), and K_2O-MgO-FeO-Al_2O_3-SiO_2-H_2O (KMFASH), for the phases biotite, garnet, cordierite, orthopyroxene, muscovite, sillimanite, K feldspar, quartz and water. A complete petrogenetic grid would contain 36 invariant points for KMASH and KFASH, and 9 invariant points for KMFASH. To make the calculations more manageable Vielzeuf and Boivin (1984) considered only quartz and water present equilibria. This reduces the total number of invariant points to 21 and 6 respectively. Petrogenetic grids for KMASH or KFASH (a partial grid only), and KMFASH are shown in figures 5.1 and 5.5 respectively. Reactions in KMASH/KFASH and KMFASH are listed in tables 5.1 and 5.2. The interested reader is referred to Vielzeuf and Boivin (1984) for a complete explanation of the construction of the grids.

The more complex system K_2O-MgO-FeO-Al_2O_3-SiO_2-H_2O (KMFASH) provides a more realistic model for subsolidus phase equilibria in natural systems, than do KMASH or KFASH.

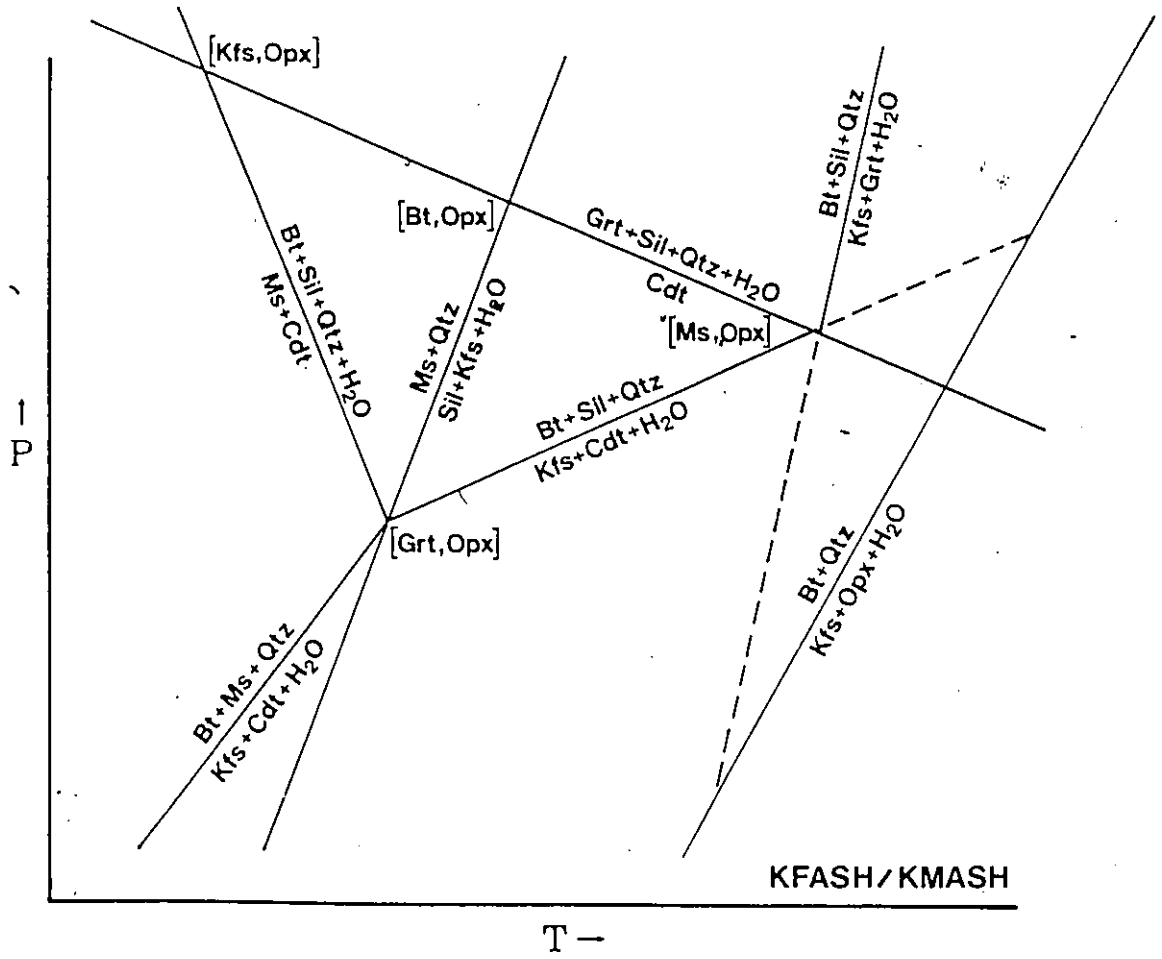

Figure 5.1. Schematic phase relations in the system KFASH or KMASH for the phases shown.

Table 5.1. Reactions in KMASH or KFASH.

Number	Reaction
M-1	Biotite + Sillimanite + Quartz = K feldspar + Cordierite + H_2O
M-2	Muscovite + Quartz = Sillimanite + K feldspar + H_2O
M-3	Muscovite + Cordierite = Biotite + Sillimanite + Quartz + H_2O
M-4	Biotite + Muscovite + Quartz = K feldspar + Cordierite + H_2O
M-5	Biotite + Sillimanite + Quartz = K feldspar + Garnet + H_2O
M-6	Cordierite = Garnet + Sillimanite + Quartz + H_2O
M-7	Biotite + Quartz = K feldspar + Orthopyroxene + H_2O

The most significant difference for phase relations in the system KMFASH compared to those in KMASH or KFASH is that univariant reactions must have balanced Fe-Mg ratios between ferromagnesian phases on both sides of the reaction. Univariant reactions in the system KFASH and KMASH become divariant fields in the system KMFASH.

Equilibria in the systems KFASH and KMASH may be integrated into the system KMFASH in the following manner. In the system KMFASH, the two end-points of non-degenerate univariant equilibria are constrained by the position of the KFASH and KMASH end-member invariant points containing the same phases as those found in the univariant equilibria. The end-member invariant points in KMASH and KFASH will contain the same phases and number of phases as univariant equilibria in KMFASH, and one less phase than KMFASH invariant points, since the end-member systems contain one less component, either MgO or FeO. For Fe-Mg phases the position of a univariant reaction in KMFASH is constrained by the intersection of any two of the divariant reactions at equal X_{Mg} isopleths for a common ferromagnesian phase (cf. Holdaway and Lee 1977).

As an example we will examine univariant reaction MF-1. Equilibria involving the breakdown of sillimanite, biotite, and quartz are important indicators of metamorphic grade in the present study-area and in many high-grade metamorphic terrains. Reaction MF-1 is constrained by the intersection of the Fe and Mg end-member reactions: M-1, M-5, M-6, and M-8, as shown in figure 5.2. The reaction MF-1 is also constrained by the intersection of lines of equal cordierite composition for end-member reactions M-1 and M-6 or by the intersection of lines of equal garnet composition for the end-member reactions M-5 and M-6 (figure 5.3). The relative stability of end-member reactions M-5 and M-1 is considered to be

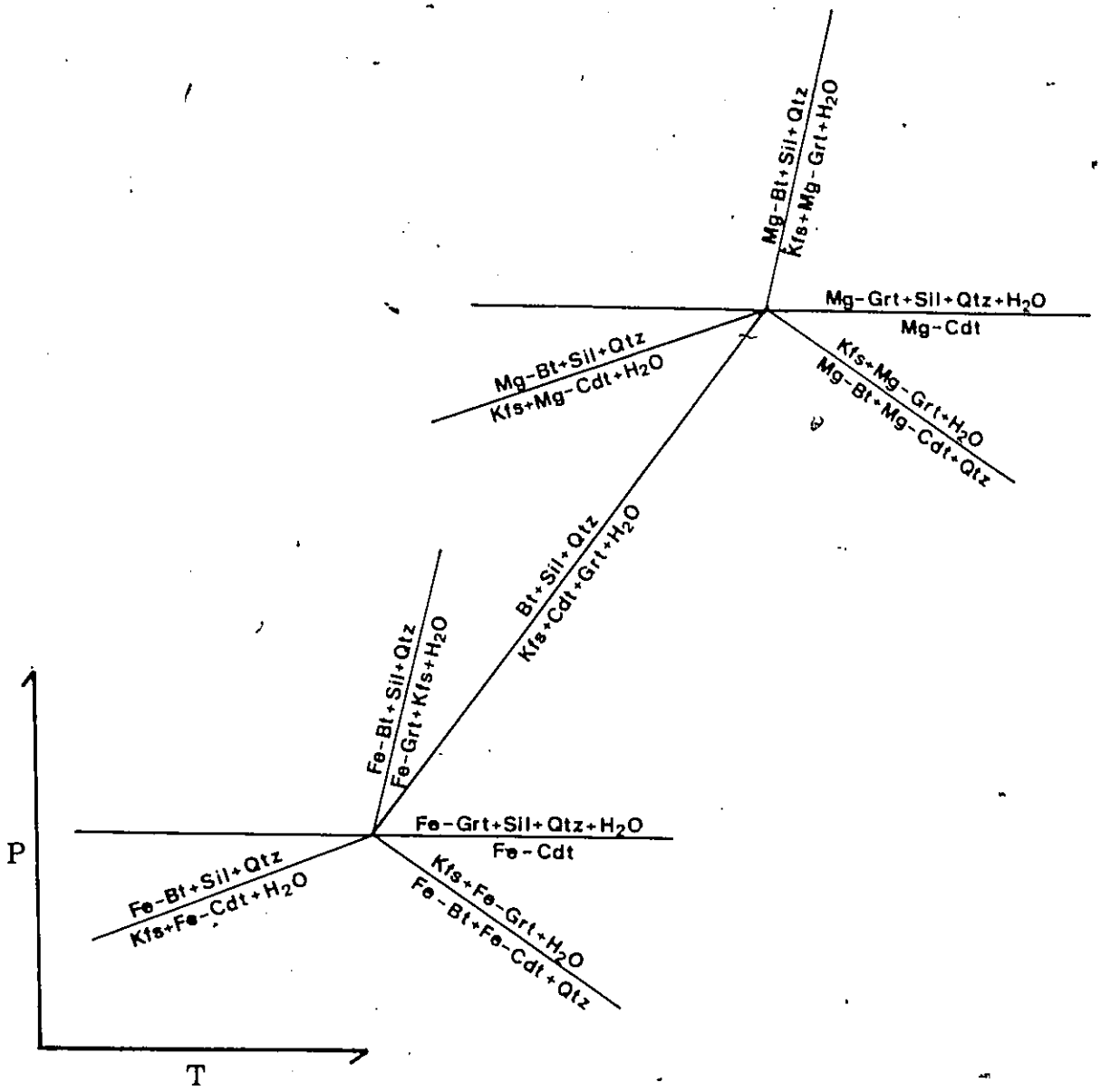

Figure 5.2. Schematic topology of reaction MF-1, constrained by the Fe and Mg endmember invariants containing the phases Qtz-Kfs-Als Bt Grt Cdt-H_2O.

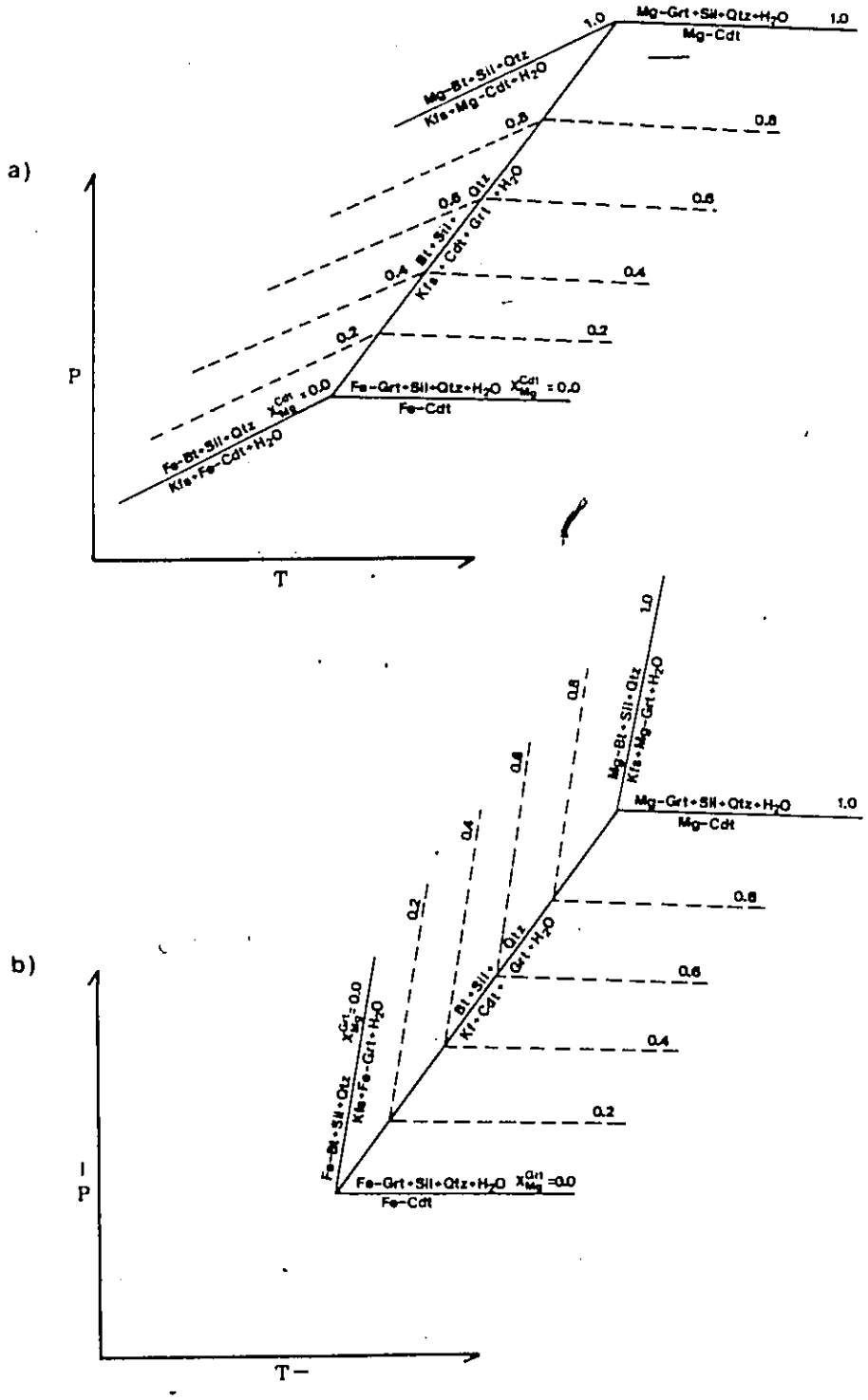

Figure 5.3. Schematic topology of reaction MF-1, constrained by the intersection of the divariant fields of: (a) reactions Bt+Sil+Qtz=Kfs+Cdt+H2O and Cdt=Grt+Sil+Qtz+H2O at equal cordierite compositions; or (b) reactions Bt+Sil+Qtz=Kfs+Grt+H2O and Cdt=Grt+Sil+Qtz+H2O at equal garnet compositions.

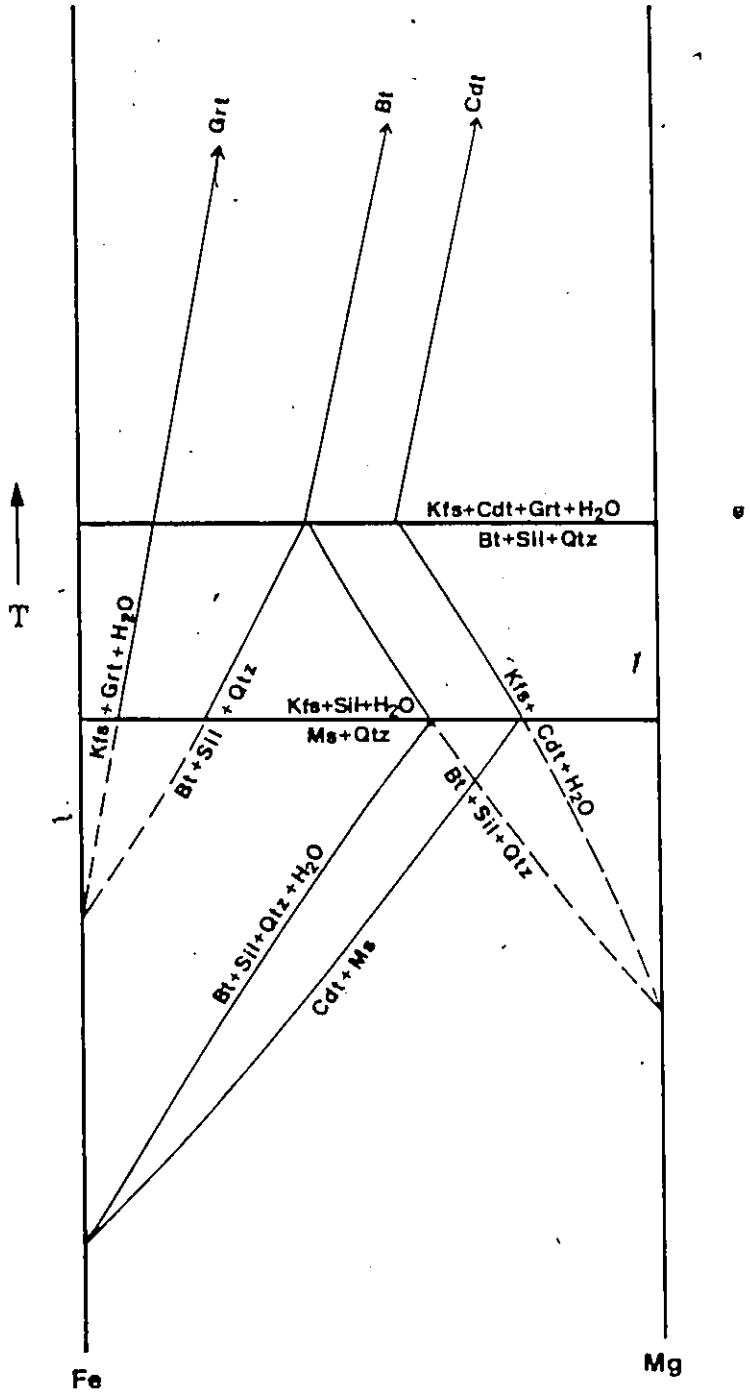

Figure 5.4. Schematic T-X_{Fe-Mg} section for divariant reactions emanating from univariant reaction (Bt+Sil+Qtz=Kfs+Cdt+Grt+H2O)$_{FMF}$ (after Thompson 1976).

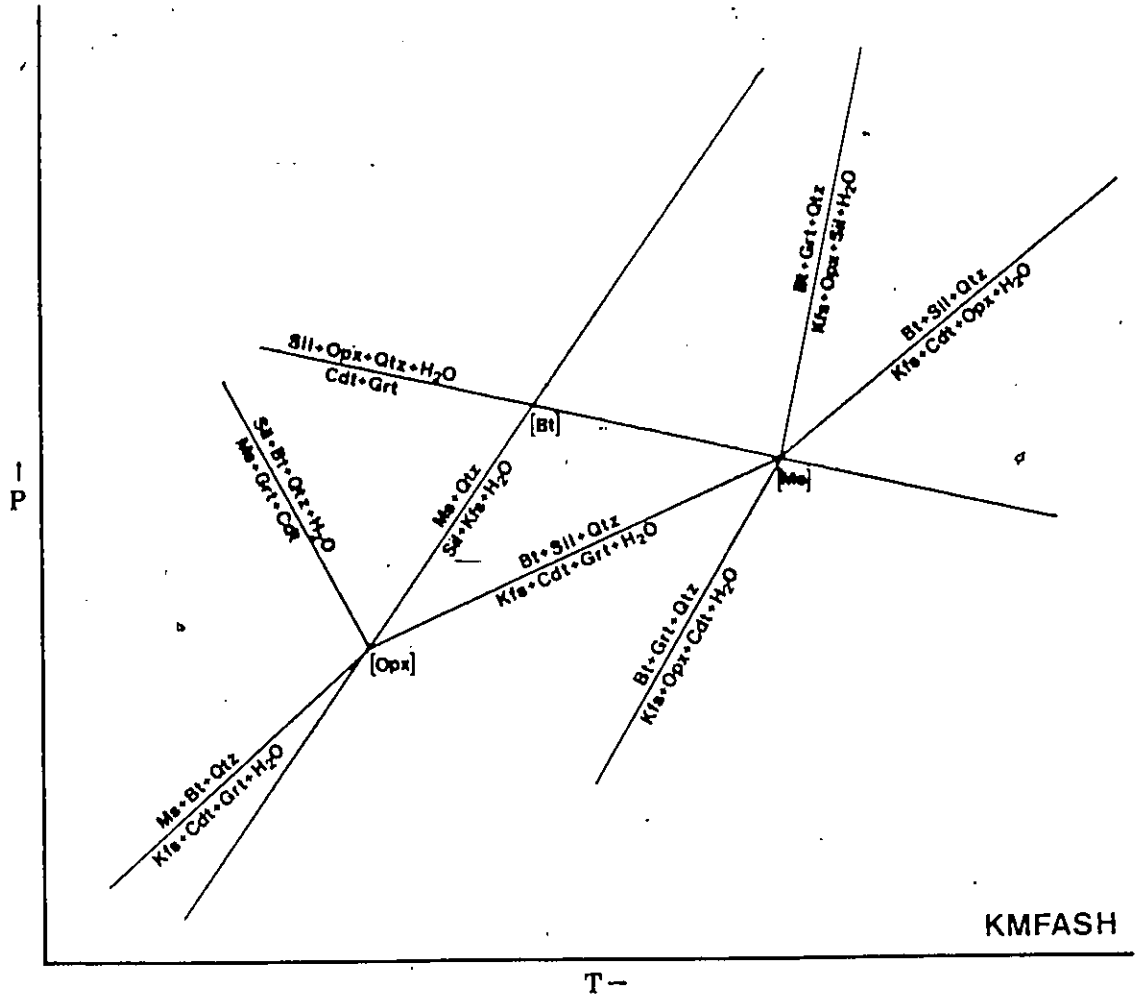

Figure 5.5. Partial Schematic P-T grid of phase relations in the system KMFASH for the phases Qtz-Kfs-Als-Ms-Bt-Grt-Cdt-Opx-H_2O. After Vielzeuf and Boivin (1984).

Table 5.2. Reactions in KMFASH.

Number	Reaction
MF-1	Biotite + Sillimanite + Quartz = K feldspar + Cordierite + Garnet + H_2O
MF-2	Muscovite + Quartz = Sillimanite + K feldspar + H_2O
MF-3	Muscovite + Garnet + Cordierite = Sillimanite + Biotite + Quartz + H_2O
MF-4	Muscovite + Biotite + Quartz = K feldspar + Cordierite + Garnet + H_2O
MF-5	Biotite + Garnet + Quartz = K feldspar + Orthopyroxene + Cordierite + H_2O
MF-6	Cordierite + Garnet = Sillimanite + Orthopyroxene + Quartz + H_2O
MF-7	Biotite + Sillimanite + Quartz = K feldspar + Cordierite + Orthopyroxene + H_2O
MF-8	Biotite + Garnet + Quartz = K feldspar + Orthopyroxene + Cordierite + H_2O

a function of the Fe/Mg ratio of the rock (Thompson 1976). This can be shown graphically by an isobaric T-X section for continuous reactions emanating from the discontinuous reaction MF-1 (Figure 5.4).

Hess (1969) derived a grid similar to the grid derived by Vielzeuf and Boivin (1984), but which differs in the position of the $[Ms]_{MF}$ invariant point. The discrepancy arises because Hess did not consider the full extent of reaction MF-6. The partial P-T grid shown in figure 5.5 is consistent with phase relations deduced by Reinhardt (1968) for metamorphism of pelitic rocks in the Frontenac Axis of Ontario, and by Grant (1973). Grant (1973) was able to show that equilibria radiating from the invariant points $[Ms]_{MF}$, $[Bt]_{MF}$, and $[Opx]_{MF}$ are compatible with a considerable amount of natural data.

At conditions of a_{H2O} near unity the invariant $[Opx]_{MF}$ will lie below the stability of the assemblage Fe-garnet-sillimanite-quartz-water and is therefore metastable (cf. Holdaway and Lee 1977, Grant 1985).

5.2.3 Phase Relations in the System KNMFASH

Supersolidus phase relations (above the granite solidus) of the metasedimentary rock types in the present study will be treated in the system KNMFASH, and will include all of the phases considered for the system KMFASH, plus plagioclase (albite) and granite melt. K feldspar in the system KNMFASH contains an albite component. A partial, schematic P-T grid, consistent with Schreinemakers analysis, has been developed by Grant (1985) for univariant curves radiating from the invariant points $[Ms,Opx]_{NMF}$ and $[Ms,Sil]_{NMF}$ (figure 5.6). Univariant curves radiating from the $[Opx,Cdt]_{NMF}$ invariant point are also included in figure 5.6. The tonalite solidus is included in figure 5.6 for the consideration of H_2O-

phase[1] present melting of plagioclase-quartz (no K feldspar) assemblages. Reactions in KNMFASH are listed in table 5.3.

The position of the $[Ms,Sil]_{NMF}$ invariant point from Grant (1985) requires that the melt composition produced by melting reactions NMF-7 and NMF-6 be granitic. However, experimental studies have indicated that the melt produced may be granodioritic in composition for H_2O-phase-present melting (Knabe 1970a and 1970b). Percival (1983) deduced the formation of granodioritic melts for H_2O-phase-absent melting, based on natural observations. Percival (1983) positions reaction Bt+Pl+Qtz=Opx+Melt[2] at the intersection of the tonalite solidus curve (NMF-14) and subsolidus reaction Bt+Qtz=Kfs+Opx+H_2O (equivalent to NMF-3) (figure 5.7).

H_2O-phase-absent melting according to reaction Bt+Pl+Qtz=Opx+Melt (H_2O in melt is derived from biotite breakdown) results in H_2O contents in the melt of 1.1 wt. % for a granodioritic melt composition and 1.8 wt. % for a granitic melt composition[3]. Both melts are extremely H_2O undersaturated. Wyllie (1983) estimates that for melting of crustal gneiss containing 2 wt. % water temperatures in excess of 900° C are required to form granodioritic melts. Calculations of the H_2O content of granitic

---

[1] In natural rock systems, water that is not an essential structural constituent of minerals may form part of a discrete vapour phase, or part of a disordered grain-boundary/channel phase. To keep the discussion consistent with both possibilities, non-structural water will be referred to as the "H_2O-phase", unless a discrete "vapour" phase is implied.

[2] Reaction Bt+Pl+Qtz=Opx+Granodiorite Melt from Percival (1983b) would be equivalent to Bt+Pl+Qtz+Grt=Opx+Cdt+Granodiorite Melt in the system KNMFASH, assuming that all K feldspar produced is incorporated into the melt, and that the Fe/Mg ratio in biotite and orthopyroxene are equal.

[3] Calculations are based on the simplified reaction Bt + 3Qtz = Kfs + 3Opx + H_2O, with all Kfs and H_2O entering the melt. Granodioritic and granitic melts represent average MG_2 leucosome compositions from this study.

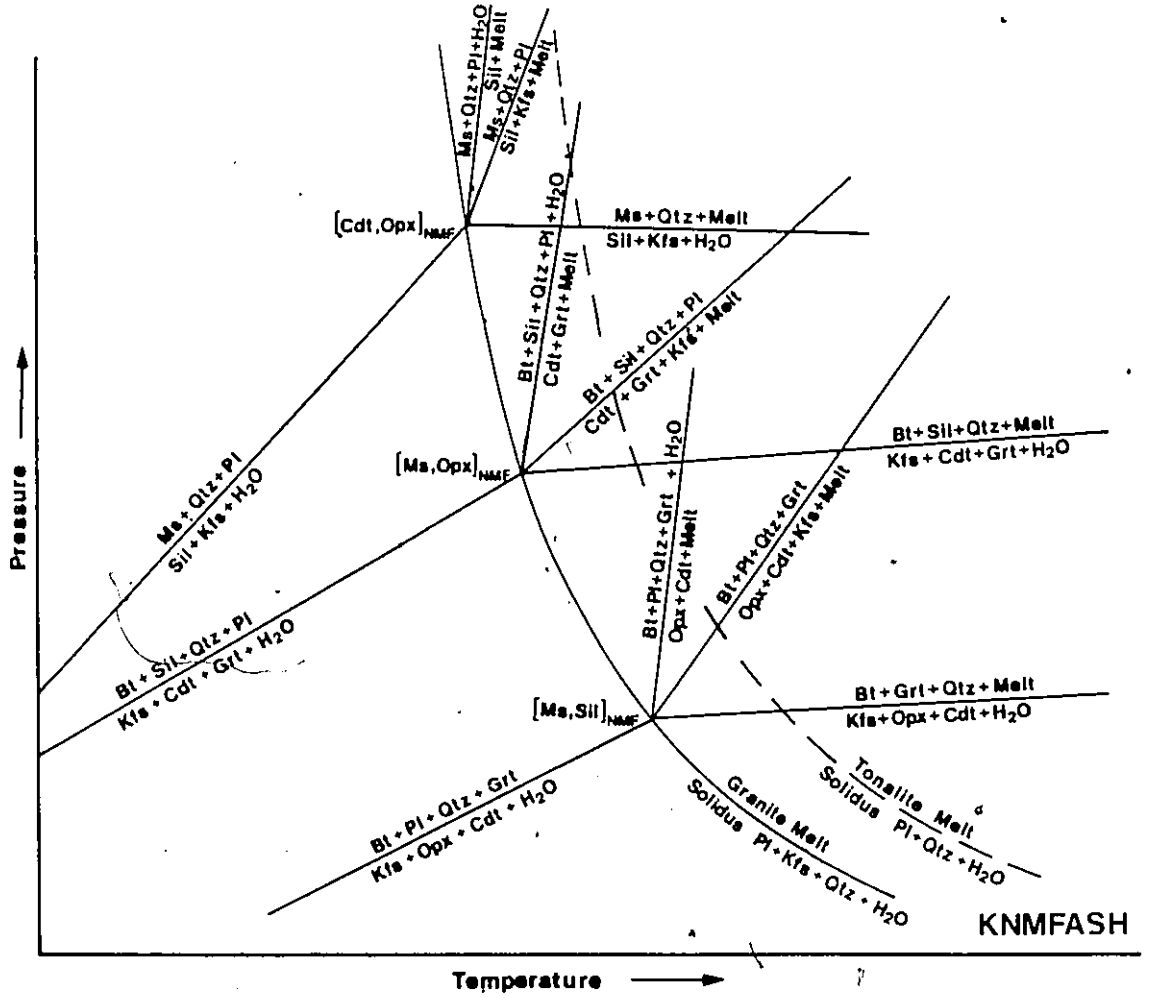

Figure 5.6. Schematic phase relations in the system KNMFASH for the phases Qtz-Kfs-Pl-Ms-Bi-Als-Cdt-Grt-Opx-H_2O, radiating from the invariants $[Bt,Cdt,Grt,Opx]_{NMF}$, $[Ms,Opx]_{NMF}$, and $[Ms,Sil]_{NMF}$ (Modified after Grant, 1985). To simplify phase relations the solubility of Fe and Mg in the melt is assumed to be zero.

Table 5.3. Reactions in KNMFASH.

Number	Reaction
NMF-1	Biotite + Sillimanite + Quartz + Plagioclase = K feldspar + Cordierite + Garnet + H_2O
NMF-2	Muscovite + Quartz + Plagioclase = Sillimanite + K feldspar + H_2O
NMF-3	Biotite + Plagioclase + Quartz + Garnet = K feldspar + Orthopyroxene + Cordierite + H_2O
NMF-4	Plagioclase + K feldspar + Quartz + H_2O = Granite Melt
NMF-5	K feldspar + Orthopyroxene + Cordierite + H_2O = Biotite + Garnet + Quartz + Granite Melt
NMF-6	Biotite + Plagioclase + Quartz + Garnet = Orthopyroxene + Cordierite + K feldspar + Granite Melt
NMF-7	Biotite + Plagioclase + Quartz + Garnet + H_2O = Orthopyroxene + Cordierite + Granite Melt
NMF-8	K feldspar + Cordierite + Garnet + H_2O = Biotite + Sillimanite + Quartz + Granite Melt
NMF-9	Biotite + Sillimanite + Quartz + Plagioclase = Cordierite + Garnet + K feldspar + Granite Melt
NMF-10	Biotite + Sillimanite + Quartz + Plagioclase + H_2O= Cordierite + Garnet + + Granite Melt
NMF-11	Sillimanite + K feldspar + H_2O = Muscovite + Quartz + Granite Melt
NMF-12	Muscovite + Quartz + Plagioclase = Sillimanite + K feldspar + Granite Melt
NMF-13	Muscovite + Quartz + Plagioclase + H_2O = Sillimanite + Granite Melt
NMF-14	Plagioclase + Quartz + H_2O = Tonalite Melt

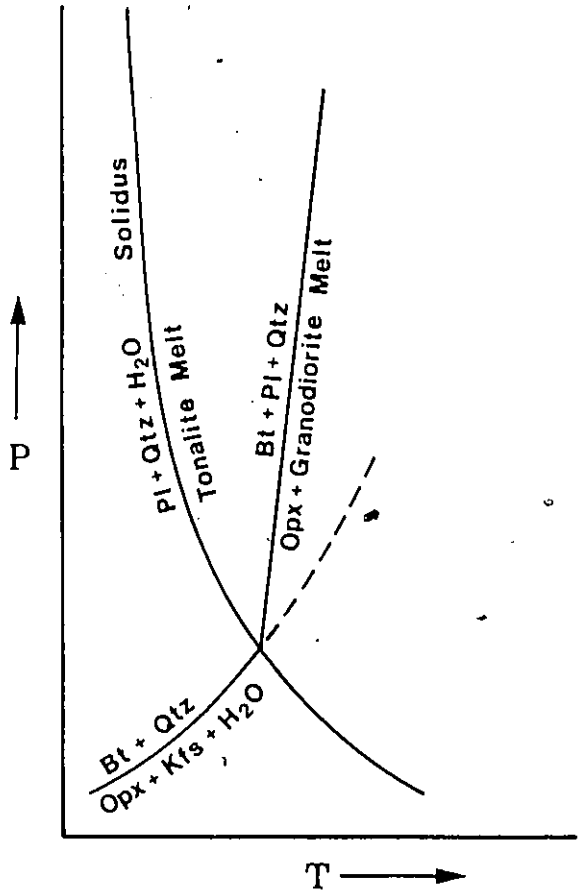

Figure 5.7. Topology of vapour absent melting for the assemblage Bt-Pl-Qtz proposed by Percival (1983).

melts based on the equations of Burnham (1979) and presented in Johannes (1985) indicate that granitic melts with equilibrium H_2O contents of less than 2 wt. % will not form at temperatures less than about 875^{o} C. Therefore, at temperatures of about 700 ^{o}C strongly undersaturated melts will not form. Furthermore, in the presence of plagioclase, Percival's reaction Bt+Qtz=Opx+Kfs+H_2O should produce a granite melt at conditions exceeding the granite solidus. H_2O-phase-absent melting reactions must, therefore, produce K feldspar in excess of that which could be incorporated into the melt (cf. Thompson 1982, Grant 1985), to allow for higher H_2O contents in the melt, resulting in the formation of granitic melts (ie.

reaction Bt+Pl+Qtz=Opx+Cdt+Melt should in fact be NMF-6). The interpreted position of reaction Bt+Pl+Qtz=Opx+Melt of Percival (1983b) is not reasonable and that of Grant (1985) which shows the correct form of the reaction (NMF-6) will be adopted in this study.

Reaction NMF-7 does not share the H_2O content restriction of reaction, NMF-6. For reaction NMF-7 or other H_2O-phase-present, incongruent, biotite melting-reactions melts may in fact be granodioritic, particularly at higher pressures where reaction NMF-7 moves further away from the granite solidus. It is also worth noting that at pressures greater than the intersection of reaction NMF-7 with the tonalite solidus, initial H_2O-phase saturated melting of assemblages of Biotite-Plagioclase-Quartz (no aluminosilicate) will produce tonalitic melts (see figure 5.6). It is clear from figure 5.6 that different P-T paths during metamorphism will result in very different melting patterns for a rock.

During prograde metamorphism, H_2O-phase-present melting reactions will lower the proportion of H_2O in the remaining solid rock. Therefore during metamorphism, initial melting of the rock mass is likely to be the result of H_2O-phase-present melting reactions, and later melting the result of H_2O-phase-absent melting reactions (Thompson 1982). Natural high-grade metamorphic rocks probably contain a very small amount of H_2O not tied up in the crystal structure of minerals in the rock. The amount of this "free" water would in fact be buffered internally by the hydrated minerals (Powell 1983). Only a small amount of melt could probably be formed by H_2O-phase-present melting reaction of natural high-grade metamorphic rocks, without an influx of water into the system. A much larger proportion of melt could be formed by H_2O-phase-absent melting reactions, in which H_2O released from the hydrated mineral goes directly into the undersaturated melt (Thompson 1982).

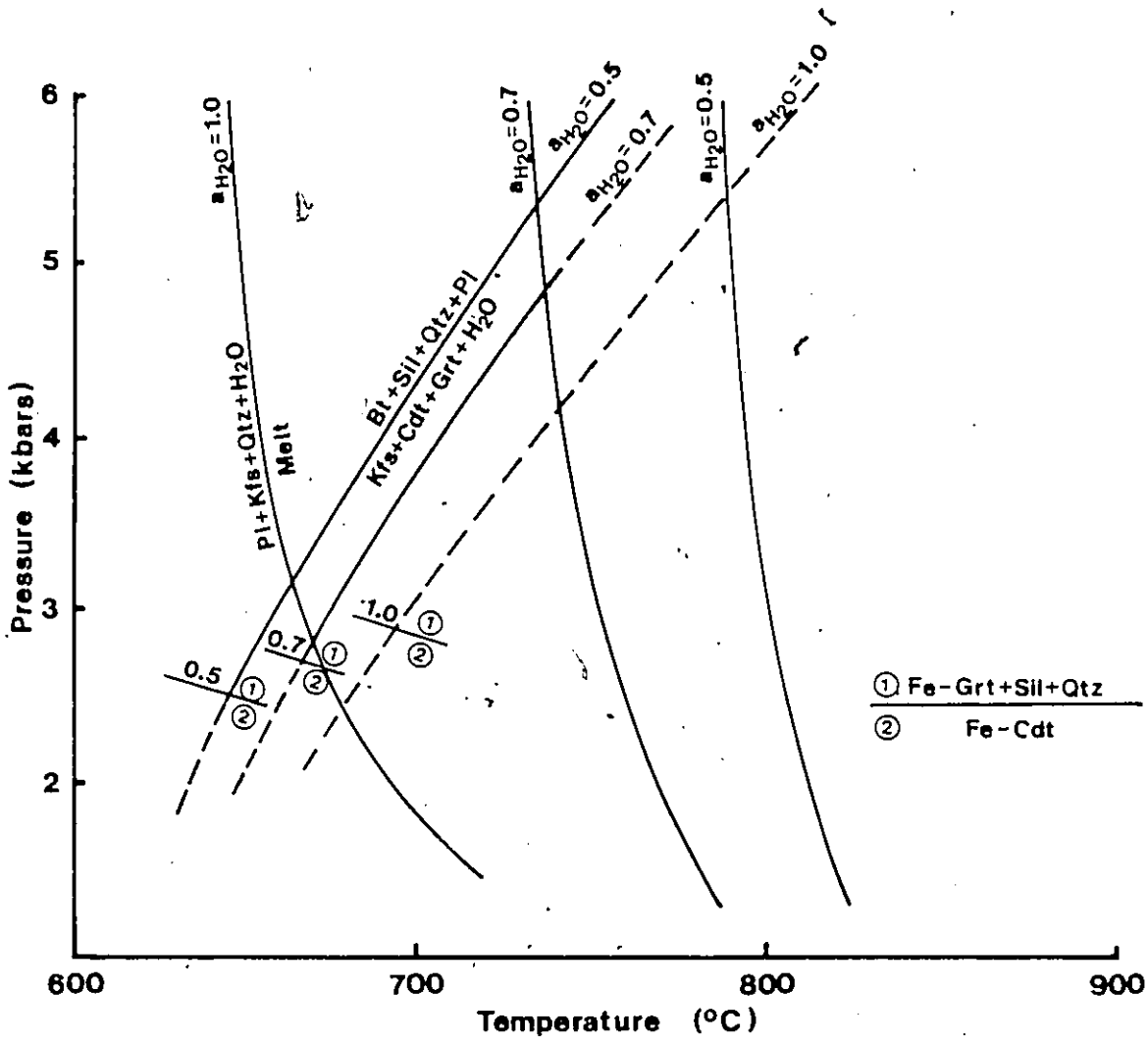

Figure 5.8. Intersection of reactions NMF-1 and NMF-4 (granite solidus) in P-T space at variable ratios of P_{H2O}/P_{total}. Metastable sections of reactions are shown as dashed lines. Position of reaction NMF-1 from Holdaway and Lee (1977), reaction NMF-4 from Johannes (1985).

A degree of freedom is gained for H_2O-phase-present reactions by considering variations in the a_{H2O}. In general, decreasing the a_{H2O} will shift subsolidus dehydration reactions towards lower temperatures and H_2O-phase-present melting reaction towards higher temperatures. H_2O-phase-absent melting reactions are not shifted by variations in the a_{H2O}. The net result of the shifts in univariant curves is that decreasing the a_{H2O} will shift the invariant points in figure 5.6 towards higher pressures along the H_2O-phase-absent melting curves.

The position of the invariant $[Ms,Opx]_{NMF}$ and reactions involving the breakdown of biotite, sillimanite, and quartz are of particular importance in this study and will be considered further. Experimental studies by Holdaway and Lee (1977) and Hoffer and Grant (1980) have indicated that at $a_{H2O} = 1$ the subsolidus reaction NMF-1 is metastable, and melting reaction NMF-9 will occur instead. However, for the lower values of a_{H2O} a portion of the subsolidus reaction becomes stable. The intersection of reaction NMF-1 from Holdaway and Lee (1977) with the granite solidus (NMF-4) from Johannes (1985), at different ratios of P_{H2O}/P_{total} ($\simeq a_{H2O}$) is shown in figure 5.8. This intersection defines the position of the invariant $[Ms,Opx]_{NMF}$. The lower stability limit of NMF-1 is constrained by the reaction:

Fe-cordierite = Fe-garnet + Aluminosilicate + Quartz + Water.

The upper stability limit of NMF-1 is constrained by the granite solidus. From figure 5.8, reaction NMF-1 will be stable at values of $a_{H2O} < 1$. While there is considerable uncertainty in the absolute position of reactions NMF-1 and NMF-4 due to the combined uncertainties in the experimental data and thermodynamic calculations (see Holdaway and Lee

(1977) and Johannes (1985) for a discussion of errors), the relative positions are valid.

5.3 The Activity of H_2O

5.3.1 A General Discussion of the Behaviour of H_2O in High-grade Metamorphic Rocks

There are at least two ways in which water within a rock during high-grade metamorphism may be viewed. A common assumption used by petrologists is that water, possibly combined with other volatile components, exists as a discrete fluid phase in a metamorphic rock system. A second possibility is that within medium- to high-grade metamorphic rocks, water may exist in a solid grain-boundary/channel phase as adsorbed molecules at grain boundaries, and/or as molecular H_2O in cavities and channels within a cation-oxygen framework, somewhat analogous to the zeolite structure (Ramberg 1952, Kretz Personal Communication). Water present in this manner in a rock will be referred to as part of a grain-boundary/channel phase, which clearly can not be viewed as a fluid. With this second view of the behaviour of water in a high-grade metamorphic rock, the activity of water may be altered in two ways:

1) Dilution of water with another volatile component (eg. CO_2), by the influx of the volatile component or by devolatization reactions other than dehydration reactions occurring within the rock (eg. decarbonation reactions).

2) Removal of water from the system, with or without the presence of another volatile component. The progressive removal of water from the system would decrease the mole

fraction of water in the grain-boundary/channel phase, resulting in a lowering of the a_{H2O} within the rock.

If the volatile components are viewed to occupy a discrete fluid phase, then only dilution with another vapour phase can bring the a_{H2O} below unity. In the presence of a pure water vapour phase, the a_{H2O} must be unity, and will be independent of the amount of water present. If water in some metamorphic rocks does indeed exist within a disordered grain-boundary/channel phase it could account for reduced activities of H_2O, even when water is the only volatile component present. The two cases need not be mutually exclusive. If the amount of water and other volatile components within a rock was in excess of that which could be incorporated into the grain-boundary/channel phase, then water could exist as a part of a fluid phase. This might be the case during dehydration reactions if excess water could not be transported out of the rock as quickly as it is being produced. The amount of water present in a rock is equally as important as the activity but is commonly not considered.

For experimental studies of dehydration reactions at values of $a_{H2O} < 1$, it is necessary to consider water as a component of a discrete fluid phase. These studies may provide a reasonable approximation for natural rock systems where a discrete fluid phase may not exist (Kretz Unpubl. Manuscript).

5.3.2 Activity of H_2O in the Study-area

In the study-area there are several features which suggest that the activity of water was less than unity:

1) The development of dehydration rims in mafic gneiss at the contact with metagreywacke indicates a lower a_{H2O} in the metagreywacke relative to the mafic gneiss.

2) The coexistance of sodic plagioclase, quartz, and K feldspar in leucocratic biotite-garnet-K feldspar gneiss with metamorphic textures at P-T conditions (from geothermometry and geobarometry) in excess of those required for melting with a_{H2O} = 1 (refer to section 5.4.2 for a more detailed discussion).

3) Orthopyroxene is present in mafic gneiss and locally in metatonalite, which is though to require values of a_{H2O} of less than unity to form at geologically reasonable P-T conditions in the crust (Winkler 1979, Turner 1981).

There is no evidence for the presence or absence of volatile components other than water in the rocks in the study-area. However, if water, under metamorphic conditions, existed as part of a grain-boundary/channel phase, then the presence of additional volatile components is not a prerequisite for reduced values of a_{H2O}. The production of water by metamorphic reaction, followed by escape of the H_2O produced, could conceivably result in reduced activities of H_2O, as could partial melting. This point will be discussed further, in section 5.4.

5.4 Metamorphism and MG_1 (Internal) Migmatization of Metasedimentary rocks in the Study-area

5.4.1 Application of Model Systems to the Present Study

In the present study, the chemical system for the metasedimentary rocks (metapelite and metagreywacke) may be expressed by the components K_2O-FeO-MgO-Al_2O_3-SiO_2-MnO-$FeTiO_3$-CaO-Na_2O-H_2O[4]. By applying the following

[4] Water is treated as a discrete phase although it is recognized that water may not form a discrete phase or may only exist as a discrete phase periodically as dehydration reactions occur.

simplifying assumptions the system can be simplified to KNMFASH for subsolidus phase relations and to KNMFASH for phase relations involving a melt phase:

1) Ilmenite is present in excess and does not react, fixing the chemical potential of $FeTiO_3$.

2) MnO present in minor amounts in garnet, can be neglected.

3) All Fe is assumed to be in the ferrous state.

4) Plagioclase of constant composition does not participate in subsolidus reactions and is present in excess which fixes the chemical potential of CaO and Na_2O in KNMFASH. In KNMFASH, only the albite component of plagioclase is modeled.

Mineral phases present in metapelite in the study-area include; biotite, garnet, cordierite, sillimanite, muscovite, K feldspar, and quartz (plus plagioclase and ilmenite). Gahnite, and graphite are present in minute amounts in some samples, but are not considered as part of the model system. The components TiO_2 and MnO, present in minor amounts in metapelite and metagreywacke, will affect the stability of biotite and garnet respectively.

CaO, contained predominantly in plagioclase, does not introduce any new phases, thereby increasing the variance of plagioclase present reactions in KNMFASH by one, and extending the stability field of plagioclase bearing assemblages to higher temperatures. The system KNMFASH does however provide useful constraints on the melting (solidus behaviour) of rocks containing sodic rich plagioclase. Johannes (1984) has shown experimentally that the granite solidus curve in the system quartz-orthoclase-albite-anorthite-H_2O at 5 kbars varies by less than 10^{o} C for plagioclase compositions more sodic than An_{40}. Therefore, it is reasonable

to neglect the influence of anorthite on granite solidus temperatures. Similarly, for plagioclase more sodic than An_{25} tonalite solidus temperatures differ by less than 15^{o} C (Johannes 1985).

Johannes (1985) has evaluated many of the existing studies, related to the influence of excess FeO, MgO, Al_2O_3, TiO_2, and MnO on melting temperatures and concluded that it is unlikely that the excess solubility of any of these components will significantly reduce solidus temperatures in granitic and tonalitic systems.

5.4.2 Metapelite

Metapelite in the study-area is characterized by four assemblages, which define a prograde transition from medium- to high-grade metamorphism. Muscovite-quartz medium-grade assemblages (A-4) are the lowest grade assemblage observed in the study-area. Assemblage A-3 is characteristic of the sillimanite-K feldspar zone of high-grade metamorphism. A-2 assemblages are characteristic of the cordierite-garnet-K feldspar-zone. A coexisting MG_1 leucosome (assemblage A-1) is associated with cordierite-garnet-K feldspar-zone metapelite. K feldspar is present in the melanosome of cordierite-garnet-K feldspar-zone metapelite in about 1/3 of the samples examined, but is invariably present in the coexisting MG_1 leucosomes observed with both quartz-bearing and quartz-absent melanosome assemblages. Cordierite-garnet-K feldspar-zone metapelite persists into the orthopyroxene-zone of high-grade metamorphism, defined by the presence of orthopyroxene in hornblende-bearing rocks.

Muscovite-quartz-zone and sillimanite-K feldspar-zone metapelite is restricted in occurrence to the southeast corner of the study-area, near Hollingsworth Lake, within 5 km of the southern subprovince boundary. Metamorphic grade decreases towards the southern subprovince boundary. The

sequence of isograds is shown in figure 3.1, although the patchy distribution of metapelite has allowed for only the approximate placement of the isograds. The sequence of isograds is similar to those observed by Breaks et. al (1978) in the Lake St. Joseph area, near the northern subprovince boundary, although they observed lower grade, staurolite-bearing assemblages.

West of Hollingsworth Lake (see figure 3.1), the isograd sequence is disrupted by the Pashkokogan Lake-Kenoji Lake mylonite zone. This mylonite zone separates orthopyroxene-zone and cordierite-garnet-K feldspar-zone rocks to the north, from the Smoothrock Lake pluton to the south, which contains rafts and screens of muscovite-quartz-bearing medium-grade schists.

The univariant assemblage (in KMFASH and KNMFASH) biotite-sillimanite-cordierite-garnet-quartz-K feldspar-plagioclase (A-2c) was observed in the northern-most portion of the study-area at Whiteclay Lake, and may represent the northern limit of cordierite-garnet-K feldspar-zone metamorphic conditions (see figure 3.1). This assemblage would lie directly on the univariant reaction MF-1 (or NMF-1) in figure 5.5 (or figure 5.6). All other metapelite assemblages observed are divariant and would lie in the divariant fields separating univariant reactions.

The absence of any evidence of internal migmatization associated with the transition from assemblage A-4 to assemblage A-3 metapelite, indicates it formed by subsolidus reaction MF-2 (or NMF-2). The P-T path of metamorphism must, therefore, have passed below the $[Opx,Cdt]_{NMF}$ invariant point in figure 5.6.

The transition from assemblage A-3 to A-2a,b or c is coincident with the first appearance of MG_1 leucosome in metapelite, in accord with observations elsewhere in the ERSp (cf. Harris 1976, Breaks et al. 1978).

Several observations indicate this leucosome formed by internal migmatization of metapelite:

1) The melanosome of MG_1 metapelite migmatite is clearly depleted in certain elements and enriched in others relative to paleosome compositions from lower grade portions of the ERSp. The differences in element oxide concentrations between MG_1 metapelite migmatite melanosome and metapelite paleosome, can be attributed to the removal of a quartz-K feldspar leucosome (see figure 4.3).

2) The alkali feldspar granite to quartz syenite composition of MG_1 metapelite leucosome is unique to metapelite layers.

3) MG_1 leucosome forms isolated lenses and pods within the coexisting melanosome.

The transition from assemblage A-3 to assemblages A-2a, A-2b, and A-2c will result from reaction MF-1 (or NMF-1) at pressures less than the invariant point $[Ms,Opx]_{NMF}$, and from one of the equivalent melting reactions, NMF-10 or NMF-9, at pressures greater than the invariant point.

Ignoring, for a moment, the question of whether or not the reaction involved the generation of a melt phase, there are several lines of evidence to support the formation of cordierite, K feldspar, and garnet from the prograde metamorphic reaction of biotite, sillimanite, and quartz:

1) The instability of coexisting biotite, sillimanite, and quartz under cordierite-garnet-K feldspar-zone conditions is indicated by the two different stable assemblages found at this grade, as shown below:

Inferred partial reaction:

Bt + Sil + Qtz = Cdt + Grt + Kfs (NMF-1, NMF-9, or NMF-10)

Stable Cdt-Kfs-zone sub-assemblages:

Bt, Sil, Cdt, Grt, Kfs (Qtz-absent A-2a)

Bt, Qtz, Cdt, Grt, Kfs (Sil absent, Qtz-bearing A-2b)

Quartz-bearing metapelite (A-2b) contains sillimanite only as minor inclusions restricted to the cores of cordierite grains (see plate 3.6b). Quartz-absent metapelite (A-2a) contains sillimanite in contact with all other phases and as abundant inclusion trails throughout cordierite grains (see plate 3.6a). Reaction of biotite, sillimanite and quartz to produce K feldspar, cordierite, and garnet continued until one or more of the reactants was consumed, which in quartz-bearing metapelite was sillimanite, and in quartz-absent metapelite was quartz. Biotite which is much more abundant than sillimanite or quartz, was therefore not consumed (ie. present in excess).

2) The transition from A-3 to A-2 assemblages has been found to approximately coincide with the prograde appearance of orthopyroxene in hornblende-bearing mafic rocks, which is in agreement with other studies (eg. Waters and Whales 1984).

If it can be shown that the reaction to form K feldspar, cordierite, and garnet did involve the formation of a granitic melt, then migmatization would necessarily have been a melting process. If however the reaction was in fact a subsolidus reaction then migmatization would have been a subsolidus process. Therefore consideration of the possibility that MG_1

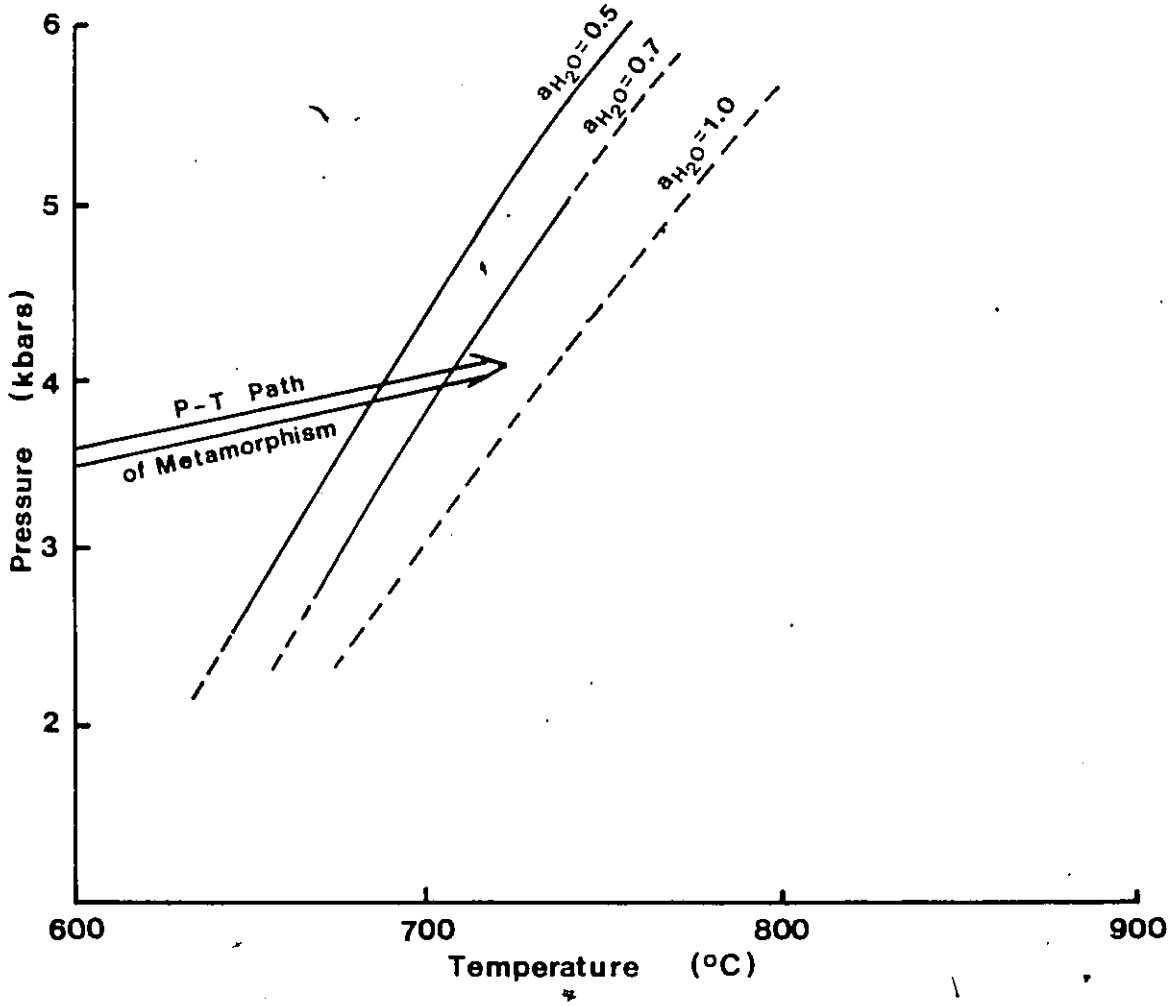

Figure 5.9. Stable portions of reaction NMF-1 superimposed on an inferred geothermal gradient for the study-area.

leucosome formed from a melt may shed light on the nature of the reaction to form K feldspar, cordierite, and garnet.

The alternatives for the generation of MG_1 metapelite leucosome are; 1) metamorphic differentiation in the presence of a mixed volatile phase, 2) metamorphic differentiation in the absence of a free-vapour-phase, or 3) partial melting.

An inferred geothermal gradient[5] for the study-area is shown with the position of the invariant $[Ms,Opx]_{NMF}$ at different values of a_{H2O} in figure 5.9. From figure 5.9, the reaction forming K feldspar, cordierite, and garnet in metapelite may have been a subsolidus reaction if the a_{H2O} were less than about 0.7 and a melting reaction for higher values of a_{H2O}. Melting of metapelite is therefore reasonable at high values of a_{H2O}.

The chemical composition of MG1 metapelite leucosome differs significantly from experimentally determined eutectic and cotectic granite compositions. The normative ratio of quartz-orthoclase-albite for metapelite leucosome is compared with the experimentally determined eutectic and cotectic compositions for granitic melts from Tuttle and Bowen (1958) and Luth et al. (1964) in figure 5.10. Metapelite leucosomes lie towards either the orthoclase or quartz apex away from eutectic compositions. Equilibrium partial melts from metapelite should produce initial eutectic melts. If at some point in the melting of metapelite, either K feldspar or quartz was consumed, the melt composition would shift along the quartz-albite or albite-orthoclase cotectic lines, consequently becoming more enriched in albite, or albite and quartz. To produce melts more orthoclase- or quartz-rich than eutectic melts, would require the

---

[5] Estimated geothermal gradient is constructed by joining a straight line between 25 ^{o}C, 0 Kbars, and 700 ^{o}C, 4 Kbars. Conclusions are still valid however for lower geothermal gradients.

consumption of plagioclase before K feldspar or quartz. This is clearly not possible because, plagioclase is present in metapelite melanosome and is not present in metapelite leucosome. The chemical composition of MG_1 metapelite leucosome is inconsistent with the formation of metapelite migmatite by internal anatectic migmatization, based on existing experimental data. However, there is no existing experimental data on melt compositions derived from melting of pelitic compositions, and the application of haplogranite eutectic melt compositions may be erroneous to melting in small closed systems (cf. Ashworth 1976, 1986).

For metamorphic differentiation, during subsolidus reaction MF-1 (or NMF-1), to be a reasonable process, at temperatures above the vapour saturated granite solidus, some account must be made of the H_2O produced by this reaction. If this water exists as a relatively pure aqueous vapour phase, then melting would occur. Therefore, dilution with another vapour phase is required to allow reaction MF-1 (or NMF-1) to occur. There is no indirect petrographic evidence, for the presence of a vapour phase other than water in metapelite.

MG_1 metapelite leucosomes lack the zoning which characterizes subsolidus segregations described by Sawyer (1986) in the Quetico Belt. Furthermore quartz is consumed by reaction MF-1 (or NMF-1), making it difficult to understand the mechanism, which would result in the diffusion of quartz into the leucosome, during this reaction. Saywer (1986) noted this problem and attributed pressure solution as the main source of silica for segregation veins, but at lower metamorphic grades. If pressure solution has acted in MG_1 metapelite migmatites, then plagioclase should also be present in the leucosome (cf. Sawyer 1986).

In some metapelite layers the proportion of leucosome is insufficient to account for the depletion of the melanosome. This suggests that

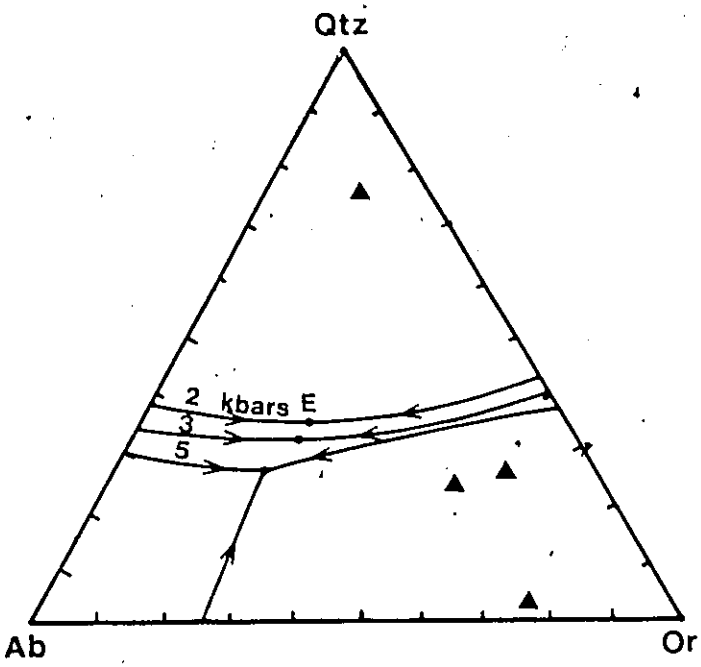

Figure 5.10. Weight percent Qtz-Or-Ab diagram showing the experimental determined position of the water saturated eutectic compositions from Tuttle and Bowen (1958), Luth et al. (1964), and the position of MG_1 metapelite leucosome.

leucosome has moved out of these metapelite layers during migmatization. For example, sample 147 contains 26 vol. % cordierite and only about 2 vol. % K feldspar. The breakdown of biotite to form 26 vol. % cordierite will produce about 10 vol. % K feldspar, of which only about 1/5 is still present in the rock.

The absence of K feldspar and in some cases quartz in the melanosome and their presence in the leucosome of many MG_1 metapelite migmatites indicates that these phases have been effectively partitioned into the leucosome during internal migmatization. Direct evidence of the movement of K feldspar, comes from an outcropping in which thin (<1m) boudinaged metapelite layers occur in metagreywacke. MG_1 leucosome is found in the low pressure zones separating boudins (see Plate 3.5b). In some instances, K feldspar and quartz have moved at least 1 m from the site of reaction in

the melanosome. In contrast, in thicker metapelite layers, MG_1 leucosome is generally evenly distributed throughout the rock, with the distance of movement in the order of several cm (see Plate 3.6). Leucosome in thinner metapelite layers has apparently migrated in response to local pressure gradients.

There is no clear resolution to the mechanism of MG_1 migmatization of metapelite. Examination of the chemical data does not help resolve the problem. Partial melting is the logical choice given the high metamorphic grade, distances of leucosome movement in the order of 1 m in some layers, and coincidence of migmatization with a K feldspar producing dehydration reaction. The absence of plagioclase from the leucosome can not be explained by existing experimental studies in the granite system. However, the absence of plagioclase is equally difficult to explain if one turns to metamorphic differentiation as a mechanism. Sawyer (1986) has noted the presence of plagioclase in all vein segregations in Quetico rocks, except for low-grade veins (lower greenschist). Metamorphic differentiation in metapelite in this study, further requires the presence of vapour phase other that H_2O.

The presence of quartz-bearing leucosome in quartz-absent metapelite melanosome (A-2a) would at first glance seem to represent a clear case of non-equilibrium. Closer examination of coexisting phases however reveals that quartz in the leucosome is always isolated from sillimanite and biotite, by a thin rim of plagioclase, cordierite, and garnet around the margin of the leucosome.

Quartz-bearing metapelite melanosomes preserve localized equilibrium in the form of sillimanite inclusions in the cores of cordierite and garnet grains. Sillimanite may persist as inclusions as long as it remains isolated from quartz and biotite. The extent of equilibrium within the

metapelite, at least for univariant reactions appears to be in the order of several millimeters in scale. A single thin section contains a collection of isolated local equilibrium systems rather than one pervasive equilibrium system.

A zinc-rich hercynite spinel is present as a minor phase in quartz-absent metapelite. It is suggested that the absence of quartz and the Zn-rich composition of the spinel are the determining factors in allowing it to form. A possible reaction for the formation of spinel is:

$$\text{sillimanite} + \text{biotite} + \text{Zn} = \text{cordierite} + \text{K feldspar} + \text{spinel} \qquad \text{(R-1)}$$

In the presence of quartz, reaction (R-1) would not occur, and reaction MF-1 (or NMF-1) would occur instead. Zn in the spinel may have an influence on the stability of spinel, analogous to the effect of Mn on garnet stability, such that Zn-rich spinel forms at lower metamorphic grades, than Zn-absent hercynite spinel. The amount of spinel would be controlled by the amount of Zn available. Biotite breakdown according to reaction MF-1 (or NMF-1) represents the most likely source of Zn, as biotite contains up to 550 ppm Zn. These conclusions are in agreement with the interpreted stability of similar spinels in pelitic rocks in southwest Finland (Dietvorst 1980).

5.4.3 Metagreywacke and Leucocratic Garnet-K feldspar Gneiss

Metagreywacke (A-5) and leucocratic garnet-K feldspar gneiss (A-11) differ in mineral assemblage only by the absence of K feldspar in metagreywacke. No mineralogical variations are observed over the range of metamorphic conditions observed within the study-area. The peak metamorphic conditions experienced by these rocks are defined by divariant

reaction MF-5 (or NMF-3), since orthopyroxene is absent from both rock types.

A small proportion of migmatitic leucosome (< 5%), with in situ characteristics is present locally in cordierite-garnet-K feldspar-zone metagreywacke. However, the evidence of an internal derivation for these leucosomes is not conclusive. The leucosomes occur as isolated lenses and pods within metagreywacke. Melanosomes are only rarely developed (2 of 20 samples observed). Mesosome fractions of MG_1 migmatitic metagreywacke do not differ in chemical composition from non-migmatitic metagreywacke, beyond what can be attributed to original compositional variability (see table 4.3). Chemical analyses of leucosome revealed that MG_1 metagreywacke leucosome is generally granodioritic in composition. If leucosome formed by internal migmatization, there is the problem of the source of K feldspar, which is not observed within non-migmatitic metagreywacke or in metagreywacke mesosome. The breakdown of biotite does not represent a reasonable source of K feldspar, because no suitable reaction products (eg. orthopyroxene and cordierite) are present. One possibility is that only metagreywacke originally containing small amounts of K feldspar underwent anatectic migmatization at the granite solidus, which effectively segregated K feldspar into the leucosome.

The low proportion of MG_1 leucosome, and its localized occurrence indicates that if MG_1 (internal) migmatization of metagreywacke did occur it was a minor process. Significant internal migmatization of metagreywacke would probably not have occurred until the breakdown of biotite + plagioclase + quartz occurred, which would likely be a melting reaction (ie. NMF-6).

Leucocratic biotite-garnet-K feldspar gneiss is not migmatitic. This is significant because it contains plagioclase, quartz, and K feldspar

which would produce granitic melts at temperatures exceeding the granite solidus, in the presence of an aqueous vapour. The absence of evidence of melting in leucocratic biotite-garnet-K feldspar gneiss indicates that the a_{H2O} in leucocratic gneiss was less than one, because peak metamorphic conditions lie above the granite solidus (see chapter 6) at $a_{H2O} = 1$ (see figure 5.9). Given the very low proportion of hydrous minerals in leucocratic Bt-Grt-Kfs gneiss, it is is reasonable that the a_{H2O} and/or amount of H_2O is lower than in metapelite or metagreywacke.

5.4.4 Grey Metatonalite

Throughout most of the study-area, grey metatonalite contains hornblende, biotite, and minor cummingtonite in the orthopyroxene-zone. Orthopyroxene is generally restricted to mafic metadiorite xenoliths within metatonalite. Cummingtonite is secondary after orthopyroxene and is not part of the stable peak metamorphic assemblage. No grey metatonalite plutons were observed outside of the orthopyroxene-zone.

Grey metatonalite plutons at Mojikit Lake differ from those elsewhere in the study-area, in that they contain orthopyroxene throughout and not only in mafic xenoliths. Two different assemblages, A-12a and A-12b, were observed in metatonalite at Mojikit Lake.

There is no evidence based on phase equilibria of other rock types or geothermometry or geobarometry (see chapter 6) that this area was exposed to a higher grade of metamorphism than elsewhere in the study-area. A lower activity of water at Mojikit Lake during metamorphism could explain the stabilization of orthopyroxene throughout the plutons, however this is impossible to verify.

The absence of K feldspar in grey metatonalite would suggest that orthopyroxene has formed from hornblende and not biotite. This is in

agreement with the petrogenetic grid of Froese and Jen (1978) which shows that hornblende breakdown reactions forming orthopyroxene occur at lower temperatures than biotite breakdown reactions forming orthopyroxene.

5.4.5 Mafic Hornblende Gneiss

Mafic hornblende gneiss, although highly variable in mineralogy, invariably contains a high proportion of hornblende. The appearance of orthopyroxene in these rocks (assemblages A-6 to A-10) defines the prograde transition into the orthopyroxene-zone from the cordierite-garnet-K feldspar-zone, which is defined by metapelite assemblages.

The variation in mineral assemblages found in orthopyroxene-zone mafic hornblende gneiss is the result of variations in bulk composition and not the result of variations in metamorphic grade, because as many as three different assemblages were observed in mafic hornblende gneiss at a single outcropping.

5.5 Summary of Metamorphic Conditions

Metamorphic conditions in the study-area have been qualitatively constrained, in the system KNMFASH, from phase assemblage data. The highest metamorphic grade observed, which may be defined by phase relations in the cordierite-garnet-K feldspar-zone metapelite and metagreywacke, must lie within the space bounded by reactions NMF-1, NMF-3, NMF-7, and NMF-9 (see figure 5.6). The appearance of orthopyroxene in mafic-hornblende gneiss defines the lower limit of the orthopyroxene-zone, which is not recognised in the system KNMFASH in the study-area. Sillimanite-K feldspar-zone and muscovite-quartz-zone metamorphic assemblages are present only within 5 km of the southern subprovince boundary in the southeast corner of the study-area.

MG_1 (internal) migmatization of metapelite and metagreywacke is best explained by partial melting. However, the unusual alkali-feldspar composition of MG_1 metapelite leucosome remains an unresolved problem.

The mineral assemblages observed in the study-area are consistent with areas of orthopyroxene-zone metamorphism studied further west in the English River Subprovince (Harris 1976, Breaks et. al 1978, Perkins and Chippera 1985). There is petrographic evidence that the activity of H_2O was less than one in some rock types, namely mafic hornblende gneiss and leucocratic Bt-Grt-Kfs gneiss, at orthopyroxene-zone and cordierite-garnet-K feldspar-zone metamorphic conditions.

The study-area and the English River subprovince as a whole is a transitional granulite terrain within the five-fold granulite classification scheme proposed by Newton and Perkins (1982). Transitional granulite terrains are typified by pressures of less than about 6.5 kbars, and temperatures of less than 750 ^{o}C, which are lower than those found in massif granulite terrains, the other major group (Newton and Perkins 1982).

6. GEOTHERMOMETRY AND GEOBAROMETRY

6.1 Introduction

Metapelite, metagreywacke, mafic hornblende gneiss, and locally metatonalite contain mineral assemblages suitable for geothermometry and geobarometry. Temperature estimates are based on Fe-Mg exchange between coexisting ferromagnesian phases which have been shown to be sensitive to changes in temperature and only slightly pressure dependent. Coexisting biotite and garnet in metapelite, metagreywacke and grey metatonalite were used to estimate metamorphic temperatures, based on the calibrations of Ferry and Spear (1978) and Perchuck and Lav'entera (1983). Coexisting orthopyroxene and garnet in mafic hornblende gneiss and grey metatonalite were used to estimate temperature, based on the calibration of Sen and Bhattacharya (1984).

Geobarometers based on equilibria among coexisting plagioclase-garnet-aluminosilicate-quartz and plagioclase-garnet-orthopyroxene-quartz are sensitive to changes in pressure and relatively insensitive to changes in temperature. Pressures based on coexisting plagioclase-garnet-orthopyroxene-quartz in hornblende mafic gneiss and grey metatonalite was calculated using Perkins and Newton (1981) geobarometer. Coexisting plagioclase-garnet-aluminosilicate-quartz was used to calculate pressures based on the geobarometer of Newton and Haselton (1981).

All Fe was assumed to be in the ferrous state for the purposes of geothermometry. Activity models for components in plagioclase, garnet, and orthopyroxene are those used in the calibrations, except that the activity model of anorthite in plagioclase from Newton and Perkins (1982) is used for the Newton and Haselton (1981) plagioclase-garnet-aluminosilicate-

quartz geobarometer. A temperature of 700 ^{o}C was assumed for geobarometry and a pressure of 4 kbars was assumed for geothermometry, based on the results of geothermometry and geobarometry in a study further west in the ERSp (Perkins and Chippera 1985).

The plagioclase-garnet-sillimanite-quartz geobarometer for metapelite melanosome, was used, despite the absence of either one of quartz or sillimanite. Within the study-area plagioclase, garnet, aluminosilicate, and quartz do not coexist. Reaction MF-1 (or NMF-1) resulted in the complete consumption of either quartz or sillimanite from the metapelite. All four phases did however coexist (presumably in equilibrium) up until the point at which either quartz or sillimanite was completely consumed by reaction MF-1.

At metamorphic conditions greater than reaction MF-1, divariant reaction R-1 would continue towards the right in metapelite, because plagioclase, the only reactant, is still present:

$$\underset{\text{(In Pl)}}{\text{Anorthite}} \rightleftharpoons \text{Sillimanite} + \underset{\text{(In Grt)}}{\text{Grossular}} + \text{Quartz} \qquad \text{(R-1)}$$

The garnet-sillimanite-plagioclase-quartz geobarometer is valid for cordierite-K feldspar metapelite (free of either quartz or sillimanite) if the following conditions are met: 1) the mole fractions of grossular in garnet and anorthite in plagioclase are not affected by divariant reactions other than R-5, and 2) the pressure is increasing. If pressure is decreasing then the pressure recorded should represent the pressure at which reaction MF-1 was crossed.

Univariant reaction MF-1 contains garnet as a product, and may therefore change the mole fraction of Ca in the garnet by diluting the garnet with Fe and Mg. However, reactions MF-1 and R-5 should behave in a

coupled manner until either quartz or sillimanite was consumed by reaction MF-1, at which point only reaction R-5 controls the mole fractions of grossular and anorthite.

6.2 Microprobe Strategy

Minerals were checked for zoning. It was found that zonation was restricted to a thin zone at the edge of garnet and orthopyroxene grains enriched in Fe relative to core analyses. No zoning was detected in biotite and plagioclase. In order to minimize the effects of re-equilibration rim analyses were avoided. All samples analyzed are from the orthopyroxene-zone.

Two strategies were followed in the selection of coexisting minerals for analysis:

1) Analysis of coexisting minerals in direct contact

2) Analysis of minerals in close proximity but not in direct contact.

This selection strategy follows the study of Indares and Martingole (1985), which suggests that the selection of mineral pairs not in direct contact may minimize the effects of re-equilibration during cooling. No systematic differences were noted between temperatures and pressures based on strategies 1 and 2.

6.3 Results of Geothermometry

Garnet-biotite temperature estimates using the calibration of Perchuck and Lav'entera (1983) yield an overall temperature range of 570-710 ^{o}C and a mean temperature of 670 ^{o}C (table 6.1). The results of the Ferry and Spear (1978) garnet-biotite calibration show an overall temperature range of 550-820 ^{o}C and a mean value of 720 ^{o}C (table 6.1).

Table 6.1. Results of Grt-Bt and Grt-Opx geothermometry.

		Grt-Bt Perchuck and Lav'entera			Grt-Bt Perry and Spear			Grt-Opx Sen and Bhattacharya		
Sample No.	Rock Type	Range (°C)	Mean (°C)	Number of Estimates	Range (°C)	Mean (°C)	Number of Estimates	Range (°C)	Mean (°C)	Number of Estimates
64B	p	610-690	660	4	581-750	680	4	640-690	660	3
147	p	670-730	700	2	720-840	780	2			
203	p	680-710	700	3	740-810	780	3			
3D	n	590-630	600	4	560-630	590	4			
111C	w	680-720	690	5	720-820	760	5			
157A	w	640-670	650	5	650-700	670	5			
28	l	640-650	640	3	650-700	660	3			
64C	l	660		1	690		1			
153A	l	640-660	650	2	660-680	670	2			
200	l		720	2	810-830	820	2			
1A	t	670-710	690	2	730-820	780	2			
139B	m							640-750	680	3
199A	m							620-710	670	2

Rock Types: p = Metapelite Melanosome, w = Metagreywacke Mesosome, l = MG2 Migmatite Leucosome, t = Grey Metatonalite, m = Mafic Gneiss

Table 6.2. Results of Grt-Sil-Pl-Qtz and Grt-Opx-Pl-Qtz geobarometry.

		Grt-Opx-Pl-Qtz Newton and Perkins			Grt-Sil-Pl-Qtz Newton and Haselton		
Sample No.	Rock Type	Range (kb)	Mean (kb)	Number of Estimates	Range (kb)	Mean (kb)	Number of Estimates
64B	p				3.8-5.0	4.3	3
147	p				3.5-4.0	3.8	2
203	p				3.0		2
28	li					5.3	1
1A	t	4.3-4.8	4.5	3			
139B	m	3.7-4.8	4.1	3			
199A	m	3.4-4.7	4	3			

Rock Types: p = Metapelite Melanosome, t = Grey Metatonalite, m = Mafic Gneiss, li = Metapelite inclusion in MG2 Migmatite Leucosome

The Garnet-orthopyroxene thermometer yields an overall temperature range of 618-750°C, and a mean value of 670°C (table 6.1).

There is good agreement between the garnet-biotite geothermometer of Perchuck and Lav'entera and the garnet-orthopyroxene geothermometer of Sen and Bhattacharya, both yielding mean values of 670°C. The Ferry and Spear calibration yields higher average temperatures. Several samples yield temperatures of greater than 800 °C, using the Ferry and Spear calibration, which is anomolously high given the absence of orthopyroxene in metapelite and metagreywacke. A garnet-clinopyroxene temperature of 730°C was obtained for a rock from within the study-area using the calibration of Ellis and Green (1979) (Percival et al. 1985).

6.4 Results of Geobarometry

Garnet-orthopyroxene pressure estimates yields a overall pressure range of 3.4-4.8 kbars, and a mean pressure of 4.2 kbars (table 6.2). Garnet-sillimanite geobarometry yields a overall pressure range of 3.0-5.3 kbars, and a mean pressure of 4.4 kbars (table 6.2).

There is good agreement between the two geobarometers used with cumulative mean pressures of 4.2 and 4.4 kbars. The results are in general agreement with those of Perkins and Chippera (1985).

6.5 Regional Temperature and Pressure Variations

The mean value, calibration uncertainty, and the 95% confidence interval[1] for the pressure and temperature estimates are given in table 6.3.

---

[1] 95% confidence interval = 1.96 x (sample standard deviation) / (square root of sample size).

Table 6.3. Summary of means, calibration uncertainties and 95% confidence intervals for pressure and temperatures estimates

Calibration	Mean	Calibration Uncertainty	95% confid. interval
Perchuck and Lav'entera (1983): Grt-Bt	670 °C	50	20
Ferry and Spear (1978): Grt-Bt	720 °C	50	50
Sen and Bhattacharya: Grt-Opx	670 °C	50	1
Newton and Haselton (1981): Grt-Als-Pl-Qtz	4.4 kb	1.5	-
Perkins and Newton (1982): Grt-Opx-Pl-Qtz	4.2 kb	1.5	- |-- 0.5[1]

1 Calculated for combined pressure estimates to obtain an adequate sample size.
i Insufficient sample size..

In each case the 95% confidence interval for the mean pressure or temperature estimate, based on natural variation, is less than the calibration uncertainty, except for the Ferry and Spear calibration where they are equal. This analysis indicates that there is no statistically valid temperature or pressure variation (gradient) within the orthopyroxene-zone, in the study-area.

7. STRUCTURE

Schistosity and gneissosity of all rock types strike east to southeast and dip generally steeply north, suggesting an overall monoformal structure. Biotite foliations, present in most metamorphic rocks, define an S1 surface parallel to lithologic contacts, including those between supracrustal rock types. Hence, the S_0 surface parallels the S_1 surface, or has been rotated into parallelism, to form a composite S_0/S_1 surface, although low angle S_0-S_1 intersections were observed locally. Hornblende lineations (L_1) are developed on the biotite foliation plane in grey metatonalite. A lack of distinctive marker horizons makes it impossible to evaluate the extent of isoclinal folding and/or faulting (D_1). Fault indicators (shearing, chloritized zones, and pseudotachylite (Station 225 in figure 3.2)) were observed locally, and minor folding of S_1 layering is common.

Lithologic contacts and foliations parallel the southern and northern subprovince boundaries. East of Smoothrock Lake the southern subprovince boundary is the Pashkokogan Lake-Kenoji Lake mylonite zone (PKmz), an easterly trending, vertically dipping zone, averaging 0.5 km in width. The well developed foliation in the mylonite zone forms the S_3 surface. Here, the PKmz separates metasedimentary and white granitoid rocks of the ERSp to the north from dominantly intermediate to mafic metavolcanic rock of the Wabigoon subprovince to the south (see figure 3.1). At Hollingsworth Lake, where the mylonite zone is well exposed, there is a northward transition from relatively undeformed metavolcanic rock into mafic mylonite (probably mylonitized mafic metavolcanic rock) into felsic mylonite and protomylonite (white granite and metagreywacke equivalents) and finally into non-mylonitic metasedimentary and white granitoid rock.

West of Hollingsworth Lake, at Smoothrock Lake, the PKmz bifurcates into two zones. The northern splay of the PKmz swings north into the ERSp, whereas the southern splay follows the southern subprovince boundary. The point at which the fault bifurcates is the eastern-most extent of the Winnipeg River Subprovince (cf. Card and Ciesielski 1986). West of this intersection, the northern splay of the PKmz separates orthopyroxene-zone rocks to the north, from medium grade rocks of the Winnipeg River Subprovince to the south.

Small scale disharmonic folding and ductile shearing (D_2) are common structures in metasedimentary rock exposures containing a significant proportion of intrusive migmatite leucosome. Small scale fold axes show no preferred orientation. The widespread appearance of disharmonic folding indicates that a strong competency contrast existed between MG_2 leucosome and the metasedimentary mesosome at the time of deformation, with the leucosome behaving in a less competent manner.

Evidence of a late shearing is preserved locally as C and S fabrics in metasedimentary rock, cutting the S_1 fabric. The late shearing and faulting may or may not be related to faulting at the subprovince boundary.

Convoluted and swirled inclusion trails of acicular sillimanite needles in cordierite of quartz-free metapelite, may record a deformation earlier than D_1. Alternatively they may simply represent disruption of the earlier L_1 sillimanite lineation by the nucleation and growth of the cordierite. The latter interpretation is favoured because there is no apparent pattern to the convolution of the inclusion trails.

The relative timing of deformation events recognized within the study-area is summarized in Table 7.1. Deformation events correlate well with, and represent a subset of those recognized by Thurston and Breaks

(1978), within a large portion of the western English River and Uchi Subprovinces.

Table 7.1. Relative timing of deformation events in the Whitewater-Mojikit Lakes study-area.

Deformation	Foliation	
	S_0/S_1	Lithologic contacts between supracrustal units, which parallels biotite foliation surface. (S_0 & S_1)[1]
D_1		Isoclinal folding and or faulting not recognized, but inferred to be present. (D_1)
D_2		Disharmonic folding associated with emplacement of intrusive migmatite leucosome. (D_2)
D_3	S_3	Late development of mylonite in major fault zone at southern boundary of ERSp. Possibly synchronous development of late shearing. (D_4 and S_4)

1 Values in parentheses represent corresponding deformation events of Thurston and Breaks (1978)

8. MG_2 (EXTERNAL) MIGMATIZATION

8.1 Introduction

The evidence of an external source for MG_2 leucosome was discussed in chapter 3. Chemical data, presented in chapter 4, showed that, at the level of exposure in the study-area, coexisting metagreywacke and metapelite could not represent the source of MG_2 leucosome. Metagreywacke, the dominant rock type, has the same chemical composition throughout the study-area regardless of metamorphic grade, and there is no evidence of significant depletion of any elements, with respect to lower grade equivalents. Cordierite-garnet-K feldspar- and orthopyroxene-zone metapelite melanosomes have been depleted in certain elements, however, these depletions are accounted for in the coexisting MG_1 leucosome. Furthermore, the composition of MG_1 metapelite leucosome differs from MG_2 leucosome. MG_2 leucosome must, therefore, have been derived from a source at depth and emplaced at the level of exposure.

The source of and process(es) which gave rise to MG_2 leucosome are examined in this chapter. A model for the origin of MG_2 migmatite is proposed which is consistent with the metamorphic and MG_1 migmatitic history of the study-area, and phase relations in the system KNMFASH.

8.2 The MG_2 (External) Migmatization Process

All MG_2 leucosome compositions are common igneous granitoid compositions (see figure 4.1), lacking the unusual chemical compositions of MG_1 metapelite leucosome. The majority are granites, with a smaller number of tonalites. Granodiorites are less common.

Discordant contacts between MG_2 leucosome and metasedimentary mesosome are common. Deformation of MG_2 migmatite with leucosome/mesosome ratios of greater than about 1/3, has resulted in the formation of disharmonic convolute folds in which there is not a consistent orientation of the axial surface of the folds. The development of disharmonic fold structures in MG_2 migmatite suggests that deformation occurred while the leucosome was less competent than the metasedimentary rock (mesosome).

The available evidence is consistent with an igneous origin for MG_2 leucosome. The style of folding is inconsistent with a subsolidus origin for MG_2 leucosome. The abundance of outcrop scale disharmonic folds associated with MG_2 leucosome (see plate 6.1) would be a logical consequence of the syntectonic intrusion of magma into a solid rock, which would greatly decrease the strength of the resulting rock-magma mixture (cf McLellan 1984). Hollister and Crawford (1986) have argued that melt enhanced deformation is a common feature in many high-grade metamorphic terrains.

Although necessarily biased by the lack of understanding of subsolidus migmatization processes, the available evidence leads to the conclusion that MG_2 leucosome was emplaced as magma.

8.3 Possible and Probable Origins of MG_2 (External) Migmatite Leucosome

The source region in which the parental melts of MG_2 leucosome formed must lie at some depth below that presently exposed in the study-area. Possible source rocks would include; metasedimentary rock, grey metatonalite, and deep crustal or mantle rock.

The absence of other syn-MG_2 leucosome plutonic rocks from which MG_2 leucosome could have evolved, would argue against the formation of MG_2 leucosome from mantle derived melts. For example, if the origin of MG_2

leucosome were calc-alkaline arc type magma, then one would expect a variety of syn-MG_2 plutonic rocks and not only granitoid MG_2 leucosome compositions as observed. The only plutonic rocks which may be syn-MG_2 leucosome are the pink granite dykes, intrusive into grey metatonalite. The chemical composition of these dykes is similar to that of granitic MG_2 leucosome. However, it is unlikely, for several reasons, that pink granite and MG_2 leucosome share a common parent, with assimilation of metasedimentary rock responsible for the differences between them. For one, pink granite is restricted to granite in composition, and it is unlikely that an originally granitic melt could assimilate enough plagioclase and quartz (which would raise the solidus temperature) to produce the variability of MG_2 leucosome observed. Even if it were possible, assimilation would also be expected in pink granite resulting in more tonalitic variants.

Partial melting of grey metatonalite is also a possible source material for MG_2 leucosome (and perhaps a probable source for pink granite). However, if metatonalite underwent partial melting at depth, then the much more abundant metasedimentary rock should also have partially melted. Unless the proportion of grey metatonalite or similar rock is much greater at depth than at the level of exposure, the proportion of grey metatonalite is insufficient to account for the large quantity of MG_2 leucosome. Based on gravity modeling further west in the ERSp, Gupta and Barlow (1983) have estimated that metagreywacke, with smaller amounts of interlayered metapelite, extends to a depth of about 10 km below the level presently exposed.

There are several features of MG_2 leucosome that are commonly associated with S-type granitoid rocks, interpreted to form by the partial

melting of metasedimentary rock (cf. Chapple and White 1972). These features include:

1) The mafic minerals present in MG_2 leucosome are also present in the metasedimentary rock in the study-area and their chemical compositions are the same.

2) The white colour of MG_2 leucosome and the presence of ilmenite as opposed to magnetite or hematite as the opaque mineral.

3) The An content of plagioclase in MG_2 leucosome is less than or equal to that of plagioclase in metasedimentary mesosomes.

Partial melting of the abundant metasedimentary rock at depth is the most logical source for MG_2 leucosome. At the level of exposure in the study-area, significant melting has not occurred in metagreywacke, but may have in metapelite. Aside from the difference in composition between MG_1 metapelite leucosome and MG_2 leucosome, the proportion of leucosome which could be produced from metapelite is insufficient to account for the proportion of MG_2 leucosome in the study-area. The proportion of metapelite is, in total, only about 10%, which is approximately one-third on the proportion of MG_2 leucosome. Metagreywacke, which constitutes approximately 65% of the study-area, represents the most probable source at depth, of MG_2 leucosome, with metapelite and leucocratic Bt-Grt-Kfs gneiss making contributions.

Depending on the a_{H2O} and the P-T path of metamorphism, initial melting of metagreywacke could occur either at the tonalite solidus or reaction NMF-7. In addition, a significant proportion of melt could be produced by H_2O-phase absent melting of metagreywacke by the reaction NMF-6. A reaction similar to NMF-6 has been inferred in other metasedimentary terrains in the Superior Province exposed to somewhat higher metamorphic grades (Percival 1983b and personal communication 1987).

Initial H_2O-phase present melting of metagreywacke may therefore produce vapour-saturated tonalitic melts (cf. Ashworth 1976, 1985, Percival 1983b). With increasing temperature, biotite begins to break down by reaction NMF-7 or NMF-6, and melts produced will be granitic. Partial melting of metapelite and leucocratic Bt-Grt-Kfs gneiss will produce granitic melts. Partial melting and mixing of melts from metagreywacke, metapelite, and leucocratic Bt-Grt-Kfs gneiss could produce the variability in MG_2 leucosome compositions observed in the study-area.

8.4 A Model of the Origin of MG_2 (external) Migmatite in the Whitewater-Mojikit Lakes Study-area

A model will be developed for the origin of MG_2 (external) migmatite in the study-area, which is consistent with phase and melting relations discussed in chapter 5 and with metamorphic conditions in the study-area. The phase relations in the system KNMFASH are shown in figure 8.1, along with an inferred geothermal gradient for the study-area. The model is outlined in figure 8.2 and is keyed to the reactions in figure 8.1. The model is consistent with or without melting having occurred in the metapelite at the present level of exposure. The absence of significant melting in metagreywacke is critical to the model.

Partial melting occurred at some depth below that which is presently exposed in the study-area. Metapelite and leucocratic biotite-garnet-K feldspar gneiss were the first rocks to melt at temperatures exceeding reaction NMF-9 and the granite solidus respectively. Melting in metapelite probably occurred at the level presently exposed. Melting of leucocratic Bt-Grt-Kfs gneiss occurred at deeper levels, because it contained a lower a_{H2O} or a lower absolute abundance of H_2O. Migration of the melt was limited by the surrounding metagreywacke, which was still solid.

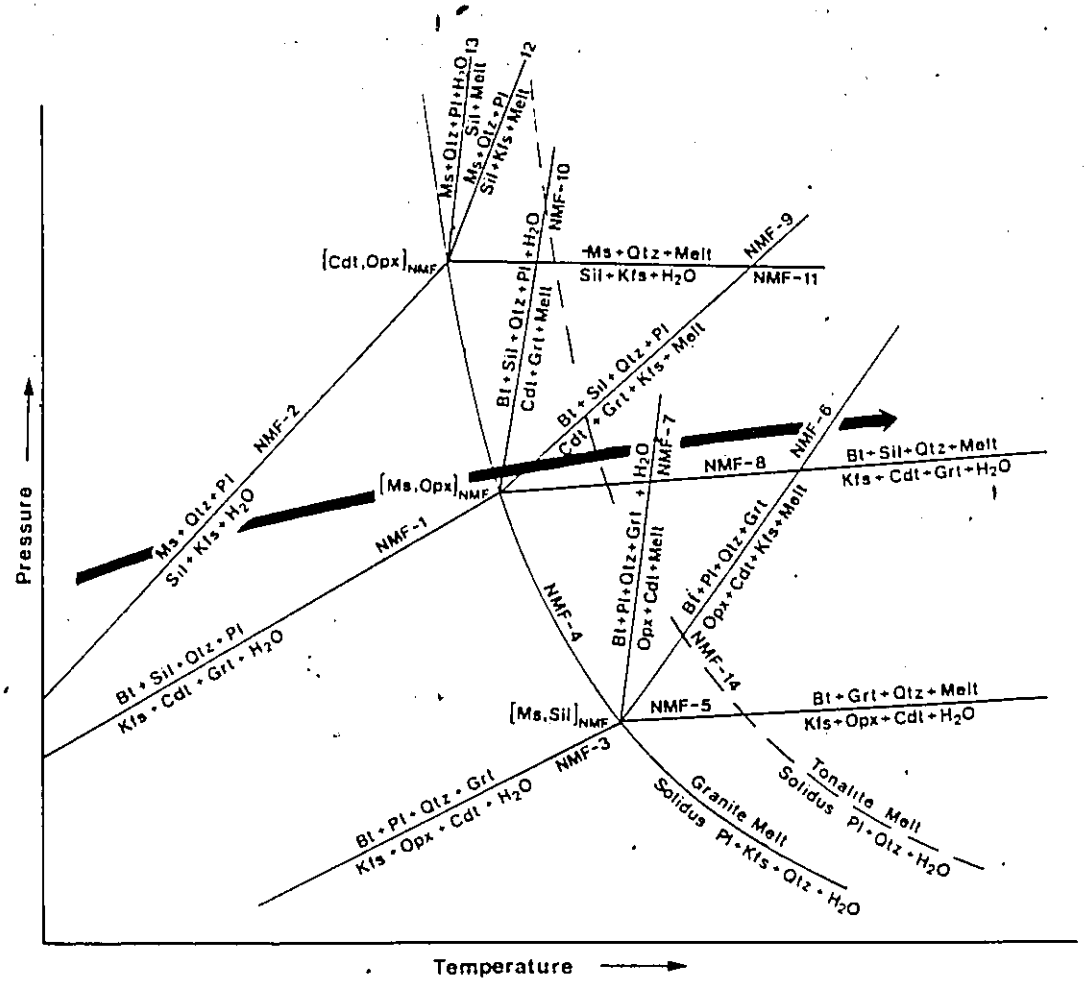

Figure 8.1. Schematic phase relations in the system KNMFASH, resulting in a topology consistent with the internal (MG_1) and external (MG_2) migmatization of the study area.

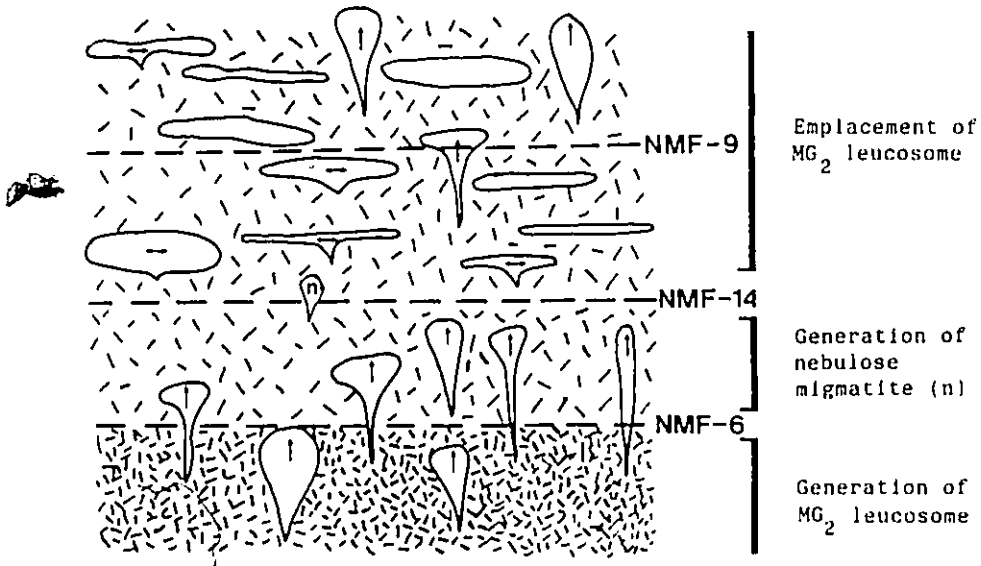

Figure 8.2. Schematic model cross section, for the generation of migmatites in the Whitewater-Mojikit Lakes area.

Initial melting of metagreywacke occurred at conditions exceeding the tonalite solidus (NMF-14) yielding tonalitic melts. Additional melting may have occurred as temperature exceeded reaction NMF-7. Subsequent melting occurred by reaction NMF-6 (H_2O-phase-absent), resultant in the formation of granitic melts.

Melting would continue without significant segregation or migration of the melt until some critical volume of melt was produced in metagreywacke (cf. van der Molen and Paterson 1979). Once this critical proportion of melt was achieved the rock would respond to stress in a melt dominated system, and partial melts from all rock types would begin to separate from the residual crystals, and to rise and coalesce. Tonalitic to granitic metagreywacke partial melts and granitic metapelite and leucocratic biotite-garnet-K feldspar gneiss partial melts would mix in variable proportions depending on their relative abundance in the source region. Granodioritic and tonalitic magmas would also assimilate MG_1 metapelite and metagreywacke leucosome as they rose through the rock column.

Emplacement of these magmas at the present level of exposure resulted in the MG_2 migmatization of the study-area. The introduction of magma into metagreywacke and metapelite host rock under orthopyroxene-zone conditions could result in the partial assimilation of the host rock into the MG_2 leucosome, modifying leucosome and host rock compositions. This would explain the development of schlieric migmatite in exposures where the proportion of MG_2 leucosome is high. Deformation would be facilitated by the intrusion of MG_2 leucosome magma, giving rise to the abundant small scale deformation structures, which are most common when MG_2 leucosome is present in large amounts.

Where the proportion of external leucosome is low, the extent of assimilation would be low, since the mesosome would not be heated to the same extent, and the intrusive magma would cool more rapidly. Where the proportion of MG_2 leucosome is low, evidence of assimilation of MG_2 stromatic migmatite external leucosome is limited to the local development of thin melanosome rims a few millimeters wide, at the leucosome-mesosome contacts.

The thermal contribution of MG_2 migmatization is not primarily responsible for MG_1 migmatization in metapelite, because MG_1 migmatization predates MG_2 migmatization. MG_1 migmatization is therefore inferred to be a consequence of the same regional thermal event which gave rise to MG_2 magma production at depth.

Further modification of MG_2 leucosome compositions towards more tonalitic compositions could result from the extraction of eutectic or near eutectic granitic melts during the final stages of crystallization of granodioritic to tonalitic MG_2 leucosome. These granitic melts could give rise to the late white biotite pegmatite dykes and possibly some of the more potassic MG_2 leucosome found throughout much of the study-area. This would account for the close chemical similarity of white biotite pegmatite and MG_2 leucosome (see figure 4.4). The granoblastic texture of tonalitic MG_2 leucosome is consistent with early emplacement and crystallization, followed by solid state adjustment of grain boundaries.

The virtual absence of orthopyroxene from MG_2 leucosome is likely a combination of residual orthopyroxene being separated from the melt during ascension of the magma and complete reaction of the remaining orthopyroxene with the melt during crystallization, to form biotite (cf. Clemens and Wall 1981).

The occurrence and habit of cordierite in MG_2 leucosome is very similar to that reported by Phillips et al. (1981) for the Strathbogie batholith in Australia. These authors interpreted the crystallization of the melt to have begun at a temperature of 750-850 ^{o}C and a pressure of greater than 4 kbars. Cordierite was interpreted to be a late crystallizing phase. An experimental study by Clemens and Wall (1981), has shown that cordierite is a near solidus phase at pressures near 5 kbars. Cordierite in MG_2 leucosome, produced by reaction NMF-6 and/or NMF-7 in metagreywacke, would be incorporated into the melt, and cordierite subsequently crystallized as tabular euhedral crystals.

The nebulose migmatite at Mojikit lake, which has the same bulk chemical and mineralogical composition as metagreywacke mesosome, can not be explained simply by assimilation of metasedimentary rock into MG_2 leucosome. The nebulose migmatite may have formed by H_2O-phase-present partial melting of metagreywacke, at the tonalite solidus, followed by emplacement, without significant liquid-crystal segregation, at a higher level as a crystal mush. Spatial variations in the a_{H2O} in metagreywacke may be responsible for the localized occurrence of nebulose migmatite. It is possible that some of schlieric migmatite may also have formed in a similar manner, but underwent a higher degree of liquid-crystal segregation prior to emplacement.

Rather than a simple process of emplacement of melts derived by partial melting at depth, external (MG_2) migmatization in the Whitewater-Mojikit Lakes study-area was a complex and dynamic process involving the step-wise melting of several rock types at depth, combined with the processes of assimilation, magma mixing, and variable degrees of liquid-crystal segregation.

9. CONCLUSIONS

The lithology of Whitewater-Mojikit Lakes study-area is dominated by migmatitic metasedimentary rock, mainly metagreywacke, with subordinate metapelite, and minor metamorphosed banded iron formation and mafic hornblende gneiss. Foliated grey metatonalite represents the only recognizable pre-metamorphic intrusive rock type.

Metamorphic grade is in the orthopyroxene-zone, except for a small area in the southern part of the study-area, where metamorphic grade decreases to muscovite-quartz zone, medium-grade conditions, near the southern subprovince boundary. Geothermometry and geobarometry indicates metamorphic conditions reached at least 670 ± 50^{o} C and 4 ± 1.5 kbars.

Progressive metamorphism has resulted in two phases of migmatization. Early (MG_1) internal migmatization is recognized within metapelite and possibly within metagreywacke. MG_1 migmatites are believed to have formed by partial melting, although the evidence is equivocal. Migmatization is absent in leucocratic Bt-Grt-Kfs gneiss, indicating that the a_{H2O} was less than unity in this rock type and/or had a low abundance of H_2O.

Later MG_2 (external) migmatization occurred as a result of the intrusion of magma generated by melting of the crust at depth, and was responsible for most of the migmatite leucosome in the study-area. Partial melting of metagreywacke by reactions NMF-14 (tonalite solidus), NMF-7, and NMF-6 represents the most likely source of external (MG_2) leucosome, with a contribution from metapelite and leucocratic Bt-Grt-Kfs gneiss. Melting of metagreywacke can result in the generation of melts of granitic to tonalitic composition, whereas melting of metapelite should produce only granitic melts (for the P-T path inferred). Melting of metasedimentary rock, primarily metagreywacke, can produce the chemical variability of MG_2

leucosomes observed. The removal of water enriched, near-eutectic melts during the final stages of crystallization of MG_2 leucosome magma may have further modified MG_2 magma compositions and may have given rise to the late, white biotite pegmatite dikes common in the study-area. Textural evidence, comparison with existing experimental studies, and field observations indicate that cordierite crystallized in a melt in MG_2 leucosomes.

The metamorphism and migmatization of the metagreywacke and metapelite could be treated in the system KMFASH for melt-absent equilibria and in the system KNMFASH for melt-present equilibria. Quantification of the equilibria in these systems awaits more complete and consistent thermodynamic data, an area in which rapid progress is being made.

The lithology and distribution of metamorphic zones in the Whitewater-Mojikit Lakes study-area is characteristic of the English River Subprovince (cf. Breaks et al. 1978, Thurston and Breaks 1978), and therefore the conclusions reached in this study should be applicable to the metamorphism and migmatization of the English River Subprovince as a whole.

Further research is required in the areas surrounding the present study-area, to delimit the full extent of orthopyroxene-zone high-grade metamorphism. Further petrographic and chemical data on MG_1 migmatites would aid in identifying the mechanism of migmatization more conclusively.

References

Ashworth, J.R. (1985) Introduction; in Migmatites. J.R. Ashworth (Editor), Blackie, London, pp. 1-35.

Ashworth, J.R. (1976) Petrogenesis of migmatites in the Huntly-Portsoy area, northeast Scotland; Mineralogical Magazine, Vol. 40, pp. 661-682.

Ashworth, J.R. and McLellan, E. (1985) Textures; in Migmatites. J.R. Ashworth (Editor), Blackie, London, pp. 180-203.

Beakhouse, G.P. (1977) A subdivision of the western English River subprovince; Canadian Journal of Earth Sciences, Vol. 14, pp. 1481-1489.

Bowen, N.L. (1913) The melting phenomena of the plagioclase feldspars; American Journal of Science, Vol. 35, pp. 577-599.

Breaks F.C., Bond W.D. and Stone D. (1978) Preliminary geological synthesis of the English River Subprovince, Northwestern Ontario and its bearing upon mineral exploration; Ontario Geological Survey, Miscellaneous Paper 72.

Burnham, C.W. (1979) Magmas and hydrothermal fluids; in Geochemistry of Hydrothermal Ore Deposits (2nd Edition.), H.L. Barnes (Editor), John Wiley, New York, pp. 71-136.

Card, K.D. and Ciesielski (1986) DNAG #1. Subdivisions of the Superior Province of the Canadian Shield, Geoscience Canada, Vol. 13, No. 1, pp. 5-13.

Chappell, B.W. and White, A.J.R. (1974) Two contrasting granite types; Pacific Geology, Vol. 8, pp. 173-174.

Clemens, J.D. and Wall, V.J (1981) Origin and crystallization of some peraluminous (S-type) granitic magmas, Canadian Mineralogist, Vol. 19, pp. 111-131.

Davies, J.C. and Pryslak, A.P. (1966) Savant-Caribou Lakes Sheet, District of Thunder Bay; Ontario Department of Mines, Preliminary Geological Map P. 352.

Dietvorst, E.J.L. (1980) Biotite breakdown and the formation of gahnite in metapelitic rocks from Kemio, southwest Finland; Contributions to Mineralogy and Petrology, Vol. 75, pp. 327-337.

Ellis, D.J. and Green, D.H. (1979) An experimental study of the effect of Ca upon garnet-clinopyroxene Fe-Mg exchange equilibria; Contributions to Mineralogy and Petrology, Vol. 71, pp. 13-22.

Ferry, J.M. and Spear, F.S. (1978) Experimental calibration of the partitioning of Fe and Mg between biotite and garnet; Contributions to Mineralogy and Petrology, Vol. 66, pp. 113-117.

Grant, J.A. (1985) Phase equilibria in low-pressure partial melting of pelitic rocks; American Journal of Science, Vol. 285, pp. 409-435.

Grant, J.A. (1973) Phase equilibria in high-grade metamorphism and partial melting of pelitic rocks; American Journal of Science, Vol. 273, pp. 289-317.

Gupta, V.K. and Barlow, R.B. (1984) A detailed gravity profile across the English River Subprovince, northwestern Ontario; Canadian Journal of Earth Sciences, Vol. 21, No. 2, pp. 145-151.

Hanson, G.N. (1978) The application of trace elements to the petrogenesis of igneous rocks of granitic composition; Earth and Planetary Science Letters, Vol. 38, pp. 26-43.

Harris, N.B.W. (1976) The significance of garnet and cordierite from the Sioux Lookout region of the English River Gneiss Belt, northern Ontario; Contributions to Mineralogy and Petrology, Vol. 55, pp. 91-104.

Harris, N.B.W. and Goodwin, A.M. (1976) Archean rocks from the eastern Lac Seul region of the English River Gneiss Belt, northwestern Ontario, part 1. Petrology, chemistry, and metamorphism; Canadian Journal of Earth Sciences, Vol. 13, pp. 1201-1211.

Hess, P.C. (1969) The metamorphic paragenesis of cordierite in pelitic rocks; Contributions to Mineralogy and Petrology, Vol. 24, p. 191-207.

Hoffer, E. and Grant, J.A. (1980) Experimental investigation of the formation of cordierite-orthopyroxene parageneses in pelitic rocks; Contributions to Mineralogy and Petrology, Vol. 73, pp. 15-22.

Holdaway, M.J. and Lee, S.M. (1977) Fe-Mg cordierite stability in high-grade rocks based on experimental, theoretical, and natural observations; Contributions to Mineralogy and Petrology, Vol. 63, pp. 175-198.

Hollister, L.S. and Crawford, M.L. (1986) Melt-enhanced deformation: A major tectonic process; Geology, Vol. 14, pp. 558-561.

Indares, A. and Martingole, J. (1985) Biotite-garnet geothermometry in granulite-facies rocks: an evaluation of equilibrium criteria; Canadian Mineralogist, Vol. 23, pp. 187-193.

Johannes, W. (1985) The significance of experimental studies for the formation of migmatites; in Migmatites. J.R. Ashworth (Editor), Blackie, London, pp. 36-85.

Johannes, W. (1984) Beginning of melting in the granite system Qz-Or-Ab-An-H_2O; Contributions to Mineralogy and Petrology, Vol. 86, p. 264-273.

Johannes, W. (1983) On the origin of layered migmatites; in Migmatite, Melting and Metamorphism. M.P. Atherton and C.D. Gribble (Editors).

Johannes, W. (1978) Melting of plagioclase in the system Ab-An-H_2O and Qz-Ab-An-H_2O at P_{H2O}=5 kbars, an equilibrium problem; Contributions to Mineralogy and Petrology, Vol. 66, pp. 295-303.

Johannes, W. and Gupta, L.N. (1982) Origin and evolution of a migmatite; Contributions to Mineralogy and Petrology, Vol. 79, pp. 114-123.

Knabe, W. (1970a) Reaktionen des Biotits bei der anatexis; Geol. Jb. Abb, Vol. 88, pp. 355-372.

Knabe, W. (1970b) Anatexis von Quarz-Plagioklas-Biotit-Metamorphiten; Geol. Jb. Abb., Vol. 89, pp. 1-32.

Kretz, R. (1966) Metamorphic differentiation at Einasleigh, north Queensland; Geological Society of Australia Journal, Vol. 13, pp. 561-582.

Krogh, T.E., Harris, N.B.W. and Davis, G.L. (1976) Archean rocks from the eastern Lac Seul region of the English River Gneiss Belt, northwestern Ontario, part 2. Geochronology; Canadian Journal of Earth Sciences, Vol. 13, pp. 1212-1215.

Lindh, A. and Wahlgren, C (1985) Migmatite formation at subsolidus conditions - an alternative to anatexis; Journal of Metamorphic Geology, Vol. 3, pp. 1-12.

Luth, W.C., Jahns, R.H. and Tuttle, O.F. (1964) The granite system at pressures of 4 to 10 kb; Journal of Geophysical Research, Vol. 69, pp. 759-773.

McLellan, E. (1984) Deformational behaviour of migmatites and problems of structural analysis in migmatite terrains; Geological Magazine, Vol. 121, pp. 339-345.

Mehnert, K.R. (1968) Migmatites and the Origin of Granitic Rocks. Elsevier, Amsterdam.

Misch, P. (1968) Plagioclase compositions and non-anatectic origin of migmatitic gneisses in Northern Cascade mountains of Washington state; Contributions to Mineralogy and Petrology, Vol. 17, pp. 1-70.

Newton, R.C. and Haselton, H.T. (1981) Thermodynamics of the garnet-plagioclase-Al_2SiO_5-quartz geobarometer; in Thermodynamics of Minerals and Melts. R.C. Newton, A. Navrotsky and B.J. Wood (Editors), Springer-Verlag, New York, pp. 131-147.

Newton, R.C. and Perkins, D. (1982) Thermodynamic calibration of geobarometers based on the assemblages garnet-plagioclase-orthopyroxene (clinopyroxene)-quartz; American Mineralogist, Vol. 67, pp. 203-222.

Oliver, G.J.H. (1977) Feldspathic hornblende and garnet granulites and associated anorthosite pegmatites from Doubtful Sound, Fiordland, New Zealand; Contributions to Mineralogy and Petrology, Vol. 65, pp. 111-121.

Olsen, S.N. (1985) Mass balance in migmatites; in Migmatites, J.R. Ashworth (Editor), Blackie, London, pp. 145-179.

Olsen, S.N. (1983) Open- and closed-system migmatites in the Front Range, Colorado; American Journal of Science, Vol. 282, pp. 1596-1622.

Perchuck, L.L. and Lav'rentera, I.V. (1983) Experimental investigation of exchange equilibria in the system cordierite-garnet-biotite; in Kinetics and Equilibrium in Mineral Reactions (S.K. Saxena Editor), Springer Verlag, New York, p. 199-239.

Percival, J.A. (1983a) Preliminary results of geological synthesis of the Western Superior Province; in Geological Survey of Canada, Paper 83-1A, p. .

Percival, J.A. (1983b) High-grade metamorphism in the Chapleau-Foleyet Area, Ontario; American Mineralogist, Vol. 68, pp. 667-686.

Percival, J.A., Stern, R.A. and Digel, M.R. (1985) Regional geological synthesis of western Superior Province, Ontario; in Geological Survey of Canada, Paper 85-1A, pp. 385-397.

Perkins, D. and Chippera, S.J. (1985) Garnet-orthopyroxene-plagioclase-quartz barometry: refinement and application to the English River subprovince and the Minnesota River valley; Contributions to Mineralogy and Petrology, Vol. 89, pp. 69-80.

Perkins, D. and Newton, R.C. (1981) Charnockite geobarometers based on coexisting garnet-pyroxene-plagioclase-quartz; Nature, Vol. 292, pp. 144-146.

Phillips, G.N., Wall, V.J and Clemens, J.D. (1981) Petrology of the Strathbogie Batholith: A cordierite-bearing granite; Canadian Mineralogist, Vol. 19, pp. 47-63.

Plant, A.B. and Lachance, G.R. (1973) Quantitative electron microprobe analysis using an energy dispersive spectrometer; Proceedings of the Eighth National Conference of Electron Probe Analysis, New Orleans, Paper 13.

Powell R. (1983) Equilibrium Thermodynamics in Petrology; Harper and Row, London.

Pye, E.G. and Harris, F.R. (1965) Mojikit Lake Sheet, District of Thunder Bay; Ontario Department of Mines, Preliminary Geological Map P. 267.

Ramberg, H. (1952) The Origin of Metamorphic and Metasomatic Rocks.

Reinhardt, E.W. (1968) Phase relations in cordierite-bearing gneisses from the Gananoque area, Ontario; Canadian Journal of Earth Sciences, Vol. 5, p. 455-482.

Robin, P-Y (1979) Theory of metamorphic segregation and related processes; Geochimica Cosmochimica Acta, Vol. 43, pp. 1587-1600.

Sage, R.P., Breaks, F.W., Stott, G.M., McWilliams, G.M. (1974) Operation Ignace-Armstrong, Pashkokogan-Caribou Lakes Sheet, District of Thunder Bay, Ontario Division of Mines, Preliminary Map P. 962.

Sawyer, E.W. and Robin, P-Y,F. (1986) The subsolidus segregation of layer-parallel quartz-feldspar veins in greenschist to upper amphibolite facies metasediments; Journal of Metamorphic Geology, Vol. 4, p. 237-260.

Schreinemakers, F.A.H. (1915-1925) In-, mono-, and divariant equilibria (English Edition); Koninkl. Akad. Wetenschappen te Amsterdam Proc., Vol. 18-28.

Sen, S.K. and Bhattacharya, A. (1984) An orthopyroxene-garnet thermometer and its application to the Madras charnockites; Contributions to Mineralogy and Petrology, Vol. 88, 64-71.

Stormer Jr., J.C. (1975) A practical two-feldspar geothermometer; American Mineralogist, Vol. 60, pp. 667-674.

Stott, (1984) Geological compilation map of the Mojikit Lake area; Ontario Geological Survey, Compilation map P. 265 rev..

Streckeisen, A. (1976) To each plutonic rock its proper name; Earth-Science Reviews, Vol. 12, pp. 1-33.

Thompson A.B. (1982) Dehydration melting of pelitic rocks and the generation of H_2O-undersaturated granitic liquids; American Journal of Science, Vol. 282, pp. 1567-1595.

Thurston P.C. and Breaks F.W. (1978) Metamorphic and tectonic evolution of the Uchi-English River Subprovince; in Metamorphism in the Canadian Shield, Geological Survey of Canada, Paper 78-10, pp. 49-62.

Turner, F.J. (1981) Metamorphic Petrology: Mineralogical, Field, and Tectonic Aspects, Second Edition. Hemisphere, Washington.

Tuttle, O.F. and Bowen, N.L. (1958) Origin of granite in the light of experimental studies in the system $NaAlSi_3O_8$-$KAlSi_3O_8$-SiO_2-H_2O; Memoir, Geological Society of America, No. 74.

Usdansky, S.I. (1986) PERANORM: A basic program to calculate a modal norm for peraluminous granitoids; Computers and Geosciences, Vol. 12, p. 13-20.

van der Molen and Paterson, M.S. (1979) Experimental deformation of partially melted granite; Contributions to Mineralogy and Petrology, Vol. 70, pp. 299-318.

Veilzeuf, D. and Boivin, P (1984) An algorithm for the construction of petrogenetic grids: application to some equilibria in granulitic paragneisses; American Journal of Science, Vol. 284, pp. 760-791.

Waters, D.J. and Whales, C.J. (1984) Dehydration melting and the granulite transition in metapelites from southern Namaqualand, S. Africa; Contributions to Mineralogy and Petrology, Vol. 88, pp. 269-275.

White, A.J.R. (1966) Genesis of migmatites from the Palmer region of South Australia; Chemical Geology, Vol. 1, pp. 165-200.

White, A.J.R. and Chappell, B.W. (1977) Ultrametamorphism and granitoid genesis; Tectonophysics, Vol. 43, pp. 7-22.

Winkler, H.G.F. (1979) Petrogenesis of Metamorphic Rocks, Fifth Edition. Springer-Verlag, New York.

Wyllie, P.J. (1983) Experimental studies on biotite- and muscovite-granites and some crustal magmatic sources; in Migmatites, Melting and Metamorphism, M.P. Atherton and C.D. Gribble (Editors), Shiva, Cheshire, U.K., pp. 12-26.

Wyllie, P.J. (1977) Crustal anatexis: an experimental review; Tectonophysics, Vol. 43, pp. 41-71.

Yardley, B.W.D. (1978) Genesis of the Skagit Gneiss migmatites, Washington, and the distinction between possible mechanisms of migmatization; Geological Society of America Bulletin, Vol. 89, pp. 941-951.

Zen, E-an (1966) Construction of pressure-temperature diagrams for multicomponent systems after the method of Schreinemakers-a geometric approach; U.S. Geological Survey, Bulletin 1225, 56 p..

APPENDIX A

Analytical Methods, Accuracy, and Precision

Whole Rock Analysis

Thin sections of samples chosen for whole rock analysis were examined to ensure that samples were essentially unaltered. Sample size collected varied according to the grain size and heterogeneity of the rock being sampled.

Rock Type	Min. Diam. of Sample
Metagreywacke Mesosome	10 cm
Metapelite Melanosome	10 cm
Leucocratic biotite-garnet-K feldspar Gneiss	15 cm
Grey Metatonalite	10 cm
MG_2 Migmatite Leucosome	15-20 cm
MG_1 Migmatite	15-20 cm
White biotite pegmatite	15-20 cm

For MG_1 metapelite and metagreywacke migmatite samples the coexisting melanosome/mesosome and leucosome fractions were separated. These samples were cut into 1 cm thick slices, from which the leucosome and melanosome/mesosome fractions were separated by cutting out the leucosome fraction.

Samples were broken into fragments of less than 1.5 cm in a jaw crusher. The sample was then mixed and then split in half repeatedly until the sample was reduced to about 40 cm^3. This amount of sample was crushed to a fine powder (< 200 mesh) in a shatterbox. The powdered sample was submitted to Mr. R. Hartree at the University of Ottawa, for X-ray Fluorescence Analysis of major and selected trace elements.

Mineral Separation

Biotite, K feldspar, and plagioclase were separated from selected samples of metagreywacke mesosome, metapelite melanosome, and MG_2 migmatite leucosome. Small chips of sample were powdered by hand in a mortar and pestle. The powder was sieved and the 60 to 170 mesh fraction was retained for separation.

Magnetite was removed from the sample by hand with a hand magnet. Biotite, garnet, ilmenite, and cordierite (when present) were separated from feldspars and quartz using a Franz isomagnetic separator, on high amperage. Garnet was separated from biotite and cordierite with the Franz.

Final separation was performed by heavy liquid separation. Methylene iodide (S.G. 3.3) diluted with ethanol was used to produce the following separates; K feldspar, plagioclase-quartz, and garnet-ilmenite. Garnet and ilmenite were separated using Clerici's solution (S.G. 4.3). Plagioclase (S.G. 2.63-2.66) could not be separated from quartz (S.G. 2.65), so the two were analyzed together and the analyses recalculated assuming quartz is pure SiO_2. At least two passes were made with each separate fraction to ensure purity.

The resulting separates were checked for purity by examining approximately 400 grains of each sample under a binocular microscope. The K feldspar and plagioclase-quartz fractions were etched in HF and stained with sodium cobaltnitrate prior to examination. Greater than 99% purity was achieved for biotite, garnet, and K feldspar fractions. Greater than 95% purity was obtained for plagioclase-quartz fractions except for sample 64B (metapelite melanosome) for which only 90% purity could be obtained, despite repeated passes through the heavy liquid.

The separates were crushed to a fine powder and submitted for X-ray fluorescence analysis.

Precision and accuracy of X-ray Fluorescence Analysis

X-ray fluorescence analysis was carried out at the University of Ottawa, by Mr. Ron Hartree, using a Philips PW 1410/20 AHP instrument. All Fe was originally calculated as Fe_2O_3 and was recalculated into FeO by the author.

Accuracy was determined by co-analyzing natural rock standard DR/N, and little if any systematic error was detected. The standard accuracy of the XRF method may be represented by 95% confidence limits of the precision data (1.96 x Wt % (or ppm) x COV). Estimates of the standard precision of the whole rock chemical analyses (XRF) is given in table A.1, and were determined by repeat analysis (including fusion) of natural rock standards.

Table A.1. Precision of chemical analyses[1]

Oxide/Element	COV
SiO_2	0.9
Al_2O_3	0.8
TiO_2	0.8
FeO	0.8
MgO	1.0
MnO	4.0
CaO	0.8
Na_2O	2.0
K_2O	1.2
P_2O_5	4.0
Ba	10
Zr	10
Sr	4
Rb	40
Y	20
Ni	30
V	20

1 Expressed as coefficient of variation, (COV) = 100(standard deviation/mean)

Precision and accuracy of Electron Microprobe Analysis

Electron microprobe analyses were performed, by the author, at the Geological Survey of Canada, Ottawa. The analyses were obtained using a Material Analysis Company (MAC) electron microprobe, equipped with a Kevex energy dispersive spectrometer, and automated to produce simultaneous multi-element analysis and data reduction (Plant and Lachance 1973). Operating conditions were as follows: 20KV acceleration voltage, specimen current of 10 nanoamperes measured on a standard Kaersutite and a counting time of 100 seconds. The feldspars were analyzed for Na, Al, Si, K, Ca, Fe; all other minerals were analyzed for the following 10 elements: Si, Ti, Al, Cr, Fe, Mn, Mg, Ca, Na, K.

Under the above conditions of analysis, the determinations have a relative accuracy of 1 to 2% for major elements and up to 10% for minor elements. The relative accuracies were determined using natural standards (M. Bonardi, personal communication 1987).

APPENDIX B

METANORM: A volume normative calculation

Point count estimates of MG_1 and MG_2 leucosomes and metapelite melanosomes yielded inconsistent and unsatisfactory results. For metapelite melanosome the difficulties were due to the complex and variable texture and intergrowth pattern and the difficulty in distinguishing cordierite and plagioclase. For leucosomes the coarse grain size would require the examination of a great number of thin sections per sample and the resources were not available to produce the number of sections required. Point counting of stained slabs was performed for some MG_2 leucosome samples but again the results were unsatisfactory.

To overcome these problems, a volume normative calculation was applied to the rocks. The calculation coined METANORM here was developed by the author, and is loosely based on the the normative calculation PERANORM (Usdansky 1986). However, METANORM differs markedly from PERANORM in the treatment of the phases biotite, garnet, cordierite, and sillimanite. The calculation can be summarized in the following steps.

(1) Conversion of weight percent oxides to mole percent oxides.

(2) Conversion of all Fe to Fe^{2+}.

(3) FeO, MgO, and MnO were combined to form FMMO.

Oxides were combined to form minerals in the following order. Oxides in parentheses represent the oxide which determines the proportion of the mineral formed.

(4) Apatite $Ca_5(PO_4)_3(OH)$ (P_2O_5)

(5) Albite $NaAlSi_3O_8$ (Na_2O)

(6) Biotite (K_2O) To account for Al substitution in natural biotite compositions the formula of the biotite by microprobe analysis was used.

For samples for which biotite analyses are not available, the average available biotite composition for that rock type was used.

(7) Orthoclase $KAlSi_3O_8$ (excess K_2O: if present)

(8) Garnet $(Ca,Fe,Mg,Mn)_3Al_2(SiO_4)_3$ (excess FMMO: if present)

(9) Anorthite $CaAl_2Si_2O_8$ (excess CaO)

(10) Cordierite $(Fe,Mg)_2Al_4Si_5O_{18}$ (excess FMMO, SiO_2, or Al_2O_3: if present)

(11a) <u>For metapelite melanosome only</u>

Sillimanite Al_2SiO_5 (Al_2O_3)

(11b) <u>For granitoid rocks and metagreywacke mesosome</u>

Corundum (Al_2O_3)

(12) Garnet was combined with SiO_2 and Al_2O_3 to form additional cordierite until one is consumed

(13) Quartz (excess SiO_2: if present)

(14) Ilmenite $FeTiO_3$ (excess TiO_2: if present)

(15) Magnetite FeO (excess FMMO)

(16) Orthoclase and Albite were combined to form K feldspar, using K feldspar compositions determined by XRF analysis of mineral separates. For samples with no mineral data, an average value from the same rock type was used.

(17) Plagioclase was formed by combining Anorthite and remaining Albite.

(18) Mole proportions were converted to volume proportions using the following molar volume data (Robie et al. 1978, Helgeson et al. 1978) and specific gravities.

Phase	Molar Volume (g/mole)
Albite	100.07
Almandine	115.28
Annite	154.32
Anorthite	100.79
Apatite	159.6
Fe-Cordierite	233.22
Mg-Cordierite	232.08
Corundum	25.58
Grossular	125.3
Ilmenite	31.69
Magnetite	44.52
Orthoclase	108.72
Phlogopite	149.91
Pyrope	113.27
Quartz	22.69
Sillimanite	44.9
Spessartine	117.9

Fe, Mg, Mn, and Ca ratios used for biotite, garnet, and cordierite are from probe data. Assumptions include; ideal mixing of endmembers in solid solutions, and that the molar volume of natural biotite is equal to that of ideal biotite.

(16) Volume proportions were recalculated to 100%.

End

The Metanorm calculations were performed by a Microsoft Basica program, written by the author. A working, but not too elegant, copy of the program is available from the author on request.

The calculation produced the following normative assemblages:

Granitoids (MG_1 and MG_2 leucosome and white pegmatite)

Normative Assemblage: Pl Kfs Qtz Bt, minor Ap Co

Actual Assemblage: Pl Kfs Qtz Bt, minor Grt Ilm

The inclusion of all Fe and Mg into biotite does not introduce significant errors for most granitoid rocks, because the other Fe-Mg phases

(garnet and ilmenite) are present in minor amounts. The Metanorm calculation was not applied to rocks with greater than about 3% garnet+ilmenite (estimated visually or from point counting of thin sections or stained slabs).

Metapelite Melanosome

Normative Assemblage: Pl Bt Cdt Grt, minor Ap Co +Sil +Qtz

Actual Assemblage: Pl Bt Cdt Grt, minor Ilm +Sil +Qtz +minor Kfs

The calculation for metapelite is very sensitive to the proportion of Al in the biotite, since excess Al_2O_3 will be combined with garnet and SiO_2 to form cordierite. Therefore the calculation was applied only to the 2 samples for which whole rock and mineral analyses were obtained. When the calculation was applied to other metapelite samples using a mean biotite composition the absence or presence of quartz or sillimanite was correctly determined, but the proportions garnet and cordierite did not always agree with visual estimates.

Metagreywacke Mesosome

Normative Assemblage: Pl Qtz Bt Grt, minor Ap Co

Actual Assemblage: Pl Qtz Bt Grt, minor Ilm

Metagreywacke samples are very homogeneous, and have simple textures allowing for good modal estimates from point counting. Point counted modal estimates may be compared to calculated volume norms for 3 metagreywacke samples in table B.1, to provide to test of the accuracy of the normative calculation. In each case there is excellent agreement between the point counted and normative mode.

Table B.1. Comparison of volume norms and point counted modes for metagreywacke mesosome

	157a		61b		132a	
	N	P	N	P	N	P
Pl	42.7	46.2	46.9	46.9	42.1	37.6
Kfs	0.0	--	0.0	--	0.0	--
Qtz	34.9	32.6	29.6	31.8	34.1	35.3
Bt	15.1	15.1	18.9	15.3	21.4	22.0
Grt	6.5	5.3	3.7	5.8	1.5	4.0
Cdt	--	--	--	--	--	--
Sill	--	--	--	--	--	--
Ms	--	--	--	--	--	--
Ilm	--	0.7	--	0.2	--	1.0
Co	0.6	--	0.6	--	0.9	--
Ap	0.3	--	0.2	--	0.1	--

N = Volume norm, P = Point counted mode

A comparison of modes determined by point counting of stained slabs is compared with volume norms in table B.2. There is good agreement between estimates in most cases.

Table B.2. Comparison of volume norms and point counted modes, for MG_2 leucosome and white Bt pegmatite.

	64c		140		158c		188b		194f		220a	
	P	N	P	N	P	N	P	N	P	N	P	N
Pl	50.7	38.3	40.8	37.9	23.5	30.3	58.7	53.7	20.2	23.8	25.4	27.9
Kfs	24.2	26.0	18.2	22.1	50.0	38.6	3.8	4.1	48.1	43.2	34.6	29.7
Qtz	22.8	31.2	32.8	31.2	25.1	28.6	28.8	30.9	28.2	28.1	33.2	32.5
Bt	1.0	3.5	8.0	7.8	1.4	1.8	8.1	9.7	3.3	4.2	5.7	9.3
Ms												
Grt	1.4		0.2		x		0.7		0.3		1.2	
Cdt	x				x							
Mgt												
Ilm	x		x		x		x		x		x	
Co		0.9		0.9		0.6		1.8		0.8		0.5
Ap		0.1		0.1		0.2		0		0.1		0.1

P = point counted mode, N = volume norm, x = mineral present in minor amounts (<1%)

APPENDIX C

Table C.1. Average Orthopyroxene Analyses (microprobe).

	Gt-Opx-Hbl Mafic Gneiss				Gt-Opx-Bt-Hbl Metatonalite	
	199A		139B		1A	
wt. %	Core	Edge	Core	Edge	Core	Edge
SiO_2	49.5	49.6	50.1	49.9	47.4	47.3
TiO_2	0.12	0.13	0.13	0.15	0.17	0.14
Al_2O_3	1.23	1.25	1.50	1.58	0.99	0.93
Cr_2O_3	0.06	0.06	0.06	0.07	0.09	0.06
FeO	34.8	34.7	32.3	32.3	40.1	40.6
MnO	0.67	0.67	0.40	0.43	1.14	1.09
MgO	13.3	13.3	15.4	15.1	9.4	9.4
CaO	0.43	0.44	0.23	0.24	0.78	0.58
Total	100.10	100.12	100.13	99.66	100.00	100.10
No. of cations on the basis of 6 O						
Si	1.96	1.96	1.98	1.96	1.94	1.94
Ti	0.00	0.00	0.00	0.00	0.01	0.00
Al	0.06	0.06	0.07	0.07	0.05	0.05
Cr	0.00	0.00	0.00	0.00	0.00	0.00
Fe^{2+}	1.15	1.15	1.05	1.06	1.38	1.40
Mn	0.02	0.02	0.01	0.01	0.04	0.04
Mg	0.78	0.79	0.89	0.88	0.58	0.57
Ca	0.02	0.02	0.01	0.01	0.03	0.03
Total	4.00	4.00	4.00	4.00	4.02	4.03
Fs	0.59	0.59	0.54	0.54	0.69	0.70
En	0.40	0.40	0.46	0.45	0.29	0.29
Wo	0.01	0.01	0.00	0.01	0.02	0.01
No. of Analyses	5	4	5	6	3	3